LAPPEENRANTA UNIVERSITY OF TECHNOLOGY
Faculty of Technology
Degree Programme in Energy Technology

Ville Kakkonen

APROS MODEL VALIDATION IN CASE OF FAST TRANSIENTS IN A BOILING WATER REACTOR

Examiners: Professor D.Sc. (Tech.) Riitta Kyrki-Rajamäki
M.Sc. (Tech.) Juha Poikolainen
Instructor: M.Sc. (Tech.) Juha Poikolainen

TIIVISTELMÄ

Lappeenrannan teknillinen yliopisto
Teknillinen tiedekunta
Energiatekniikan koulutusohjelma

Ville Kakkonen

APROS mallin validointi kiehutusvesireaktorin nopeissa transienteissa

Diplomityö

2011

82 sivua, 13 kuvaa, 6 taulukkoja ja 14 liitettä

Tarkastajat: Professori Riitta Kyrki-Rajamäki
DI Juha Poikolainen
Ohjaaja: DI Juha Poikolainen

Hakusanat: APROS, kiehutusvesireaktori, transientti

Diplomityössä selvitetään Olkiluoto 1 ja 2 ydinvoimalaitosten käytössä olevan APROS laskentamallin suorituskyky nopeissa transienteissa. Työssä on esitelty yleisesti Olkiluoto 1 ja 2 ydinvoimalaitoksia ja niiden tärkeimpiä turvallisuusjärjestelmiä. APROS-ohjelmiston toimintaperiaatteet ja Olkiluoto 1 ja 2 laitoksien pohjalta rakennetun laskentamallin kattavuus on selvitetty työn aikana. Odotettavissa olevien transienttien tapahtumaketjut on esitetty yksityiskohtaisesti ja ne toimivat perusteena laskentatulosten analysoinnissa.

Käytettyjä laskentatapauksia ovat kuormanpudotukset ja kaksi reaktorin sisemmän eristysventtiilin tahatonta sulkeutumista. Työn aikana selvitettiin perusteet ja tarvittavat lähtötiedot 3-D reaktorisydämen luomiseen ja päivitettiin 1-D reaktorisydämestä löytyneitä epätodellisia lähtötietoja.

Työssä ilmeni, että laskennan tulokset vastaavat pääpiirteittäin laitosmittauksia, mutta laskentamallin puutteista johtuvia erovaisuuksia esiintyy. Tulosten perusteella merkittävimmät eroavaisuudet johtuivat reaktorisydämestä ja syöttövesijärjestelmästä. Työn perusteella laskentamallista voidaan kehittää luotettava työkalu transienttien ja laitosmuutosten analysointiin.

ABSTRACT

Lappeenranta University of Technology
Faculty of Technology
Degree Programme in Energy Technology

Ville Kakkonen

APROS model validation in case of fast transients in a boiling water reactor

Master's thesis

2011

82 pages, 13 figures, 6 tables and 14 appendices

Examiners: Professor D.Sc. (Tech.) Riitta Kyrki-Rajamäki
M.Sc. (Tech.) Juha Poikolainen
Instructor: M.Sc. (Tech.) Juha Poikolainen

Keywords: APROS, boiling water reactor, transient

This Master´s thesis investigates the performance of the Olkiluoto 1 and 2 APROS model in case of fast transients. The thesis includes a general description of the Olkiluoto 1 and 2 nuclear power plants and of the most important safety systems. The theoretical background of the APROS code as well as the scope and the content of the Olkiluoto 1 and 2 APROS model are also described. The event sequences of the anticipated operation transients considered in the thesis are presented in detail as they will form the basis for the analysis of the APROS calculation results.

The calculated fast operational transient situations comprise loss-of-load cases and two cases related to a inadvertent closure of one main steam isolation valve. As part of the thesis work, the inaccurate initial data values found in the original 1-D reactor core model were corrected. The input data needed for the creation of a more accurate 3-D core model were defined.

The analysis of the APROS calculation results showed that while the main results were in good accordance with the measured plant data, also differences were detected. These differences were found to be caused by deficiencies and uncertainties related to the calculation model. According to the results the reactor core and the feedwater systems cause most of the differences between the calculated and measured values. Based on these findings, it will be possible to develop the APROS model further to make it a reliable and accurate tool for the analysis of the operational transients and possible plant modifications.

TABLE OF CONTENTS

SYMBOLS AND ABBREVIATIONS **4**

LIST OF SYSTEMS **6**

ACKNOWLEDGEMENTS **8**

1 INTRODUCTION **9**

2 OLKILUOTO 1 AND 2 NUCLEAR POWER PLANTS **10**

2.1. Plant's functionality 10

2.2. Reactor and reactor service system 11

2.3. Reactor safety systems 17

2.4. Main steam isolation valves 311V1-V4 19

2.5. Isolation 23

2.6. Emergency cooling systems 25

2.7. Ventilation systems 25

3 APROS CODE THEORETICAL BACKGROUND **27**

3.1. Governing equations 28

3.2. Thermal hydraulic modeling principles 34

3.3. Principles of one-dimensional two energy group model 35

3.4. Principles of three-dimensional two energy group model 40

3.5. General modeling capabilities 44

4 APROS CODE WITH OLKILUOTO 1 AND 2 MODEL **46**

4.1. Plant specific model 46

4.2. Reactor and reactor systems 46

4.3. Principles of 3-D core model creation 48

5 ANTICIPATED OPERATIONAL TRANSIENTS.....50
5.1. Pressure increase transients.....51
5.2. Pressure decrease transients.....57
5.3. Feedwater flow increase and temperature decrease transients.....59
5.4. Loss of feedwater transients.....60
5.5. Recirculation flow decrease transients.....60

6 APROS MODEL UPDATING AND SIMULATIONS.....63
6.1. CASE 1: 15.5.2010 OL2 inadvertent closure of one MSIV 63
6.2. CASE 2: 2.6.2005 OL1 loss-of-load test 64
6.3. CASE 3: 7.3.2004 OL2 inadvertent closure of one MSIV 65
6.4. CASE 4: 20.4.2002 OL1 failure in the 400 kV grid 66

7 RESULTS AND COMPARISON 67
7.1. Accuracy of the plant measurements 67
7.2. CASE 1: 15.5.2010 OL2 inadvertent closure of one MSIV 69
7.3. CASE 2: 2.6.2005 OL1 loss-of-load test 72
7.4. CASE 3: 15.5.2004 OL2 inadvertent closure of one MSIV 73
7.5. CASE 4: 20.4.2002 OL1 failure in the 400 kV grid 75

8 SUMMARY AND CONCLUSIONS.....77

REFERENCES 78

APPENDICES

Appendix 1: The cross-section of the OL1 and OL2
Appendix 2: The operating principle of the boiling water reactor
Appendix 3: The reactor shutdown and isolation circuits
Appendix 4: The monitored systems by the system 516
Appendix 5: The Controlled systems by the system 516
Appendix 6: The modeled systems in the OL1/OL2 APROS model
Appendix 7: The APROS model measurements in the system 211
Appendix 8: The APROS model figures

Appendix 9: The isolation chains
Appendix 10: The scram chains
Appendix 11: The results of the CASE 2010
Appendix 12: The results of the CASE 2005
Appendix 13: The results of the CASE 2004
Appendix 14: The results of the CASE 2002

SYMBOLS AND ABBREVIATIONS

Latin

A	surface	[m^2]
C	concentration	[ppm]
D	diffusion coefficient	[cm]
F	friction force	[N/ m^3]
h	enthalpy	[J/kg]
$\dot{m}$	mass flow	[kg/s]
n	quantity	[-]
p	pressure	[Pa]
q	heat flow	[W/ m^3]
t	time	[s]
u	velocity	[m/s]
V	volume	[m^3]

Creek

α	volume fraction	[-]
β	total fraction of delayed neutrons	[pcm]
Γ	mass change rate	[kg/ m^3s]
ϕ	neutron flux	[1/ cm^2s]
λ	decay constant	[s]
υ	neutron velocity	[m/s]
ρ	density	[kg/m^3]
Σ	cross section	[1/cm]

Subscripts

1	fast
12	from fast to thermal neutron group
2	thermal

b1	absorption in fast neutron group
b2	absorption in thermal neutron group
f	fission
fl	form loss
g	gas
i	interfacial
j	precursor group j
k	phase k
l	liquid
nc	non-condensable
pu	pump
va	valve
w	wall

Abbreviations

APRM	Average Power Range Monitor
APROS	Advanced Process Simulation environment
BWR	Boiling Water Reactor
HP	High Pressure
IVO PE	Imatran Voima Power Engineering Ltd
LP	Low Pressure
LPRM	Local Power Range Monitor
M.Sc.	Master of Science
MSIV	Main Steam Isolation Valve
NPP	Nuclear Power Plant
PRM	Power Range Monitor
SIRM	Source and Intermediate Range Monitor
TIFANY	the Internal Code for Design Basic Accident Analyses
TVO	Teollisuuden Voima Oyj
UPC	Upper Pressure Chamber
VTT	Technical Research Centre of Finland

LIST OF SYSTEMS

121	Reactor building
122	Turbine building
124	Auxiliary system building
150	Reactor containment
211	Reactor pressure vessel
214	Steam separator
215	Steam dryer
222	Control rods
311	Steam lines in reactor building
312	Feedwater system
313	Recirculation systems
314	Relief system
321	Shut-down cooling system
322	Containment vessel spray system
323	Core spray system
326	Flange cooling system
327	Auxiliary feedwater system
332	Clean up system
351	Boron injection system
411	Steam turbine
412	Steam reheat system
413	Turbine plant main steam system
421	Generator
431	Condenser and vacuum system
445	Turbine plant feedwater system
465	Turbine plant protection system
516	Trip and interlock system (reactor protection system)
517	Alarm display system
531	Neutron flux measuring system
532	Control rod operating system
546	Isolation monitoring system

551	Steam line radiation monitors
712	Shut-down service water system
734	High pressure purge water system
741	Containment gas treatment system
742	Reactor building ventilation system
749	Off-gas filter system
754	Compressed nitrogen system (pilot valve system)

ACKNOWLEDGEMENTS

This Master´s thesis was done at Teollisuuden Voima Oyj. I would like to thank the organization for the possibility to complete my Master´s thesis in such an inspiring and supporting environment.

I want to thank my instructor and examiner M.Sc. Juha Poikolainen for introducing me to this topic and for all of his support and advices during this Master´s thesis. I would also like to thank all members of the nuclear safety office for supporting my work and their interest in my Master´s thesis. Special thanks go to M.Sc. Janne Wahlman who has supported me with the APROS simulations. In addition, I would like to thank examiner Professor Riitta Kyrki-Rajamäki for the help during this thesis and all my studies.

Finally, many thanks to my family and friends for all the support and the encouragement I have received during my studies.

Eurajoki, 14.10.2011

Ville Kakkonen

1 INTRODUCTION

This Master´s thesis concerns validation of the APROS model in case of fast transients in the Olkiluoto 1 and 2 boiling water reactors. The calculation cases were selected from the limited group of happened plant transients. Total of four different cases were calculated for the validation. All calculations have been done by using the one dimensional reactor core. This thesis also consists of principles of the three dimensional core model creation and the one dimensional core model updating.

The Olkiluoto 1 and 2 nuclear power plant functionality and the relevant safety systems are presented in the chapter two. The third chapter concerns the description of the APROS code theoretical background and the general model capabilities. The modeled reactor and the reactor systems in the Olkiluoto 1 and 2 plant APROS model are presented in the chapter four. The fifth chapter introduces the methodologies of anticipated operation transients in the Olkiluoto 1 and 2 plants.

The one dimensional core model updating, the principles of three dimensional core model creation and the information about the calculated transients are presented in the chapter six. The seventh chapter introduces the results of calculations and the accuracies of the plant measurements. There are also some explanations for the differences between the calculated and measured values. The result comparison, the conclusions and the recommendations are presented in the chapter eight.

2 OLKILUOTO 1 AND 2 NUCLEAR POWER PLANTS

The olkiluoto plant site is located on the coast of the Bothnian Sea in the municipality of Eurajoki about 13 km north of the town of Rauma. There are two operating boiling water reactors (BWR), OL1 and OL2. Third one is under construction (OL3) which is going to be a pressurize water reactor. The units OL1 and OL2 were taken into operation in 1978 and 1980. (Viitanen, 2011, s. 5-6) Thermal power of the OL1 and OL2 units is 2500 MW_{th} and the net electrical power is 860MW_e. In this thesis the description is common to the units OL1 and OL2. The units were supplied by the Swedish company AB Asea Atom. TVO keeps both units running as good as new through carefully planned long term maintenance. The units are systematically upgraded to meet the today´s safety demands. (Lemmetty, 2010, s. 4)

2.1. Plant's functionality

The OL1 and OL2 units can each be divided into the three structural sections: the reactor building (121), the turbine building (122) and the auxiliary system building (124). The reactor building is the highest building, shown in appendix 1. The turbine building is on the left side of the reactor building, shown also in appendix 1. The main components in the turbine building are the steam turbine (411), the condenser (431) and the generator (421). (Lemmetty, 2010, s. 11-15)

The nuclear steam supply system includes the boiling water reactor of ASEA-ATOM design. The reactor is moderated by light water, operating at 7.0 MPa, 286 ºC. The BWR is the second most common type of an electricity generating nuclear reactor. The basic operating principle of the BWR is presented in appendix 2. The BWR uses demineralized water as a neutron moderator and a coolant. The water boils as it passes between the fuel rods. The reactor output is regulated with the recirculation pumps (313) and the control rods (222). The steam produced in the reactor core passes through the steam separators (214) and the steam dryer (215). The steam goes through the main steam lines to the high-pressure (HP) turbine. In which the steam releases part of its energy. After the HP

turbine the steam is transferred to the steam reheat system (412) where it is dried and superheated. The superheated steam is then transferred to the low-pressure (LP) turbines. The HP turbine and the LP turbines are all coaxially connected to the generator. The generator generates electricity that is then fed into the national grid. The steam goes to the condenser from the LP turbines. The condenser uses sea water as a coolant. The condensed water is conveyed through the clean-up system (332) and the feedwater heater system (445) to the feedwater system (312). The feedwater system feeds the water back into the reactor pressure vessel (211). (Lemmetty, 2010, s. 11-15)

2.2. Reactor and reactor service system

The reactor building encloses the containment of the reactor (150). The cross-section of the reactor building is shown in figure 2.1. The reactor building serves as a secondary containment. The reactor pool and the fuel pools are located in the reactor hall. The storage facilities for receiving and storing fresh fuel are located at the floor level below the reactor hall. The safety-related systems are located in the bottom part of the reactor building. The safety related systems at the Olkiluoto power plant units are divided into four redundancy systems. The systematic separation provides effective built-in protection against hazards associated with flooding, crashing aircrafts, fires, earthquakes and other external impacts. (TVO, 2008, s. 9)

The reactor containment is based on the principle of pressure suppression. The reactor containment is shown in figure 2.2. The containment is made of pre-stressed concrete and it is designed with a minimum amount of equipment installed inside. All of the components requiring service during the normal operation of the reactor are located outside the containment. (TVO, 2008, s. 11)

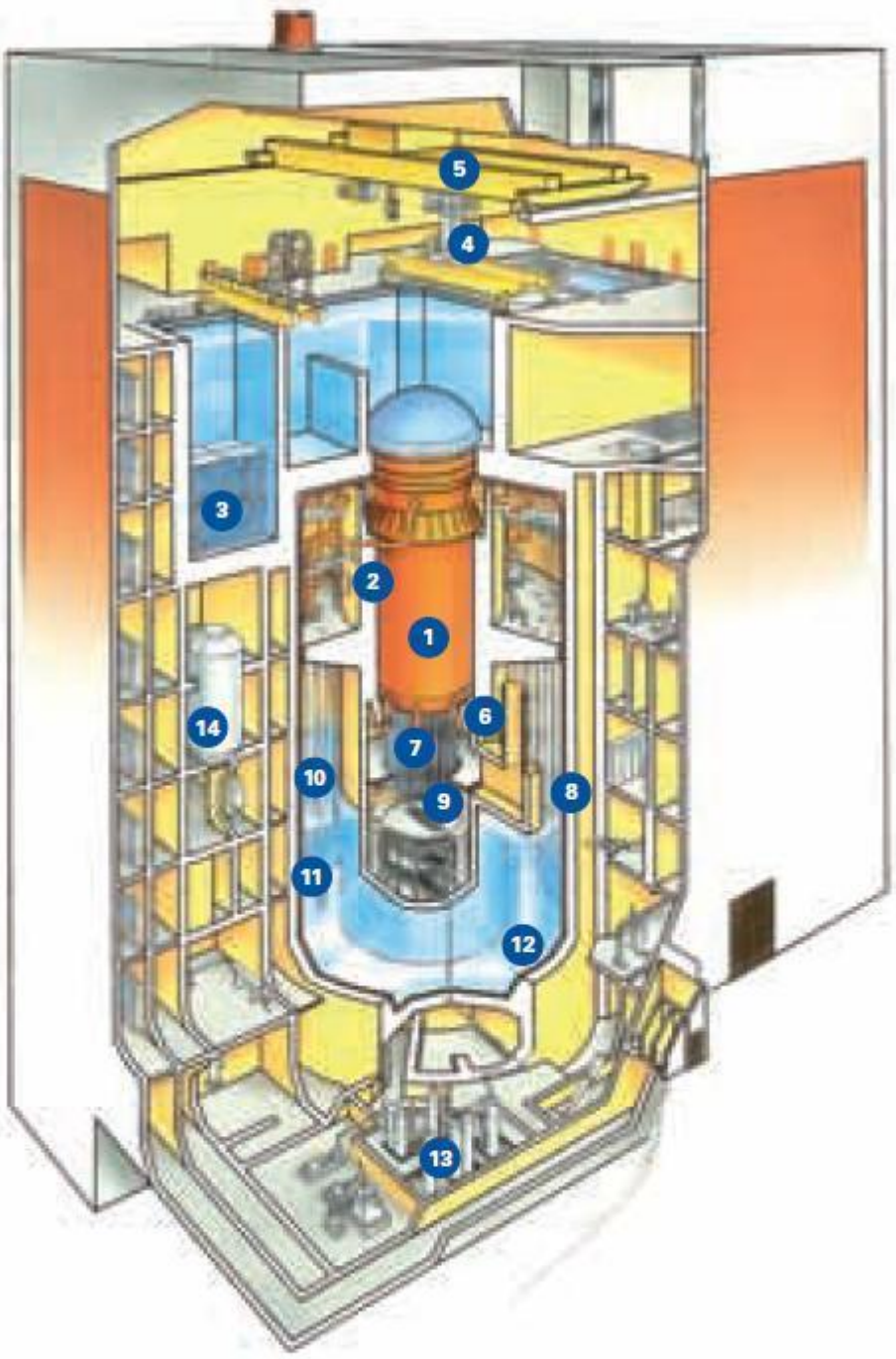

1. *Reactor pressure vessel*
2. *Main steam lines*
3. *Fuel pool*
4. *Reactor service bridge*
5. *Reactor hall crane*
6. *Recirculation pumps*
7. *Control rod drives*
8. *Containment*
9. *Control rod service platform*
10. *Blow-down pipes*
11. *Embedded steel liner*
12. *Condensation pool*
13. *Scram system tracks*
14. *SAM-scrubber*

Figure 2.1. A sectional view of the reactor pressure vessel (TVO, 2008, s. 9)

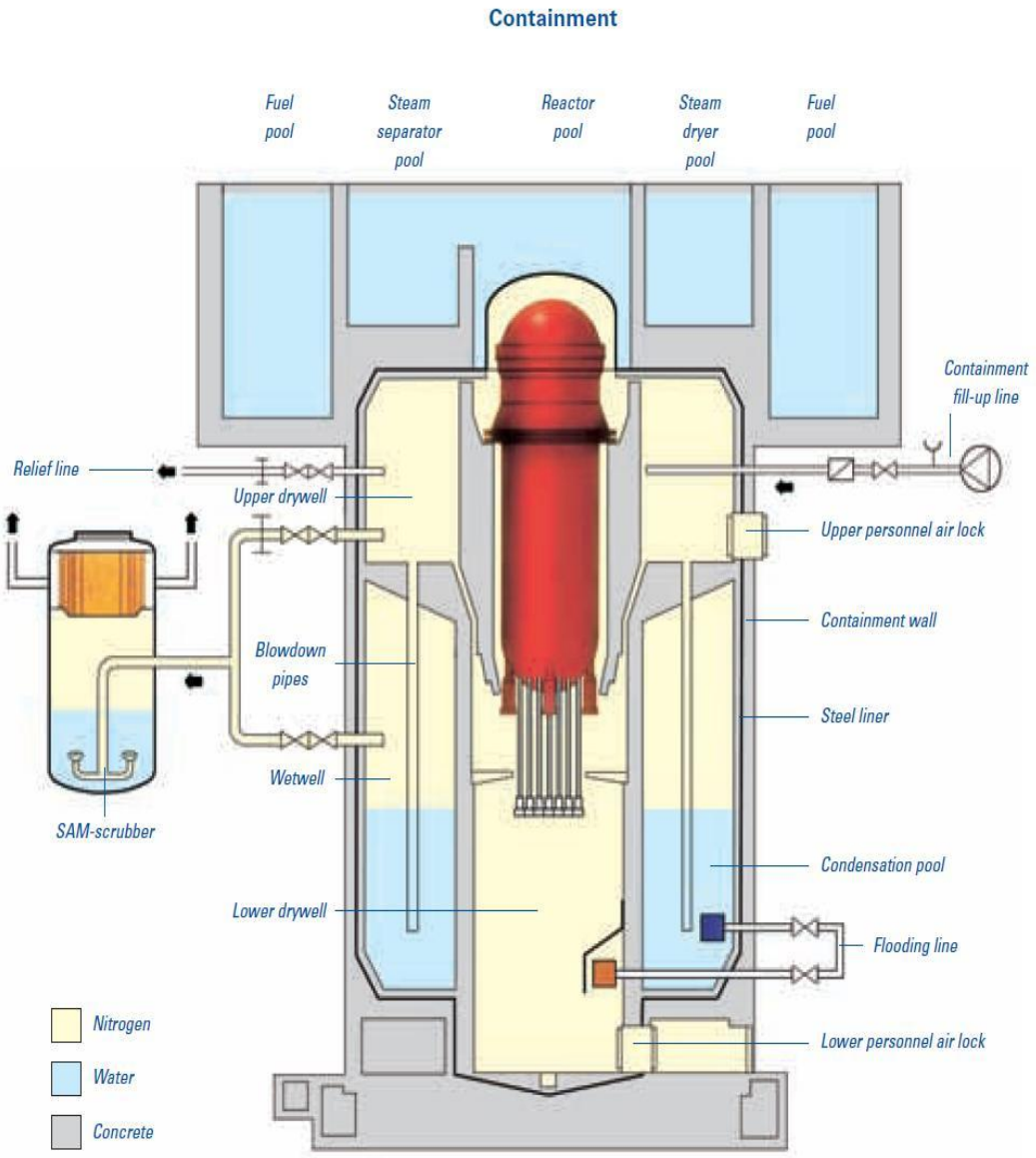

Figure 2.2. A sectional view of the containment (TVO, 2008, s. 10)

The reactor pressure vessel is seen in figure 2.3. The reactor pressure vessel is made of low-alloy steel, with a 5 mm thick lining of stainless steel. The reactor pressure vessel's inner diameter is 5.54 m and the inner height is 20.593 m. The function of the reactor pressure vessel is to be a container for the reactor core. The reactor pressure vessel also contains the steam separator system and the water supply components. The design temperature and the pressure of the reactor pressure vessel are 300 ℃ and 8.5 MPa. (TVO, 2008, s. 12)

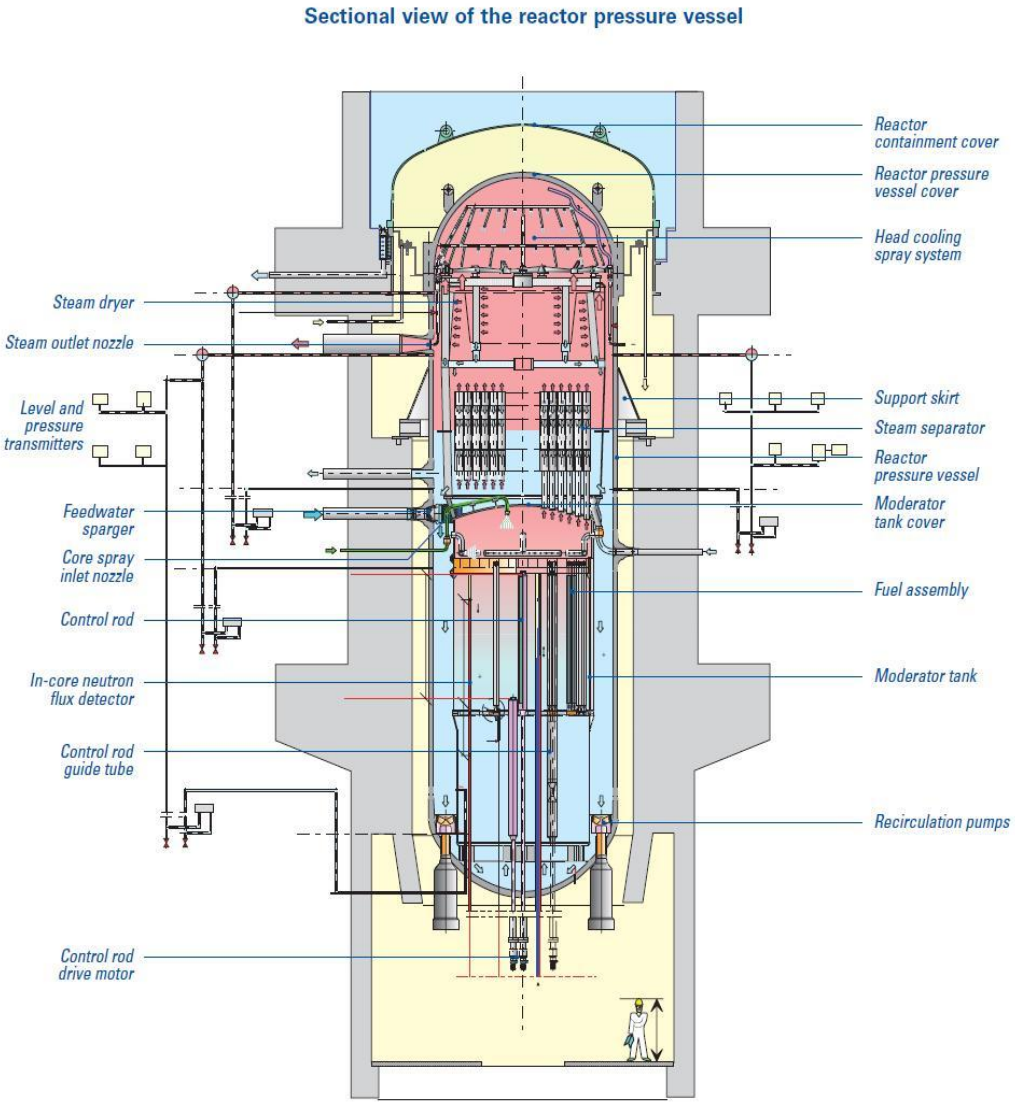

Figure 2.3. A Sectional view of the reactor pressure vessel (TVO, 2008, s. 12)

In the Olkiluoto nuclear power plants the reactor cores of the OL1 and OL2 units contain 500 fuel assemblies each. The fuel assemblies which are currently in use are designed as a 10 x 10 matrix. The form of the uranium fuel is pellets made of UO_2. The uranium U235 content in the pellets is enriched. The pellets are located in the Zircaloy-2 tubes. In the fuel design, a burnable absorber (Gd_2O_3) is used in the fuel design. Some of the absorber pellets are added in the bundle to reduce the power peaking factor and to compensate the excess reactivity during the first half of an operation period. The fuel assemblies have different radially-zoned enrichment distributions. With the different enrichment distribution, the power

peaking factor can be reduced and the fuel heat transfer capacity optimized. (Lemmetty, 2010, s. 6)

Most of the power is generated by the fission of U235 by the thermal neutrons. During the plant operation U238 is converted to plutonium. The fast neutron fission in U238 generates about 7 % of the total power. The U238 is also an important factor in reducing the power increasing transients. The increasing temperature in the fuel pellets increases the resonance absorption of neutrons and reduces the fission power. This negative temperature coefficient phenomenon is called as the nuclear Doppler-effect. The negative steam void coefficient with the Doppler-effect makes the operation of fission power possible. (Nevander, 2010, s. 4-5)

The reactor is operated in one-year cycles. One quarter of the fuel assemblies in the reactor core are replaced during each cycle. The reactor's physical measurement of the fuel assemblies determines U235 enrichment level for the fuel rods in the refueling batch. During the operating period excess reactivity in the reactor is absorbed by the control rods, by the burnable absorber and by the boiling of the coolant regulated through the primary circuit. The highest excessive reactivity is observed in the beginning of the period. The excessive reactivity decreases as the burnable absorber is consumed. During the operation period excessive reactivity can be increased by retracting the control rods in small increments. The control rods are also used for adjusting the power distribution in the reactor core. At the end of the operating period all the control rods are fully retracted. By increasing the primary circuit's flow the reactivity can been maintained. During the operating period the minor power adjustment are made by regulating the primary circuit's flow. (TVO, 2008, s. 16)

The drives for the control rods enable the use of two independent ways of moving the control rods. An electro-mechanical system for the normal operation and a hydraulic system for the fast control rod insertion. The design base is that an electrical fault cannot simultaneously render both the scram function and the electro-mechanical drive inoperative. The number of control rods in the reactor is

121. The control rods are divided into 14 scram groups of eight or nine rods each. The scram group division is made so that the reactivity coupling between the rods within a scram group is negligible. In the event of a total failure of the control rod insertion an automatic boron injection system (351) is provided to shut down the reactor. The control rod drivers are presented in figure 2.4. (Lemmetty, 2009, s. 9-10)

Used fuel assemblies are transferred from the reactor to the fuel pools in the reactor hall. The fuel assemblies are placed in the storage pools in the reactor hall for several years. During this time, the heat generation and the radioactivity of the used fuel is reduced. Used fuel is transferred into the storage facility in a water-filled transfer tank made of spheroidal graphite cast iron. The used fuel is located in water filled pools in the storage facility for several decades before they are placed in the final repository. All used fuel from Olkiluoto nuclear power plants will be transferred into the final repository at Olkiluoto. (TVO, 2008, s. 16-17)

The recirculation system cools the reactor core by circulating the water content of the reactor. The recirculation system contains six 620 kW pumps which are located inside the reactor vessel. The pumps are driven by a wet electrical motor. The motors are attached to the reactor vessel and connected to the pump through a shaft penetrating the reactor vessel wall. The pumps are located onto the bottom of the reactor vessel. This design eliminates large pipe connections to the lower part of the reactor vessel and decreases the risk of an accident, caused by a severe loss of coolant. The water is pumped from the bottom of vessel through the reactor core. The thermal power generated by the reactor can be controlled by changing the pump speed. During normal operating all six pumps are running and controlled by the reactor power control system. (Jurvakainen, 2009, s. 9-20)

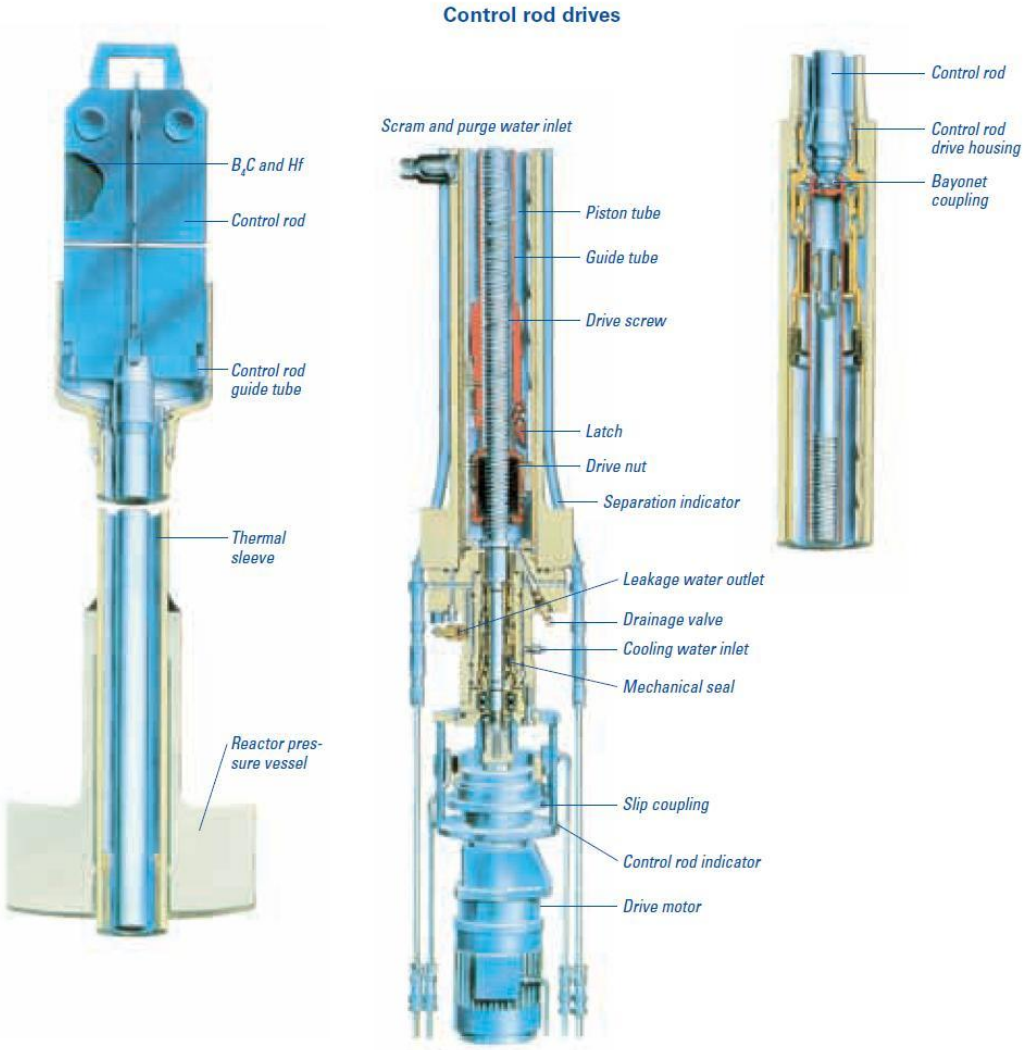

Figure 2.4. Control rod drives (TVO, 2008, s. 18)

2.3. Reactor safety systems

The reactor protection system (516) function is actuating safety functions which can limit or prevent radioactive emissions operating failure or accidents. The system 516 is designed to accept and process signals from important measured variables. All the measured variables have been analyzed to be necessary to guarantee the plant safety. The system processes so much output signals that it is possible to actuate all safety functions which are verified to be needed by the plant safety. The system 516 takes part in following executions of the safety functions (Paasikivi, 2009, s. 7-8):

- Reactor power and criticality control

- Primary circuit pressure control
- Reactor temperature and coolant reserve control
- Heat transfer to the final heat sink
- Limiting the releases of activity from containment building
- Limiting the releases of activity from other destination than containment building
- Support tasks of safety functions
- Accident management
- maintenance of consistency

The system 516 is divided into groups of subsystems which are called circuits. All input signals which can actuate same protection function are included in the same circuit. The circuits are divided into two groups. These two groups are the reactor rip circuit and the isolation circuit. More information about these two groups are presented in appendix 3, table 1. (Paasikivi, 2009, s. 60-62):

The system 516 is composed of many signal control units. The control units devise control signals which are needed to complete the system function. The system 516 input signals are binary type. The binary data is measured from the safety related switches and sensors. The system logistic processes binary information and generates the operating signals. The monitored systems and magnitudes are shown in appendix 4, table 1. The measurement systems are not included in the system 516. (Paasikivi, 2009, s. 60-62)

There are lots of systems which use output signals from the system 516. The system 516 and other systems are connected by using connection strips. The controlled systems are presented in appendix 5, table 1. There are so many controlled systems that it is not possible to process all information about the systems functions in this thesis. (Paasikivi, 2009, s. 60-62)

The function of alarm display system (517) is to notify operating personnel in a monitoring room if measured magnitudes in the system 516 exceed the limit values. The event recorder system records events which actuates alarms. Event list

is very useful to check before starting the simulation of some transient because the exact alarm times can be seen there. (Paasikivi, 2009, s. 60-62):

There are two independent systems to shutdown the reactor, the control rod system (352) and the boron system (351). The system 352 has two independent actuating systems, the hydraulic scram system and the control rod operating system. Both control rod systems are actuated by the trip and interlock system (516). The system 351 is actuated manually or by the BOR circuit in the system (516). There are different shutdown functions and their combinations. The signal to shut down the reactor originates from a number of sensors in various systems. Two common signals are 516 SS and 516 V which actuate (Paasikivi, 2009, s. 18-44):

- Control rod inserting by the hydraulic scram system
- Control rod inserting by the control rod operating system
- Reduction of main recirculation pump speed

The power will effectively be reduced even if not all scram groups are inserted in the reactor core. The boron system's capacity is high enough to shut down the reactor and keep it subcritical during cooldown even if the insertion of all control rods were to fail. During the normal scram function the heat sink is the turbine condenser. (Paasikivi, 2009, s. 39)

2.4. Main steam isolation valves 311V1-V4

Isolation is designed to minimize the environmental consequences of accidents. Generally the isolation causes the scram and the closure of the pipes which pass through the reactor containment vessel wall. The primary pipes have the internal and external isolation valves. After the pipe breaks outside the containment, the most important ways to make isolations are the internal isolation valves. The internal isolation valves are pneumatically actuated or medium operated valves, except the check valves which bring emergency water into the reactor. Purpose of use for the external isolation valve is to be a back-up for the internal isolation

valve and to isolate the reactor or the containment after a pipe break inside the containment. (Nevander, 2008, s. 5-6)

The main steam isolation valves have been exchanged during the outages in 2010 (Nousiainen, 2010, s. 1) and 2011 (Nousiainen, 2011b, s. 1). One important change is that the old inner MSIV:s had a design with risk for self closing at high steam flow but the new MSIV:s does not have that risk. When the old MSIV:s were used the inadvertent closure of one of the inner MSIV caused closure of other inner MSIV:s because of high steam flow.

The old inner MSIV is presented in figure 2.5. The isolation valves are designed to be kept in an open position with the force of a strong magnet. There are the evacuation chambers in order to open and close the isolation valve. The evacuation chamber's pressure is controlled to get same pressure on each side of the piston and to help the magnet to hold the valve open. After the fast evacution of the chamber below the piston the force on the piston will exceed the force of the magnet and the isolation valve will close or open. The valve has steam flow limit when it self-closes. The steam flow limit depends on the turbulence at the valve and the force of the magnet. In the Olkiluoto 1 and 2 units the steam flow limit was approximately 360 kg/s. (Jönssön, 2008, s. 6)

The new inner MSIV is presented in figure 2.6. and the closing sequence is presented in figure 2.7. The valves are operated by the medium actuator with the pressure principle. The steam pressure in the control system holds the valve in an open position during normal operation. The closing of the MSIV begins by opening the pilot valve. After the pilot valve opens the system steam flows into the upper pressure chamber (UPC). The MSIV starts to close when the pressure in the UPC reaches about 15 % of the system pressure. The pressure in the piston rod channel starts to decrease. The pressure decrease between the discs causes the valve discs to press together. The valve piston closes and stops against the backseat. The pressure in the piston rod channel and between the discs increases to system pressure and the discs press against the valve seats. Notice that the flow direction is different in figure 2.5 and figure 2.6. (Andersson, 2008, s. 4-8)

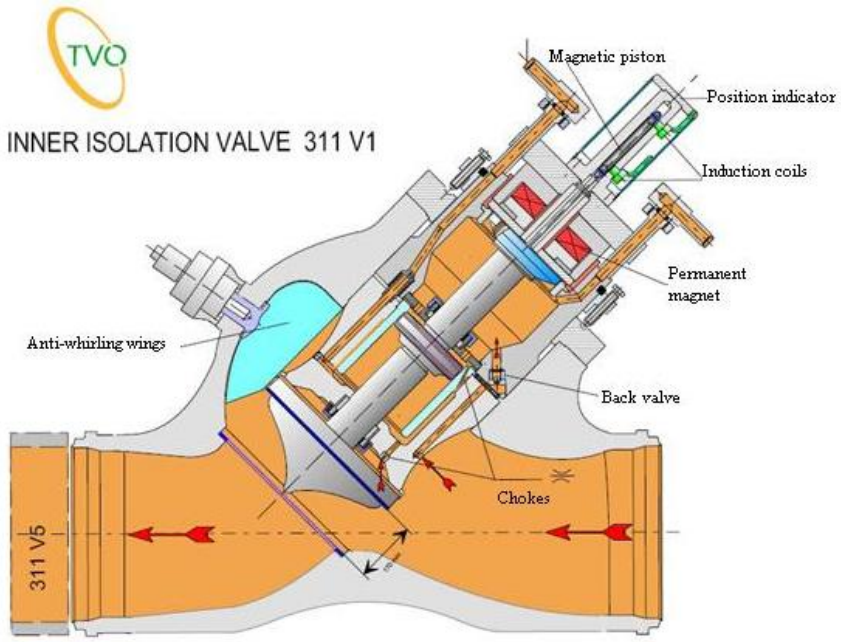

Figure 2.5. The old inner MSIV 311V1 (Dellby, 2004, s. 7)

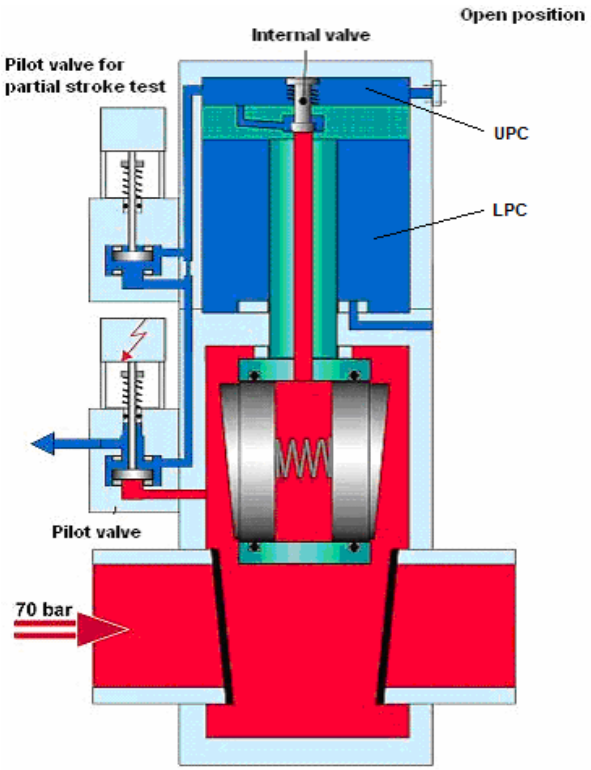

Figure 2.6. The new inner MSIV 311V1 (Nevander, 2008, s. 5)

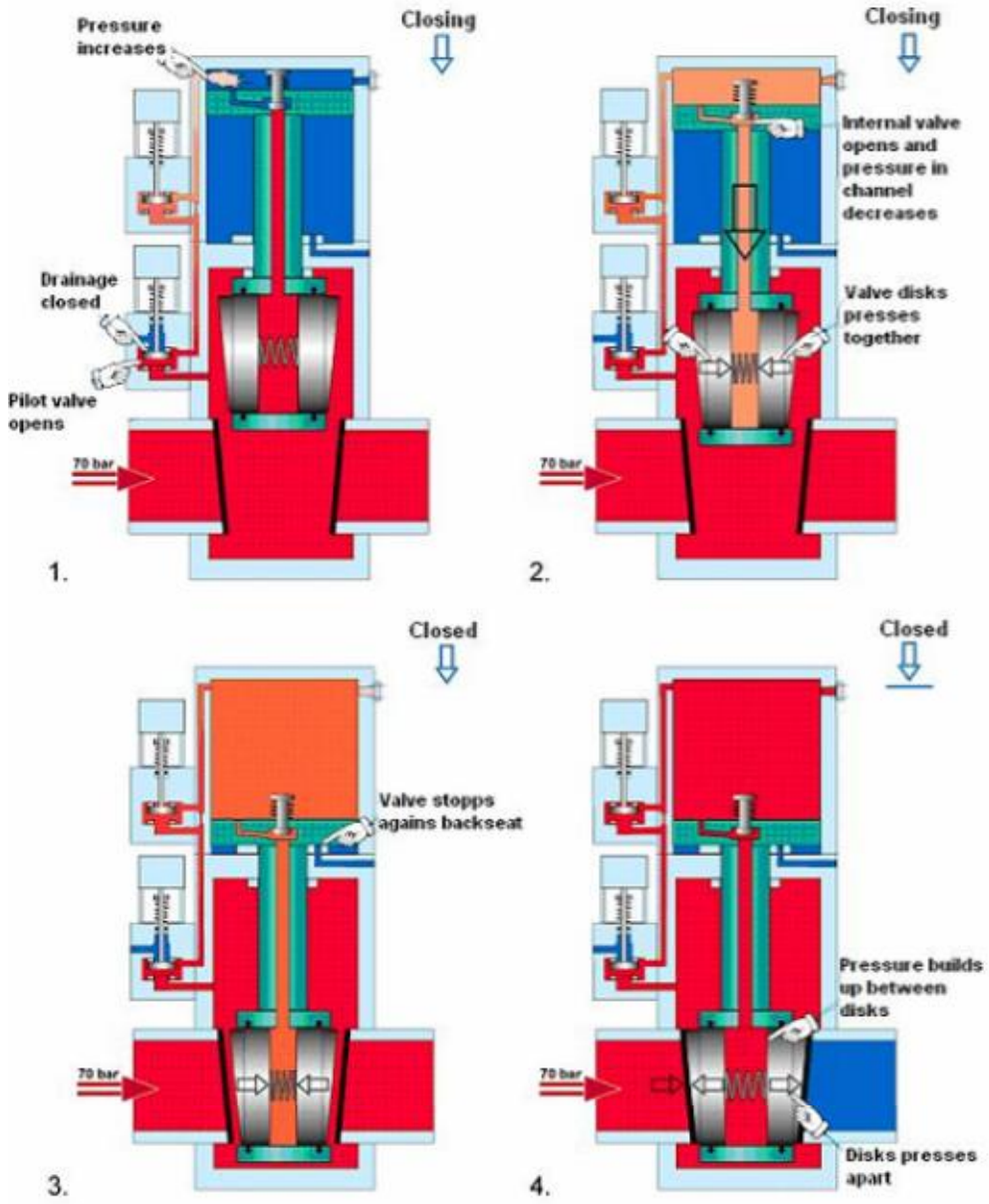

Figure 2.7. The Closing sequence of the inner MSIV (Nevander, 2008, s. 8)

2.5. Isolation

There are five different types of isolations in the OL1 & OL2 nuclear power plants. The name codes originate from the Swedish words. The code letter describes the location of the pipe break causing the isolation. These five types of isolations are (Nevander, 2008, s. 6):

- Inner isolation (I-isolation)
- Feedwater isolation (M-isolation)
- Steam isolation (A-isolation)
- Outer isolation (Y-isolation)
- Auxiliary system isolation (H-isolation)

I-isolation activation requires a pipe break accident inside the reactor containment vessel or other accidents with the potential release of radioactivity to the containment vessel atmosphere. The I-isolation measurements are the pressure and the temperature gauges in the room monitoring system (546) and the steam line radiation monitor system (551). The I-isolation signal actuates (Paasikivi, 2009, s. 29):

- Closure of isolation valves
- Start of emergency cooling system
- Stand-by auxiliary power units
- Simultaneously reactor scram

M-isolation activation requires a pipe break accident in the feedwater system (312) outside of the reactor containment vessel. The M-isolation measurements are the temperature in reactor, the water level in the reactor and the high conductivity after the main condenser. The measurements are part of the system 546 and located in the turbine building. The M-isolation signal actuates (Paasikivi, 2009, s. 33-34):

- Closure of feedwater isolation valves
- Start of emergency cooling system
- Stand-by auxiliary power units
- Stop of condensate and feedwater pumps
- Simultaneously reactor scram

A-isolation activation requires a pipe break accident in the steam lines outside of the reactor containment vessel. The A-isolation measurements are pressure and temperature gauges which belong to system 546, located in the steam line culvert and the turbine building. The A-isolation signal actuates (Paasikivi, 2009, s. 32):

- Closure of main steam isolation valves
- Start of stand-by auxiliary power units
- Simultaneously reactor scram

Y-isolation activation requires a pipe break outside of reactor containment vessel. The Y-isolation measurements are pressure and temperature which belong to the system 546 and are located in the rooms of the reactor building. Y-isolation signal actuates (Paasikivi, 2009, s. 31):

- Reactor shut down-cooling system (321), flange cooling system (326) and high pressure purge water system (734) are isolated from the reactor
- Start of stand-by auxiliary power units
- Simultaneously reactor scram

H-isolation activation requires water flooding in the emergency cooling bays. The H-isolation measurement is a level located in these bays. If any of these bays have leakage, the pipes in H-bays, the containment vessel spray system (322), the core spray system (323) and the auxiliary feedwater system (327) will be isolated and the corresponding pumps will be stopped (Paasikivi, 2009, s. 38-39).

2.6. Emergency cooling systems

The feedwater system and the auxiliary feedwater system are possible systems to supply the reactor with water at full pressure. In emergency situations where the regular feedwater system is out of power, the auxiliary feedwater system would supply the feedwater to the reactor. The core spray system is available to feed water in to the reactor when the reactor pressure is below 10 bar. When the reactor is isolated from the turbine condenser, cooling can be done with a relief system to the condensation pool. The shutdown cooling system is normally used when temperature is below 188 ℃ and the reactor pressure below 12 bar. The containment gas cooling system is isolated after most accidents. In that case the cooling of the containment atmosphere is taken over by the containment vessel spray system. The pump motors in the H-isolation bays (systems 322, 323 and 327) are all diesel-powered. The secondary system (721) which cools systems 322, 323 and 327 is separated into two subsystems. A failure in pumps, valves or another active components cannot prevent the system to do its safety function. The shutdown service water system (712) is also divided into four subsystems and it is diesel powered. (Nevander, 2008, s. 8)

2.7. Ventilation systems

The ventilation systems have different functions during the normal operation and in emergency situations. During the normal operation the ventilation system has to provide (Nevander, 2008, s. 8-9):

- Fresh air to the plant buildings
- Prevent the leakage from contaminated spaces to clean spaces
- Exhaust air from potentially contaminated rooms through filter systems before releasing to the environment

The ventilation systems have diesel backed auxiliary power and they are designed so that a single component failure would not prevent the safety shutdown of the reactor. After a pipe break or a major system leakage inside the reactor

containment vessel or in the reactor building outside the containment vessel the normal reactor building ventilation system (742) is isolated and the off-gas filter system (749) is activated. This automatic activating is connected with high radiation signals in the reactor service hall. The removal of iodine compounds with this system is nearly 100 percent. (Nevander, 2008, s. 9)

During the emergency situations the fresh air to the main control room goes through charcoal filters. The combustible gases from the reactor containment vessel after postulated accidents are removed by the containment vessel gas treatment system (741). The system 741 is divided into two subsystems for recombination of oxygen and hydrogen in the containment atmosphere. The systems are designed so that a single failure would not prevent the system to perform its safety function. (Nevander, 2008, s. 9)

3 APROS CODE THEORETICAL BACKGROUND

Advanced Process Simulator (APROS) is multifunctional software for dynamic simulations and modeling of the different processes and power plants. It has been developed by Imatran Voima Power Engineering Ltd (IVO PE) and Technical Research Centre of Finland (VTT) since 1986. The IVO PE belongs to Fortum Oyj at present. The APROS simulation environment includes tools, solution algorithms and model libraries for full-scale modeling and simulation of dynamic processes. Originally the APROS was developed for demanding use in the nuclear power plant simulators. At present the main APROS simulation objectives are the nuclear power plants, pulp and paper mills and combustion power plants. It can be also used for the desalination models, solid oxide fuel cells and district heating. APROS includes not only the process components, also the automation and electrical systems can be modeled. During the last 20 years the APROS software has been sold to 26 different countries for numerous projects. (Liuko, 2010, s. 1-2)

The APROS includes tools, solution algorithms and model libraries for full scope modeling and simulation of power plant processes. The process automation and electrical system are also available. The APROS simulation environment can be configured to meet for the design, analysis and training simulator applications. The APROS includes the model libraries based on the chemical and physical relations. The model libraries provide for fast and accurate dynamic simulation of conventional and nuclear power plant processes. (Laakso, 2011)

Process components in the APROS simulation environment are software tools that create and combine the mechanistic model building blocks such as nodes and branches automatically to describe the real components. Process components like pipes, heat exchangers and tanks are included in the general purpose process components. Most of the process components can build blocks out of any of the available thermal hydraulic models. The different thermal hydraulic models can be used in the same pipe network. Even the interconnection module is created

automatically; the user is responsible of locating the interconnection. (Laakso, 2011)

3.1. Governing equations

The six-equation model calculation is based on the conservation equations of mass, momentum and the total energy of the liquid on steam phases. If the process contains non-condensable gas, the equation of non-condensable gas is also needed. There are a total of six partial differential equations used, when equations are applied to the liquid and gas phases: The equations of mass (1), momentum (2) and energy (3) have the following forms (Hänninen & Ylijoki, 2008, s. 17):

$$\frac{\partial \alpha_k \rho_k}{\partial t} + \frac{\partial \alpha_k \rho_k u_k}{\partial z} = \Gamma_k \tag{1}$$

$$\frac{\partial \alpha_k \rho_k \mu_k}{\partial t} + \frac{\partial \alpha_k \rho_k u_k^2}{\partial z} + \alpha_k \frac{\partial p}{\partial z} = \Gamma_k u_{ik} + \alpha_k \rho_k \vec{g}$$
$$+F_{wk} + F_{ik} + f_k(v, pu, fl) \tag{2}$$

$$\frac{\partial \alpha_k \rho_k h_k}{\partial t} + \frac{\partial \alpha_k \rho_k u_k h_k}{\partial z} = \alpha_k \frac{\partial p}{\partial t} + \Gamma_k h_{ik} + q_{ik}$$
$$+q_{wk} + F_{ik} u_{ik} + \alpha_k \rho_k u_k \vec{g} \tag{3}$$

In equations 1, 2 and 3:

k	is subscript to gas or liquid	[-]
α_k	is volume fraction of phase k	[-]
ρ_k	is density of phase k	[kg/m^3]
u_k	is velocity of phase k	[m/s]
Γ_k	is mass change rate between phases	[kg/m^{3}s]
u_{ik}	is velocity difference of phases	[m/s]
$\vec{g}$	is velocity of gas	[m/s]
F_{wk}	is friction between wall and phase k	[N/m^3]

F_{ik}	is friction between phases	[N/m^3]
$f_k(va, pu, fl)$	is function to take into account the effect of valves (va), pumps (pu) and form loss (fl) coefficient describing different obstacles in the flow channel.	[kg/m^{3}s]
h_k	is enthalpy of phase k	[J/kg]
h_{ik}	is enthalpy difference of phases	[J/kg]
q_{ik}	is heat flow between phases	[W/m^3]
q_{wk}	is heat flow between wall and phase	[W/m^3]

The function f_k contains all the quantities that are not related to the basic thermal hydraulic solutions. The one-dimensional form equations include an unsteady term (time derivate), a convection term (space derivate) and the right-hand source term. The equations are discretized with the respect to time and space, and the nonlinear terms are linearized. This causes different control volumes to mass and energy than with the momentum. The pressure, enthalpy and density of both phases are called the state variables. The state variables are calculated in the middle of the mass mesh cells. The first-order upwind scheme is normally utilized to calculate enthalpies. The gas and liquid velocities are called the flow-related variables and are calculated at the border of the two mass mesh cells. The quantities are averaged over the whole mesh. The case of stratified flow is only emerged when the liquid head is taken separately into account in the pressure solution. (Hänninen & Ylijoki, 2008, s. 17-18)

The basic solution algorithm is that the liquid and gas velocities in the mass equation are substituted by the velocities from the linearized momentum equation. The linearization in the momentum equation has been made only for the local momentum flow. The upwind momentum flow uses the previous values of iteration and the phase densities are linearized with regard to pressure. The equation used for density linearization is (Hänninen, 2009, s. 23):

$$\rho_k^n = \rho_k + \frac{\partial \rho_k}{\partial p}(p^n - p) \quad (4)$$

Where,

n	refers to the unknown quantity	[-]
p	is pressure	Pa

By using the density linearization for eliminating the phase velocities with the linearized momentum equation, the linear group where the only unknown variables are pressures is formed. The density derivatives have to be positive to complete the solving process. In addition, the phase densities obtained from the table as a function of pressure and enthalpy must increase monotonically with the increasing pressure. For liquid density it is sometimes difficult to fulfill the condition of increasing density with increasing pressure because it does not change as much as the function of pressure, but depends more strongly on enthalpy. To solve this problem the tabulated pressure values must be quite dense at low pressure. (Hänninen, 2009, s. 23)

The velocities are calculated after the pressures have been solved. The velocities are calculated from linearized phase momentum equations by using the calculated pressures. After the velocities are calculated, the void fractions are calculated from the mass equations by using the new velocities. The phase enthalpies are calculated by using the discretized phase energy equations. The boron concentrations can be necessary for the nuclear applications. The boron concentrations are solved by using the mass flows of the liquid. The main assumption with the boron concentration calculations is that boron stays always dissolved in the liquid phase and the boron effect on the material properties is omitted. (Hänninen, 2009, s. 23-24)

The main idea of APROS applies solution method is that the linear equation groups of pressures, void fractions and phase enthalpies are solved one after the other. There is a function of the densities and other water material properties that uses solved pressures and enthalpies. The solutions of the interfacial friction, heat

transfer, wall friction and wall heat transfer are also calculated. The iteration is repeated as many times as the mass errors from mass balance equation of both phases have been converged. The user can define the criterions of the convergence. The solution progress is presented in figure 3.1. (Hänninen, 2009, s. 24-25)

The gas and liquid mass errors are calculated from the gas liquid and mass equations after every iteration step. The new values for densities, void fractions and velocities are used. The user can define the calculation time step. Typically the maximum time step of 0.001 to 0.1 second is used. The relative mass error limit is usually 10^{-5}. If the mass error is over the limit, the time step is reduced to half of the presently used time step and the iteration is restarted from the previous converged time step. In case of a very fast pressure and temperature change, the calculation can fail mass criterion and is not converged. In case of fast transients the maximum iteration time step should be 0.001 s or less. It is possible to change the iteration time step during the calculation. By using shorter time step during the fast changes and longer time step during the steadier situation, the calculation can be more effective. (Hänninen, 2009, s. 25)

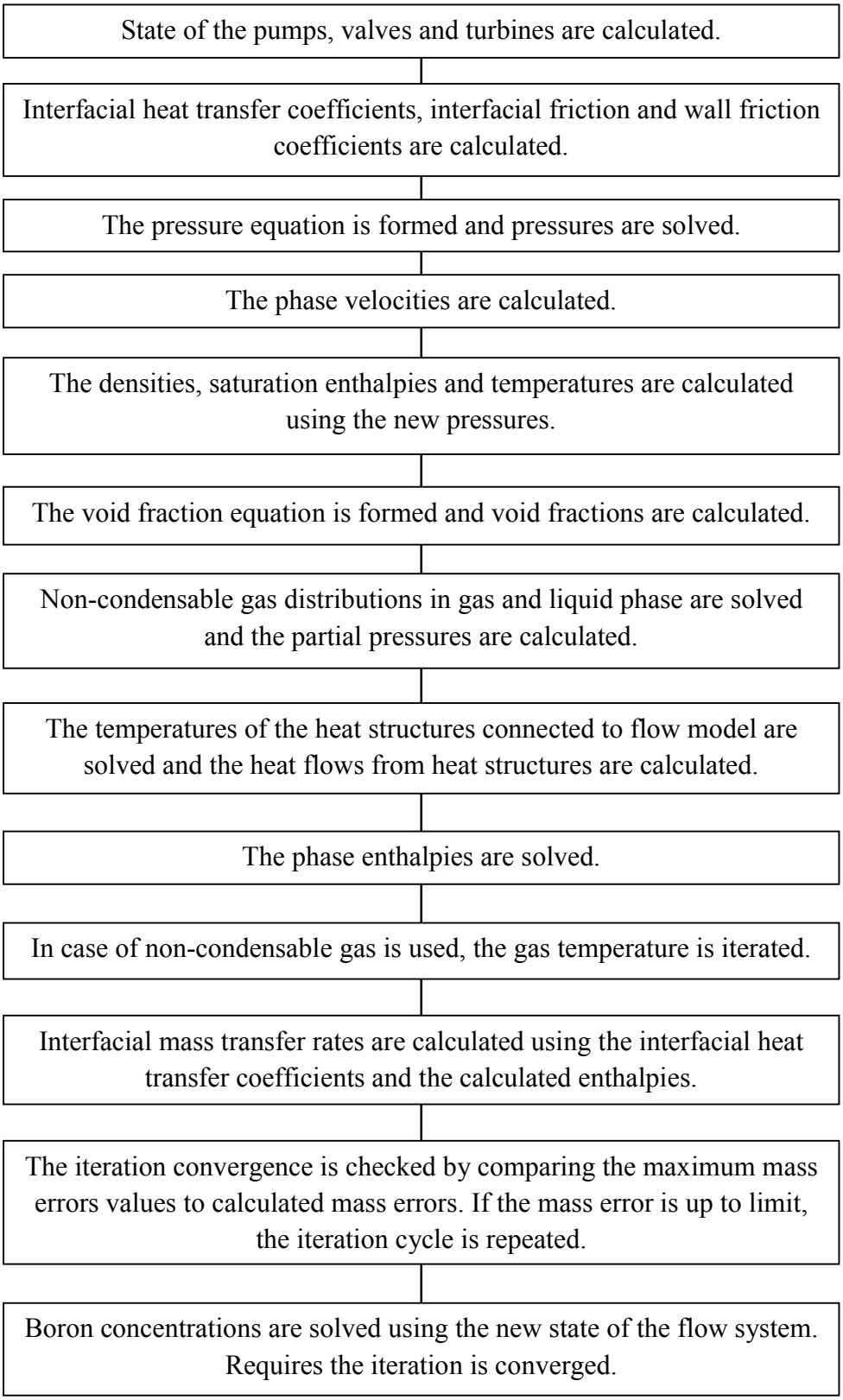

Figure 3.1. The solution progress of APROS

There are four different non-condensable gases simulated in the two-fluid APROS model. The simulated gases are air, nitrogen, helium and hydrogen. The necessary material properties for each gas are calculated using the function of temperature. The density of the gas is calculated by using the ideal gas equation. The non-condensable gas can be a part of the gas phase or it can be a dissolved component in the liquid phases. In the gas phase, the steam and the non-condensable gas forms the homogenous mixture and have the same temperature and velocity. The density of the non-condensable gas in the gas phase is solved after the pressures, velocities and void fractions. When using the dissolved gas model of the six-equation model, the maximum value of concentration of the dissolved gas is calculated using functions of pressure and temperature. The maximum and real concentration solution is based on the released gas flow calculation. The model takes into account the released gas in the gas phase solution and in the concentration solution of the dissolved gas. If the real concentration doesn't reach the maximum and the gas phase includes more of the non-condensable gas with the higher gas partial pressure than the corresponding partial pressure of dissolved gas, the gas is progressively dissolved and the small gas flow from gas to liquid is calculated. (Hänninen, 2009, s. 33-34)

The solution of non-condensable gas is related to the pressure flow solution of the six-equation model. The mass equation for the non-condensable gas can be written as (Hänninen, 2009, s. 34):

$$\partial \frac{(\alpha_g \rho_{nc})}{\partial t} + \frac{\partial(\alpha_g \rho_{nc} u_g)}{\partial z} = \dot{m}_r \tag{5}$$

Where,

α_g	is volume fraction of gas	[-]
ρ_{nc}	is density of non-condensable gas	[kg/m^3]
u_g	is velocity of gas	[m/s]
$\dot{m}_r$	is the released or dissolved mass flow of non-condensable gas	[kg/s]

Liquid and gas equations are connected by the following relationships (Hänninen & Ylijoki, 2008, s. 18):

$$\alpha_g = 1 - \alpha_l = \alpha \tag{6}$$

$$\Gamma_g = -\Gamma_l = \Gamma \tag{7}$$

$$F_{i,l} = -F_{i,g} = F_i \tag{8}$$

$$u_{i,g} = u_{i,l} = u_i \tag{9}$$

In Equations (6) to (9):

α_l	is volume fraction of liquid	[-]
Γ_g	is mass change of gas	[kg/m^{3}s]
Γ_l	is mass change of liquid	[kg/m^{3}s]
$F_{i,l}$	is interfacial friction of liquid	[N/m^3]
$F_{i,g}$	is interfacial friction of gas	[N/m^3]
F_i	is interfacial friction	[N/m^3]
$u_{i,g}$	is interfacial velocity of gas	[m/s]
$u_{i,l}$	is interfacial velocity of liquid	[m/s]
u_i	is interfacial velocity	[m/s]

3.2. Thermal hydraulic modeling principles

The thermal hydraulic model library contains three different thermal hydraulic models for one dimensional two-phase flow. The three-equation model which is generally called the homogenous model is based on the momentum, mass and energy equations. The five-equation model contains the separated equations of the mass and energy for the fluid and gas and the momentum equation for mixture of the fluid and gas. The pressures, volume flows and enthalpies of the phases are solved from the equations. There is also a correlation package for the calculation

of friction and heat transfer. The calculation speed is relatively fast also in the large applications because no iterations are needed. The six-equation model contains separated equations of mass, energy and momentum for both fluid and gas. The equations are connected with the empirical correlations describing various phenomena of the two-phase flow like heat transfer and friction for interface. The pressures, velocities, volume fractions and enthalpies of each phase are solved using an iterative procedure from the discretized equations. The six-equation model is well suitable for design calculations and safety analysis which requires simulation with dense nodalization in the fast transients. (Puska, 1999, s. 29-30)

The five- and six-equations models are usually used for the two-phase calculations on the primary system and the homogenous model for the turbine system. Generally the homogeneous model is a working solution for the auxiliary systems, the feedwater systems and the main steam systems after the turbine control valve. The homogeneous model can describe the phase change due to flashing or condensation, but not handle different phase velocities. The five- and six-equations models are suitable for the primary circuit of the nuclear power plant. (APROS, 2011, s. 1-2)

3.3. Principles of one-dimensional two energy group model

The APROS includes the one- and three-dimensional core neutronics models. Both models have six delayed neutron groups and two energy groups. The diffusion equations for fast flux ϕ_1 and thermal flux ϕ_2 (Puska, 2006, s. 5):

$$\frac{\partial}{\partial t}\frac{1}{\nu_1}\phi_1 - \nabla \cdot D_1\nabla\phi_1 + \sum_{b1}\phi_1 = (1-\beta)S_f + \sum_j \lambda_j C_j \qquad (10)$$

$$\frac{\partial}{\partial t}\frac{1}{\nu_2}\phi_2 - \nabla \cdot D_2\nabla\phi_2 + \sum_{b2}\phi_2 = \sum_{12}\phi_1 \qquad (11)$$

In equations 1 and 2,

ν_1	is fast velocity	[m/s]
ν_2	is thermal velocity	[m/s]
D_1	is fast diffusion coefficient	[cm]
D_2	is thermal diffusion coefficient	[cm]
$\sum_{b1}$	is sum of fast absorption cross section of the thermal group, control rods and boron concentration	[1/cm]
$\sum_{b2}$	is the sum of thermal absorption cross section of the control rods, soluble poisons and nuclear poisons	[1/cm]
$\sum_{12}$	is the cross section for removal from fast to thermal flux	[1/cm]
β	is the total fraction of delayed neutrons	[pcm]
λ_j	is the decay constant of the delayed neuron precursor groups	[s]
C_j	is the concentration of the precursor group j	[ppm]

The fission source S_f is expressed in equation as (Puska, 2006, s.5)

$$S_f = \nu\sum_{f1}\phi_1 + \nu\sum_{f2}\phi_2 \quad (12)$$

Where,

$\nu\sum_{f1}$	is the fast fission production cross	[1/s]
$\nu\sum_{f2}$	is the thermal fission production cross section	[1/s]

When the fission source equation (6) is taken into account, the diffusion equations for fast flux ϕ_1 and thermal flux ϕ_2 becomes (Puska, 2006, s. 5):

$$\frac{\partial}{\partial t}\frac{1}{v_1}\phi_1 - \nabla \cdot D_1\nabla\phi_1 + \sum_{b1}\phi_1 = (1-\beta)\cdot$$

$$\left(\nu\sum_{f1}\phi_1 + \nu\sum_{f2}\phi_2\right) + \sum_j \lambda_j C_j + S_o \quad (13)$$

$$\frac{\partial}{\partial t}\frac{1}{v_2}\phi_2 - \nabla \cdot D_2\nabla\phi_2 + \sum_{b2}\phi_2 = \sum_{12}\phi_1 \quad (14)$$

In the APROS one- and three-dimensional solution the time derivate of the flux is approximated as (Puska, 2006, s. 6):

$$\frac{\partial}{\partial t}\frac{1}{v_1}\phi_1 \cong \frac{1}{v_1}\frac{\partial}{\partial t}\phi_1 \; ; i = 1{,}2 \quad (15)$$

The time derivate of the flux can be presented as (Puska, 2006, s. 6):

$$\frac{\partial}{\partial t}\phi_1 = \frac{\phi_{i,t} - \phi_{i,t-1}}{\Delta t} \; ; i = 1{,}2 \quad (16)$$

Where,

Δt is time interval between time steps from t-1 to t section [s]

The second derivate discretized form can expressed as (Puska, 2009a, s. 5):

$$\frac{\partial^2\phi_i}{\partial z^2} = \frac{\phi_{i,l+1} - 2\phi_{i,l} + \phi_{i,l-1}}{(\Delta z)^2}; \; i = 1{,}2 \quad (17)$$

In the equation (17) the equal mesh spacing Δz has been assumed for simplicity.

In the discretized form of the second derivate without simplicity can be expressed as (Nuutinen, 2009, s. 12):

$$\frac{\partial^2 \phi_i}{\partial z^2} = \frac{2\phi_i^{(n+1)}}{h(h+k)} - \frac{2\phi_i^{(n)}}{hk} + \frac{2\phi_i^{(n-1)}}{k(h+k)};\ i = 1,2 \tag{18}$$

Where,

k is length of mesh spacing

h distance between the center of the two nodes

With equations (10), (11) and (12), equations (13) and (14) can be written as:

$$\frac{1}{\nu_1}\frac{\phi_1^{(n)} - \phi_{1,t-1}^{(n)}}{\Delta t} - D_1\left(\frac{2\phi_1^{(n+1)}}{h(h+k)} - \frac{2\phi_1^{(n)}}{hk} + \frac{2\phi_1^{(n-1)}}{k(h+k)}\right) +$$

$$\sum_{b1}\phi_1^{(n)} = (1-\beta)\left(\nu\sum_{f1}\phi_1^{(n)} + \nu\sum_{f2}\phi_2^{(n)}\right) + \sum\lambda_j C_j + S_0 \tag{19}$$

$$\frac{1}{\nu_2}\frac{\phi_2^{(n)} - \phi_{2,t-1}^{(n)}}{\Delta t} - D_2\left(\frac{2\phi_2^{(n+1)}}{h(h+k)} - \frac{2\phi_2^{(n)}}{hk} + \frac{2\phi_2^{(n-1)}}{k(h+k)}\right) +$$

$$\sum_{b2}\phi_2^{(n)} = \sum_{12}\phi_1^{(n)} \tag{20}$$

By organizing the terms of fast and thermal fluxes ϕ_1 and ϕ_2 equations (19) and (20) can be formed as:

$$-\frac{2D_1}{k(h+k)}\phi_1^{(n-1)} - \left(\frac{1}{\nu_1\Delta t} + \frac{2D_1}{hk} + \sum_{b1} - (1-\beta)\nu\sum_{f1}\right)\cdot$$
$$\phi_1^{(n)} - \frac{2D_1}{k(h+k)}\phi^{(n+1)} - (1-\beta)\nu\sum \qquad \phi_2^{(n)} =$$
$$\sum\lambda_j C_j + S_0 + \frac{1}{\nu_1\Delta t}\phi_{1,t-1}^{(n)} \tag{21}$$

$$\frac{2D_2}{k(h+k)}\phi_2^{(n-1)} + \left(\frac{1}{\nu_2\Delta t} + \frac{2D_2}{hk} + \sum_{b2}\right)\phi_2^{(n)} -$$
$$\frac{2D_2}{h(h+k)}\phi_2^{(n+1)} - \sum_{12}\phi_1^{(n)} = \frac{1}{\nu_2\Delta t}\phi_{2,t-1}^{(n)} \tag{22}$$

The equations (21) and (22) can be formed as matrix form. When the matrix terms include only one nodalisation point, the equations can be formed as:

$$\begin{bmatrix} \frac{2D_1}{k(h+k)} & 0 \\ 0 & \frac{2D_2}{k(h+k)} \end{bmatrix} \begin{bmatrix} \phi_1^{n-1} \\ \phi_2^{n-1} \end{bmatrix} +$$

$$\begin{bmatrix} \frac{1}{\nu_1 \Delta t} + \frac{2D_1}{hk} + \sum_{b1} - (1-\beta)\nu\sum_{fi} & -(1-\beta)\nu\sum_{f2} \\ -\sum_{12} & \frac{1}{\nu_2 \Delta t} + \frac{2D_2}{hk} + \sum_{12} \end{bmatrix}$$

$$\begin{bmatrix} \phi_1^{(n)} \\ \phi_2^{(n)} \end{bmatrix} + \begin{bmatrix} \frac{2D_1}{h(h+k)} & 0 \\ 0 & \frac{2D_2}{h(h+k)} \end{bmatrix} \begin{bmatrix} \phi_1^{n-1} \\ \phi_2^{n-1} \end{bmatrix} =$$

$$\begin{bmatrix} \sum \lambda_j C_j + \frac{1}{\nu_1 \Delta t} \phi_{t,t-1}^{(n)} + S_0 \\ \frac{1}{\nu_2 \Delta t} \phi_{2,2-1}^{(n)} \end{bmatrix} \tag{23}$$

The equation (23) can be shown as the block-tridiagonal matrix form by using abbreviations. The used abbreviations are showed in equation (24) and the block-tridiagonal matrix form in equation (25).

$$\begin{aligned} A_{11} &= \frac{2D_1}{k(h+k)} \\ A_{12} &= 0 \\ A_{13} &= 0 \\ A_{14} &= \frac{2D_2}{k(h+k)} \end{aligned} \tag{24}$$

$$\bar{A}\bar{\phi}^{(n-1)} + \bar{B}\bar{\phi}^{n} + \bar{\mathrm{C}}\bar{\phi}^{n+1} = \bar{S}^{n} \tag{25}$$

3.4. Principles of three-dimensional two energy group model

The three dimensional core neutronics is solved by integrate equations (10) and (11) over volume V_l of a single node l (Puska, 2009b, s. 5):

$$\int_{V_l} \frac{1}{\nu_2} \frac{\phi_{1,t} - \phi_{1,t-1}}{\Delta t} dV - \int_{V_l} \nabla \cdot D_1 \nabla \phi_1 dV + \int_{V_l} \Sigma_{b1} \phi_1 dV = \quad (26)$$

$$\int_{V_l} (1-\beta)\left(\nu\Sigma_{fl}\phi_1 + \nu\Sigma_{f2}\phi_2\right) dV + \int_{V_l} \sum_j \lambda_j C_j dV$$

$$\int_{V_l} \frac{1}{\nu_2} \frac{\phi_{2,t} - \phi_{2,t-1}}{\Delta t} dV - \int_{V_l} \nabla \cdot D_2 \nabla \phi_1 dV + \int_{V_l} \Sigma_{b2} \phi_2 dV = \quad (27)$$

$$\int_{V_l} \Sigma_{12} \phi_1 dV$$

Equations (26) and (28) can be solved into form (Puska, 2009b, s. 5):

$$\left[\overline{\frac{1}{\nu_1} \frac{\phi_{1,t} - \phi_{1,t-1}}{\Delta t}}\right] V_l - \int_{V_l} \nabla \cdot D_1 \nabla \phi_1 dV + \left[\overline{\Sigma_{b1}\phi_1}\right] V_l = \quad (28)$$

$$\left[\overline{(1-\beta)(\nu\Sigma_{fl}\phi_1 + \nu\Sigma_{fl}\phi_2)}\right] V_l + \left|\overline{\sum_j \lambda_j C_j}\right| V_l$$

$$\left[\overline{\frac{1}{V_2} \frac{\phi_{2,t} - \phi_{2,t-1}}{\Delta t}}\right] V_l - \int_{V_l} \nabla \cdot D_2 \nabla \phi_2 dV + \left[\overline{\Sigma_{b2}\phi_2}\right] V_l = \quad (29)$$

$$\left[\overline{\Sigma_{b2}\phi_2}\right] V_l$$

Where the bar signify average over volume V_l, for example

$$[\overline{\Sigma_{b2}\phi_2}] = \frac{1}{V_l}\int_{V_l} \Sigma_{b2}\phi_2 dV \tag{30}$$

The volume integral can be transformed to a surface integral over the bounding surface A_l of the node V_l by using the divergence theorem. The second term on the left side in equations (10) and (11) can be presented as (Puska, 2009b, s. 5):

$$\int_{V_l} \nabla \cdot D_i \nabla \phi_i dV = \int_{A_l} D_i \overline{n} \cdot \nabla \phi_i d\,A \tag{31}$$

For simplicity it is assumed that the node 1 and all of its neighbor nodes m are identical in size and shape. The same size and shape means also that the distance between the center of the two nodes, h_{lm}, is equal to constant node width in the 1-m -direction. This simplicity is only assumed to make this presenting easier. The program can actually take into account different distances between the center of the nodes in various directions. Let the fast or thermal flux at the centre of the node 1 be ϕ_{il} where i=1 in case of fast flux and i=2 in case of thermal flux. In proportion let ϕ_{im} be the thermal or fast flux at the centre of the node m and ϕ_{ilm} be corresponding thermal or fast flux at the interface along the line connecting the node centers. By using these identifications the approximations used in the preceding equations can be presented as (Puska, 2009b, s. 6):

$$-D_i \overline{n} \cdot \nabla \phi_i = -\frac{1}{2}\left(D_{im} \frac{\phi_{im} - \phi_{ilm}}{\frac{h_{lm}}{2}} + D_{il} \frac{\phi_{ilm} - \phi_{il}}{\frac{h_{lm}}{2}} \right) \tag{32}$$

According to the continuity condition the following equation can be presented as (Puska, 2009b, s. 6):

$$\phi_{ilm} = \frac{D_{il}\phi_{il} + D_{im}\phi_{im}}{D_{il} + D_{im}} \tag{33}$$

The surface integration in equation (31) corresponds to multiplying the equation for quadrilateral lattice by the factor (Puska, 2009b, s. 6):

$$A_{lm} = \frac{V_l}{h_{lm}} = \frac{V_m}{h_{lm}} \tag{34}$$

For hexagonal lattice the surface integration corresponds to multiplying the equation by the factor (Puska, 2009b, s. 6):

$$A_{lm} = \frac{2V_l}{3h_{lm}} = \frac{2V_m}{3h_{lm}} \tag{35}$$

In case of the quadrilateral lattice the same expression is used in all directions. In case of the hexagonal lattice the expression for the quadrilateral lattice is used for the vertical neighbor nodes and the expression for hexagonal lattice is used for the six horizontal neighbor nodes.

By performing the surface integration for the terms of equation (31) and by dividing the entire fast and thermal flux equations by the common factor V_l the final equations obtained by the fuel assemblies can be presented as in equation (36) and (37). In the equation (36) the terms containing ϕ_{il} are placed to the left side and the rest to the right side. (Puska, 2009b, s. 6-7)

$$\phi_{1l} = \left[\frac{1}{\nu_1 \Delta t} \phi_{1L,t-1} + \sum_n \frac{2D_{1l}D_{1n}}{h_{ln}^2 (D_{1l} + D_{1n)}} \phi_{1n} + (1-\beta)\nu\Sigma_{f2}\phi_{2l} + \sum_j \lambda_j C_j \right] \cdot \left[\frac{1}{\nu_1 \Delta t} + \sum_n \frac{2D_{1l}D_{1n}}{h_{ln}^2 (D_{1l} + D_{1n})} + \Sigma_{b1} - (1-\beta)\nu\Sigma_{fl} \right]^{-1} \tag{36}$$

$$\phi_{1l} = \left[\frac{1}{\nu_2 \Delta t} \phi_{2L,t-1} + \sum_n \frac{2D_{2l}D_{2n}}{h_{ln}^2 (D_{2l} + D_{2n})} \phi_{2n} + \Sigma_{12}\phi_{1l} \right] \cdot \left[\frac{1}{\nu_2 \Delta t} + \sum_n \frac{2D_{2l}D_{2n}}{h_{ln}^2 (D_{2l} + D_{2n})} + \Sigma_{b2} \right]^{-1} \tag{37}$$

In proportion for the hexagonal fuel assemblies (Puska, 2009b, s. 7):

$$\phi_{1l} = \left[\frac{1}{\nu_1 \Delta t}\phi_{1l,t-1} + \sum_m \frac{4D_{1l}D_{1m}}{3h_{lm}^2(D_{1l}+D_{1m})}\phi_{lm} + \sum_n \frac{2D_{1l}D_{1n}}{h_{ln}^2(D_{1l}+D_{1n})}\phi_{ln} + (1-\beta)\nu\Sigma_{f2}\phi_{2l} + \sum_j \lambda_j C_j\right] \cdot \left[\frac{1}{\nu_1 \Delta t} + \sum_m \frac{4D_{1l}D_{1m}}{3h_{lm}^2(D_{1l}+D_{1m})} + \sum_n \frac{2D_{1l}D_{1n}}{h_{ln}^2(D_{1l}+D_{1n)}} + \Sigma_{b1} - (1-\beta)\nu\Sigma_{f1}\right]^{-1} \quad (38)$$

$$\phi_{1l} = \left[\frac{1}{\nu_2 \Delta t}\phi_{2l,t-1} + \sum_m \frac{4D_{2l}D_{2m}}{3h_{lm}^2(D_{2l}+D_{2m})}\phi_{2m} + \sum_n \frac{2D_{2l}D_{2n}}{h_{ln}^2(D_{2l}+D_{2n})}\phi_{2n} + \Sigma_{12}\phi_{1l}\right] \cdot \left[\frac{1}{\nu_2 \Delta t} + \sum_m \frac{4D_{2l}D_{2m}}{3h_{lm}^2(D_{2l}+D_{2m})} + \sum_n \frac{2D_{2l}D_{2n}}{h_{ln}^2(D_{2l}+D_{2n)}} + \Sigma_{b2}\right]^{-1} \quad (39)$$

Using the first-order discretisation for the time-derivate, the delayed neutron precursor concentration is obtained from the equation (Puska, 2009b, s. 7):

$$\frac{\partial}{\partial t}C_j = \beta_j\left(\nu\Sigma_{f1}\phi_1 + \nu\Sigma_{f2}\phi_2\right) - \lambda_j C_j \quad (40)$$

Where β_j is fraction of delayed neutrons in precursor group j.

3.5. General modeling capabilities

There are three different neutronics models in the APROS. The classical point kinetics solution should be used only when it is specially required. It is not used to calculate the nuclear power plants because the 1D-model is as fast and better in the physical description. The point kinetics solution does not contain similar variety of options as the 1D- and 3D-models and has a limited application range. The 1D- and 3D-model obtain node the wise feedback from the five- or six-equation thermal hydraulics node. The modeled reactor feedbacks are (Puska, 2006):

- Fuel temperature
- Coolant density
- Coolant void fraction
- Coolant temperature
- Coolant boron concentration
- Control rod position from automation system

The decay heat calculations can be done by the different options for the various purposes. The available options are (Puska, 2006):

- No decay heat
- Constant decay heat 3%
- User given decay heat power curse versus time
- Recommended ANSI-bases decay function with possibility to reset the decay heat according to the power level

The cross section data has to be generated before using any reactor models. Usually the cross section data is generated at VTT. The 3-D cross section data is always generated before the 1-D cross sections because the 1-D model cross sections have to be condensed from the 3-D cross sections. The comparison between the one- and three-dimension model features is presented in table 3.1. (Puska, 2006)

Table 3.1. APROS model features

Property	**1D**	**3D**
Equations	Two energy groups, six delayed neutron groups	Two energy groups, six delayed neutron groups
Solution	Direct, Bloc-Tri-diagonal	Iterative, Gauss-Seidel
Cross-section data	Condensed data for 1D	3D data
Description	Average behavior	Local phenomena
Accuracy	Core average	Node wise
Consistency	Neutronics as a patch on the electric heater, many different components	Originally designed as a nuclear reactor model
Calculation speed	Very fast	Real time can be reached

4 APROS CODE WITH OLKILUOTO 1 AND 2 MODEL

The APROS thermal hydraulic code and the nuclear library units have been validated and verified for use in light water BWR-units such as OL1 and OL2. The validation includes the cold startup and the shutdown procedures, the normal operating modes, the load rejections and various accidents & emergency situations. The APROS code validation and verification procedure is repeated before each new APROS updating. (APROS, 2011, s. 1)

4.1. Plant specific model

The APROS simulation model of OL1/OL2-units has been created in many different stages. The general boiling water reactor model was created during the TIFANY-project in 1995. The original model included only good descriptions of the reactor core and the reactor pressure vessel. Some of the most important safety systems and some other systems were also modeled, but not in detail. Since 2005 the OLI/OL2-model has been systematically updated. The reactor facility, the containment and the reactor systems have been modeled primarily by TVO. The main turbine plant has been modeled by Fortum Nuclear Service. The modeled systems are shown in table 6 in appendix 1. (Paalanen, 2009, s. 5)

4.2. Reactor and reactor systems

The modeled system 211 includes the RPV, the reactor core and many important measurement systems. The RPV dimensions and material properties have been examined by TVO in 2006. The reactor core has not been updated by TVO. The reactor core model needs to be updated before it can be used to calculate the transients in which the nuclear fuel has an important impact. The modeled parts and descriptions of the system 211 are presented in table 1 in appendix 7. The reactor pressure vessel's APROS model is presented graphically in figure 1 in appendix 8. (Paalanen, 2009, s. 17)

The system 311 includes the main steam pipelines and the inner and outer isolation valves of the containment. The critical flow is checked at the beginning

of the steam lines. The system 311 APROS models are presented graphically in figures 2 and 3 in appendix 8. There are four isolation signals to close the inner and outer isolation valves (Paalanen, 2009, s. 25):

- I-isolation
- A-isolation
- SS5-signal
- Manual isolation

The system 312 includes pipelines from the inner containment to the pressure vessel, the inner (312V1-V2) and outer (312V3-V4) feedwater system isolation valves, the heck-valves (312V9-V12) and the shut-off valves (312V5-V8). The system 312 APROS graphical models are presented in figures 4 and 5 in appendix 8. The closing signals to the valves 312V3 and 312V4 are the M-isolation, the SS5-signal and the manual closing. (Paalanen, 2009, s. 31):

The system 314 includes the steam blow-out valves 314V2-V13 and 314V19-V22. The control system of the steam blow-out system has been modeled by using the external sub-process components. The steam blow-out pipes in the drywell have been modeled as in the real plant. The steam blow out pipes in the wet well side have been modeled by using the A300/A250 pipes which are in the real plant divided into the A150 pipes. The critical flow is checked in every valve of the steam blow-out system. The steam blow-out valves can be controlled manually or with the control automation system. The system 314 APROS graphical model is presented in figure 6 in appendix 8. (Paalanen, 2009, s. 38)

The reactor protection system (516) includes two main parts, the isolation and the scram. The system 516 consist of the SS-, V-, I-, M-, E- and TB-chains. The system 516 also includes signals X1, X3 and X5. There is also the TSxD signal from the system 465. The system 516 graphical models are presented in figures 7 and 8 in appendix 8. The modeled parts and activation limits from the isolation chains are presented in table 1 in appendix 9 and the scram chains in table 1 in appendix 10. (Paalanen, 2009, s. 134-135)

4.3. Principles of 3-D core model creation

Core model creation is good to start by determine the purpose of use. The three-dimensional core model can enhance the capability of the APROS OL1/OL2 model for transient analysis and plant simulator. In case of plant simulator the real time calculation speed has to be taken into account. The number of fuel assemblies and how they are divided into the axial division define the number of neutronics nodes. In the OL1/OL2 plants the core contains 500 fuel assemblies. One fuel assembly would be realistic to divide into 25 sections. The number of neutronics nodes will then be 12500. The thermal hydraulic flow channels and how they are divided into the axial division define the number of thermal hydraulic nodes. One or more fuel assemblies can be placed into the thermal hydraulic channel. For example if two fuel assemblies are placed in one thermal hydraulic channel and thermal hydraulic channel is divided into 25 sections there will be 6250 thermal hydraulic nodes. The number of nodes has strong effect on the calculation speed. The increasing number of nodes decreases the calculation speed. The creation of the 3-D core model consists five main work phases (Puska, 2009b, s. 15-16):

1. Creation of thermal hydraulic channels
2. Creation of fuel assemblies
3. Creation of control rods
4. Creation of reflector assemblies
5. Creation of general reactor data

It is necessary to go through all five main work phases and find out all needed input values. All needed input details can be found in the three-dimensional nuclear reactor model user´s guide (Puska, 2009b). During this thesis all needed input values to build the 3D-model have been reviewed. It is recommended to create the input files by coding. A well designed code will make it possible to update the reactor core details easily. All kind of manual input creation should avoid because the probability of hidden errors increases. It is possible to make lots of hidden errors because the model can be used with unrealistic input values. All

input values and their sources must be documented if the model is used to make the safety analysis. It is also important to find out is it possible to create the cross-section data file with your knowledge and resources.

The thermal hydraulic network creating is recommended to be done with the queue files. Some component symbols can be added into the graphical user interface net for the illustration purposes. It is important to understand the purpose of all user options and find out that all input details are in the right position. For example it is possible to put the fuel input details like burnups backwards in the axial direction and the model can be still used. It is recommended to create the thermal hydraulic network and run into stable state before adding the core neutronics.

It depends on the APROS model but usually it is necessary to change other model components than reactor core also. It is recommended to increase number of calculation nodes in the reactor pressure vessel. For example if there are six recirculation pumps it will be reasonable to use six nodes instead of one. If the three-dimensional core is connected by using only one input and output node, it is possible that the calculation cannot be done. The steam dryer and the steam separator have to be checked before the core is connected into the other model. A one recommended basis of dividing is symmetry.

5 ANTICIPATED OPERATIONAL TRANSIENTS

Events with a frequency greater than 10^{-2} per annum are called anticipated operational transients. The anticipated operational transients are expected to happen during the lifetime of the plant. The anticipated transient shall not end in a serious condition at the plant, such as causing protective barriers like the fuel cladding or the reactor coolant pressure boundary to lose its function. For the transient analyses the following acceptance criteria have been determined (Rezendes, 2008, s. 8):

- No more than 0.1% of all fuel rods in the core should experience the transient dry-out.
- The capacity of the relief system shall be designed big enough to control the reactor pressure below the design pressure of the reactor coolant pressure boundary. Also any of the events shall not lead to the opening of safety valves 314V2-V5.
- Events shall not lead to water reaching the main steam line isolation valves.
- The start of the automatic depressurization system shall not happen due to any events.

The anticipated operational transients have been arranged into the nine groups of physically similar events. All modeled transients in this thesis belong to the group of pressure increase transients. These nine groups are: (Lemmetty, 2010, s. 4):

- Pressure increase transients
- Pressure decrease transients
- Feedwater flow increase/temperature decrease transients
- Loss of feedwater flow transients
- Recirculation flow increase transients
- Recirculation flow decrease transients
- Control rod withdrawal error at low power transients
- Control withdrawal error at high power transients
- Inadvertent loading transients

5.1. Pressure increase transients

The basic events which lead to a start pressure increase transient are the termination or reduction of the steam flow from the reactor pressure vessel. The reduced steam flow increases the pressure in the reactor system rapidly. The pressure increase in the RPV decreases the void fraction which results in a negative reactivity feedback. The positive reactivity increases the fission power. The higher fission power increases the prompt power to the coolant, the fuel temperature and the heat transfer from the fuel cladding to the coolant. The higher heating power to the coolant increases the boiling rate and the void fraction in the reactor core. (Rezendes, 2008, s. 26)

The fission power increase increases the neutron leakage out of the reactor core. The pressure increase increases the water saturation temperature in the reactor core. The moderator negative temperature feedback decreases the reactivity increasingly. The void fraction increase and the negative Doppler feedback effect begin to decrease the fission power. The negative Doppler feedback is the most dominant feedback in decreasing reactivity. (Rezendes, 2008, s. 26)

This is the point where the fission power reaches a maximum value and begins to decrease. The decreased heat transfer to the coolant still increases the pressure. The pressure increase decreases the void fraction and increases heat transfer from fuel to the coolant. If the reactor scram system fails to work or to get a signal from the high power or high pressure, the fission power will increase again. The typical sequence of events for the pressure increase transients is show in figure 5.1. (Rezendes, 2008, s. 26)

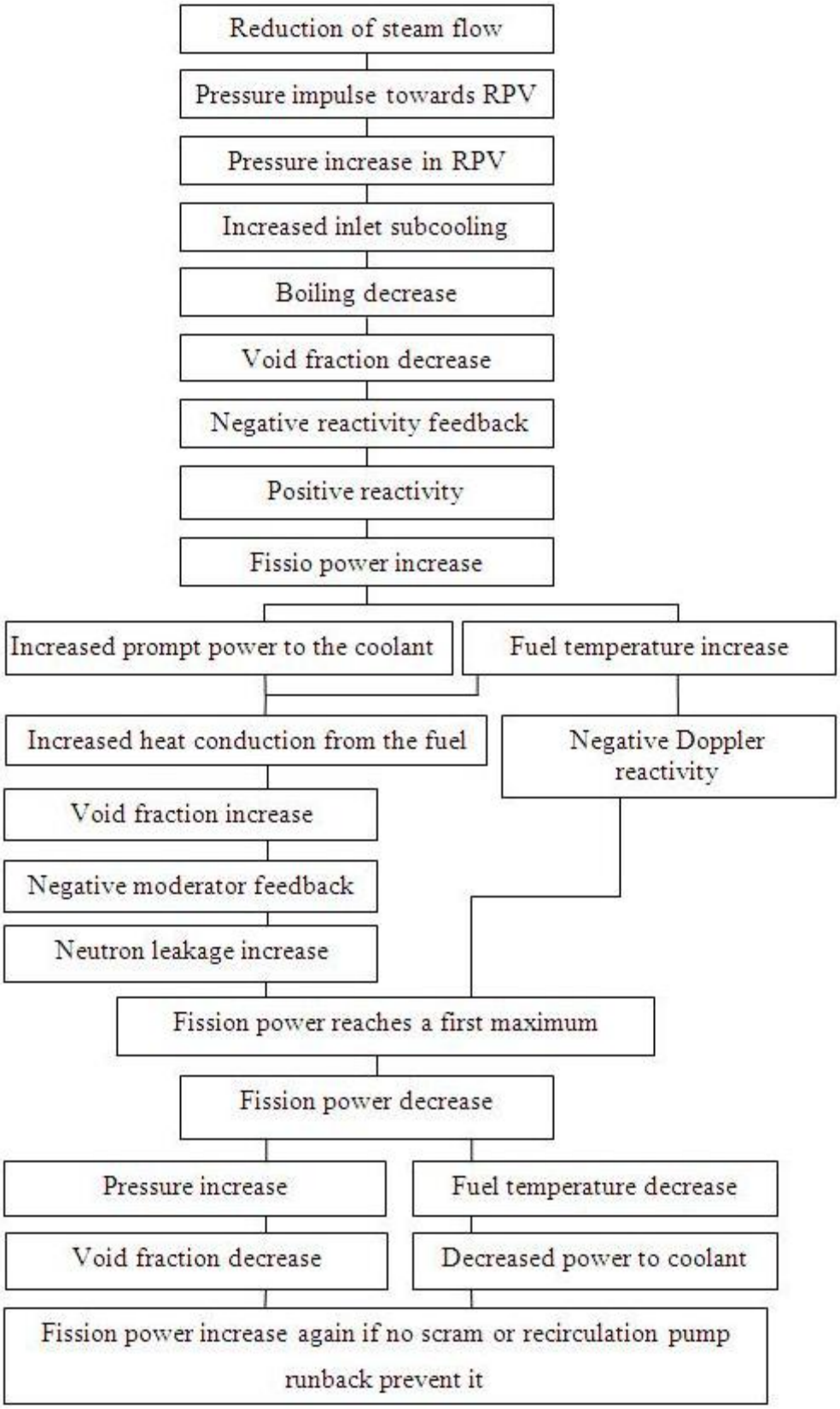

Figure 5.1. Sequence of events for the typical pressure increase transient

There are several different events that can cause the pressure increase in the pressure reactor vessel. Number of cases, names and categories are shown in table 5.1. The main phenomenon in the pressure increase transient is that the pressure increasing in the reactor vessel decreases the void fraction. The collapsing void causes a power increase because water is a more effective moderator than steam. (Rezendes, 2008, s. 15-20)

Table 5.1. Pressure increase transients

Number of cases	**Pressure increase transient name**	**Category**
1	Turbine trip with dump blocking	H2-1.1
3	Inadvertent opening of fire protection valve 416 V536	H2-1.2
3	Turbine trip with failure of one 413 dump valve	H2-1.3
3	Inadvertent closure of one 413 turbine control valve	H2-1.4
5	Inadvertent actuation of the I- or A- condition in system 516	H2-1.5
6	Inadvertent closing of one isolation valve in one main steam line	H2-1.6
13	Load rejection	H2-1.7
10	Loss of nitrogen pressure (system 754)	H2-1.8
15	Turbine trip	H2-1.9

The turbine trip with dump blocking belongs to the category H2-1.1 and means the closure of the turbine and dump valves. The closure of the turbine and dump valves causes a pressure peak into the reactor vessel. The pressure increases and the void faction decreases. The void fraction decreasing causes the power to increase. The TS-signal activates the partial scram and the power increasing absent. The TSxD-signal activates the SS11-signal and the opening of relief valves in the system 314. The SS11-signal causes the full scram and the activation of the main circulation pumps runback. The decrease of main circulation flow decreases critical power ratio. The pressure reaches a maximum in the bottom of

the reactor vessel. The reactor vessel is isolated from the turbine by the closure of the turbine and dump valves. The relief valves in the system 314 start to release steam. The pressure starts to decrease when the control rods are almost fully inserted. The pressure increase transient "The turbine trip with dump blocking" is end when all control rods are fully inserted in the core. (Rezendes, 2008, s. 15)

The opening of the fire protection valve V356 in the system 416 belongs to the category H2-1.2 and leads to the drain of oil from the turbine stop valves and the dump valves into a separate tank. The turbine stops and dump valves close generates the TSxD-signal. The events of this case would be the same as those for the event H2-1.1 "Turbine trip with dump blocking". (Rezendes, 2008, s. 16)

The turbine trip with failure of one 413 dump valve belongs to the category H2-1.3 and leads to activation of the TS-signal in the turbine protection system 465. The TS-signal activates the partial scram and closes the turbine valves. The recirculation pump runback is credited because it causes less effective heat transfer from the fuel cladding and gives a worse scenario regarding cladding integrity. The pressure in the reactor vessel increases due to the closure of turbine valves. The turbine control system compensates the pressure increase by opening the dump valves in the system 413. In this case the opening of one turbine dump valve fails. The pressure in the reactor vessel increases up to 7.4 MPa and the H4-signal actuates the SS-6 signal. Then the relief valves in the system 314 open. The SS6-signal causes the recirculation pump runback and opens the scram valves. The pressure reaches a maximum in the bottom of the reactor vessel. The reactor vessel is isolated from the turbine by the closure of turbine and dump valves. The pressure starts to decrease when the control rods are almost fully inserted. The pressure increase transient "The turbine trip with failure of one 413 dump valve" is end when all control rods are fully inserted in the core. (Rezendes, 2008, s. 16-17)

The inadvertent closure of one 413 turbine control valve belongs to the category H2-1.4. The closure of turbine control valve can occur after a fault in the turbine control system. A fault in the turbine control system also causes both dump valves

to remain closed. The events of this case would be the same as those for the event H2-1.6 "Inadvertent closure of one isolation valve in one main steam line". (Rezendes, 2008, s. 17-18)

Inadvertent actuation of the I- or A-condition in the system 516 belongs to the category H2-1.5. This event is similar to H2-1.1 "Turbine trip with dump blocking" with a difference that the I- or A-condition closes the MSIV. The MSIV starts to close when the turbine stop valves are almost fully closed. In this event the delay for SS-condition is shorter than in transient H2-1.1 where the TSxD is detected on the low oil pressure in the pilot valves. The maximum pressure is lower and transient CPR is not as worse as in the H2-1.1 event because the scram valves open earlier. Mainly the consequences for H2-1.5 are similar as those for the H2-1.1 event. (Rezendes, 2008, s. 18)

The inadvertent closure of one isolation valve in one main steam line belongs to the category H2-1.6. When the old main steam isolation valves were used the closure of one the MSIV caused a total stop of the steam flow in the steam line in issue. The closure of one the MSIV decreased the total steam flow to the turbine and increased pressure in the steam dome. The steam flow in the other steam lines increases. One of the other MSIV:s self-closed due to the steam flow reached the maximum self-closure limit. The scram activated because of the high APRM and then the relief valves opened because of the high pressure in the reactor pressure vessel. The recirculation pump runback and the control rods decrease the power. The pressure increase transient "Inadvertent closing of one isolation valve in one main steam line" is ended when all control rods were fully inserted in the core. (Rezendes, 2008, s. 18)

The new main steam isolation valves do not to the self-close due to a high steam flow. According to the test in the OL2 nuclear power plant the plant can be operated with the higher steam low by using only three main steam lines. The nominal steam flow in one main steam line is 320 kg/s. During the test the steam flow in one main steam line was 370-380 kg/s. The closure of one new MSIV decreased the total steam flow to the turbine and increased pressure in the steam

dome. The steam flow in the other steam lines increased. The pressure increase decreased the void fraction. The void fraction decrease increased fission power. The recirculation pump runback decreased the higher fission power. The full scram should not be activated. The operator can continue operate the plant with only three main steam lines or shut-down the process. (Nousiainen, 2011a, s. 1-3)

The pressure increase transient "Load rejection" belongs to the category H2-1.7. On the turbine the electrical load is abruptly removed. The speed of the turbine increases rapidly. The turbine control system closes the turbine control valves because the speed of the turbine goes over a limit value. The pressure in the steam lines start to increase immediately after the turbine control valves start to close. The turbine control system compensates the pressure increase by opening the turbine dump valves. This event is similar with event H2-1.3 "Turbine trip with failure of one 413 dump valve" except that both dump valves open. (Rezendes, 2008, s. 19)

The pressure increase transient "Loss of nitrogen pressure in the system 754" belongs to the category H2-1.8. Each of the main steam isolation valves is connected to a pilot valve in the system 754. If the nitrogen pressure drops in the system 754 the pressure in the pilot valve will decrease. The decreasing pressure in the pilot valve results in the inadvertent closure of one main steam isolation valve. This event is similar with H2-1.6 "Inadvertent closure of one isolation valve in main steam line" except that the reason for the closure of the first isolation valve is different. (Rezendes, 2008, s. 18-19)

The pressure increase transient "Turbine trip" belongs to the category H2-1.9. An electrical component failure of the turbine plant protection system (465) causes a TS-signal, which causes the closure of turbine valves, the partial scram and the recirculation pump runback. This event is similar with the event H2-1.3 except that both dump valves are opened. (Rezendes, 2008, s. 20)

5.2. Pressure decrease transients

The basic event which starts the pressure decrease transient is the loss of reactor coolant inventory, via open valves or lines. The decreasing pressure in the reactor dome causes more boiling because the water boiling temperature decreases. The increase in boiling causes the core void fraction to increase. The increasing of the void fraction causes a negativity reactivity feedback. A negativity reactivity feedback causes a decrease in fission power. The reactor power control system increases the recirculation flow and compares the fission power decrease. (Jacob, 2008b, s. 21-22)

The reactor trip signal SS5 can be activated on a high reactor liquid level H2. The SS5 signal closes all main steam isolation valves, opens the valves in the system 314 and decreases the feedwater flow. If the reactor liquid level is not high enough to activate the SS5-signal, the new steady state will be reached. The steam flow is out of control because of the open valves or lines. The plant operator can activate the plant shutdown or the high steam flow through the main isolation steam valves can lead to the self-closure of one or several MSIV. The inadvertent closure of the one MSIV causes pressure increasing transient. In Olkiluoto 1 and 2 the new inner MSIV:s have no feature to self-close due yo of the high steam flow in the main steam lines. The typical sequence of events for the pressure decrease transients is show in figure 5.2. (Jacob, 2008b, s. 21-22)

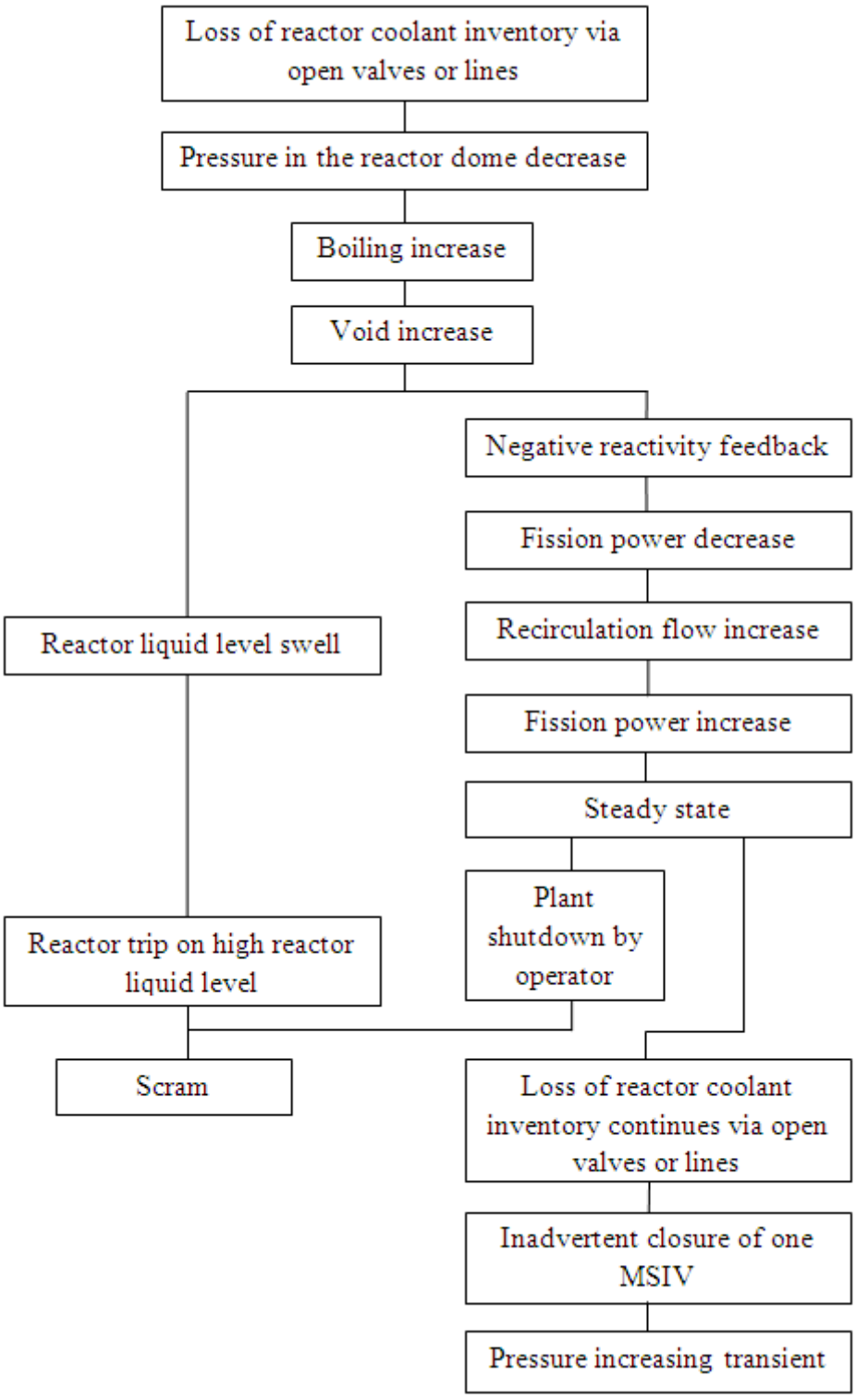

Figure 5.2. Events for the typical pressure decrease transient with old MSIV

5.3. Feedwater flow increase and temperature decrease transients

The basic event which leads to a feedwater flow increase transient is a rapid increase of the feedwater flow without the steam flow increase. The increased feedwater flow causes subcooling in the reactor. The feedwater flow temperature decrease also causes additional subcooling and the event to continues in same way as a feedwater flow increase transient. As the boiling decreases, it causes the void fraction to decrease. The void fraction increase causes on the increase of the fission power. The reactivity is positive in the core and the power control system decreases the recirculation flow rate. The transient will end to the reactor trip because of the high water level or the high neutron flux to the core coolant flow rate ratio. The typical sequence of events for the feed water flow increase and temperature decrease transients is show in figure 5.1. (Jacob, 2008a, s. 16-17)

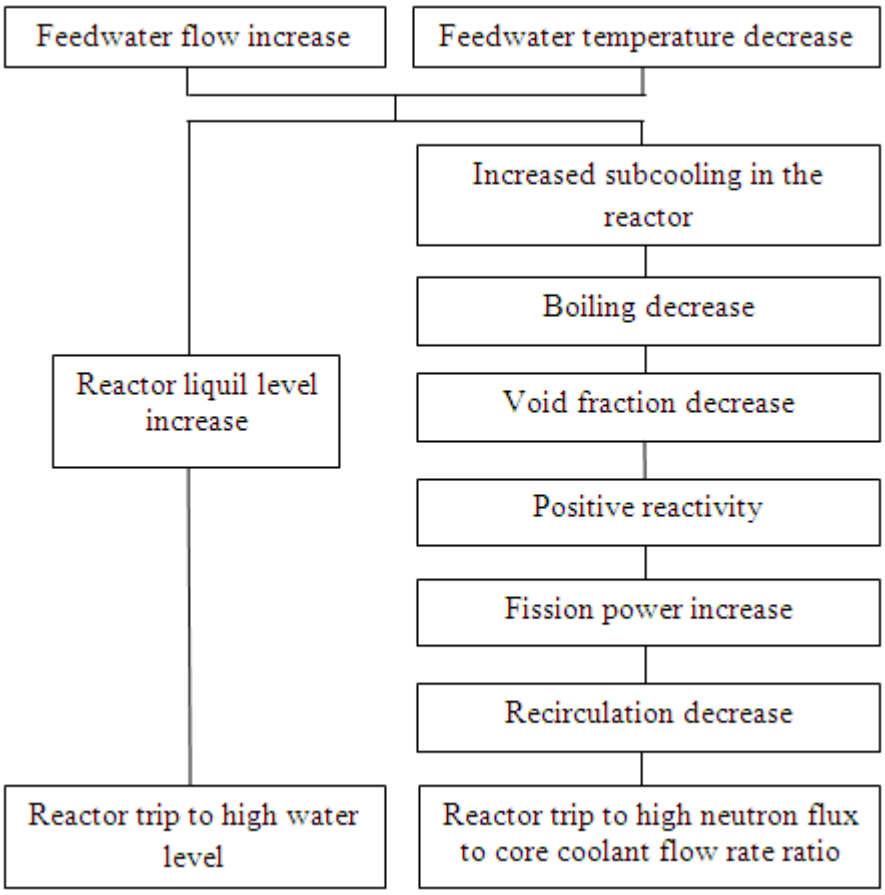

Figure 5.3. Sequence of events for the typical feedwater flow increase and temperature decrease transient

5.4. Loss of feedwater transients

The basic event which leads to a loss of feedwater transient is a rapid decrease in the feedwater flow to the reactor without the steam flow decreasing. The decreased feedwater flow causes the reactor vessel liquid level to decrease. The reactor vessel liquid level decreases under a limit L1 and the reactor power control system decreases the recirculation flow. The recirculation flow decrease causes the void fraction increasing. The reactor power decreases but the reactor vessel liquid level continues to decrease. The reactor vessel level continues to decrease and results as a low level reactor trip signal SS4 at a level set point of L2. The SS4 signal also starts the auxiliary feedwater system and the water injection into the reactor vessel downcomer with two pumps. The reactor vessel liquid level goes under a limit L3 and the two remaining subsystems in the auxiliary feedwater system start to pump water into the upper plenum. The reactor stabilizes with the reactor shut down. The typical sequence of events for the loss of feedwater transients is show in figure 5.4. (Jacob & Wallgren, 2008, s. 19-20)

5.5. Recirculation flow decrease transients

The basic event which leads to a recirculation flow decrease transient is the loss of offsite power and the failure of the house load operation. The power loss causes rapid decrease in the recirculation flow. The coolant flow through the core decreases and the boiling and the void fractions increase. The increased void fraction causes the reactor level to swell. The negative void coefficient decreases reactivity.The loss of the offsite power and the house load operation failure results in a turbine trip. The turbine trip causes pressure increasing. The pressure increase causes a decrease in the void fraction. The decreased void fraction increases the reactivity and results to the positive reactivity. The positive reactivity causes the core fission power to increase. The turbine control system (461) starts dumping steam to the condenser. The steam dumping causes the pressure decrease in the reactor core and the void fraction increases again. The core reactivity decreases and results to the reduced core power. The minimum critical power ratio occurs. The typical sequence of events for the recirculation flow decrease transients is show in figure 5.5. (Rezendes, 2008, s. 27-28)

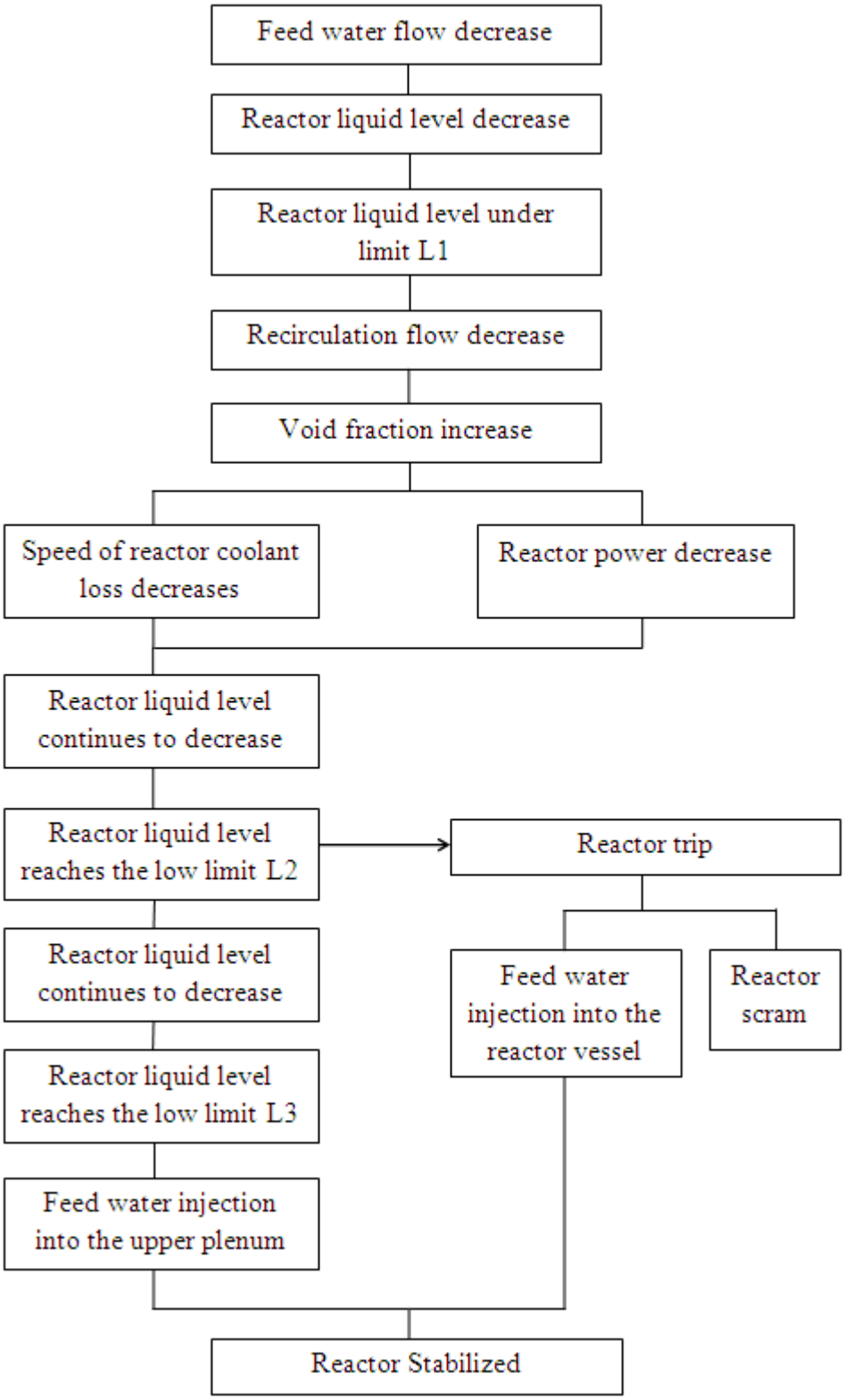

Figure 5.4 Sequence of events for the typical loss of feedwater transient

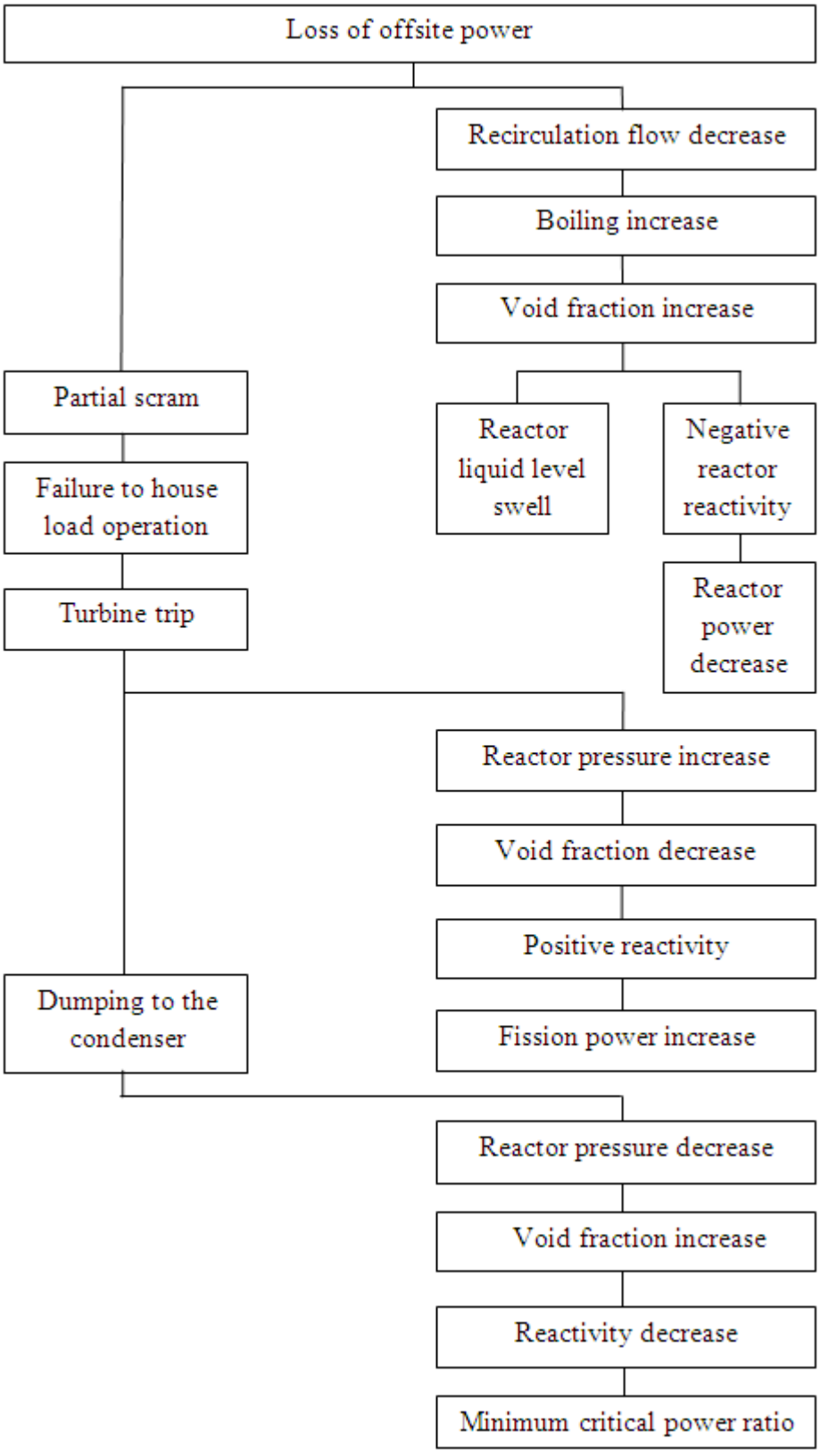

Figure 5.5. Sequence of events for the typical recirculation flow decrease transient

6 APROS MODEL UPDATING AND SIMULATIONS

All modeled transients in this thesis can be categorized to the fast transients. The core model input data should be as similar as possible with the real core data. The core model updating was done by using the BISON core input data. The BISON code is used for licensing the fuel and reactors made by Westinghouse. The most important core detail changes were the fuel enrichments, the burnups and the hydraulic diameters of the fuel assemblies. The main purpose of the core updating was to settle is it possible to use the BISON input data to make the reactor core to the APROS model. All calculations in this thesis have been done by using the 1-D reactor core model.

6.1. CASE 1: 15.5.2010 OL2 inadvertent closure of one MSIV

On the 15th of May, 2010, after the yearly overhaul, the power increased to 90 % at 11:34 h in the OL2. The old isolation valves were still used and kept in open position with the force of a strong magnet. At 12:54:15.264 the nitrogen leakage in the control system caused an open of valve 311V51. The control valve 311V51 caused the closure of the MSIV 311V1 at 12:54:15.434. The steam flow increased and after 2.71 seconds the second MSIV 311V4 closed at 12:54:18.265. During the following second, the MSIV 311V2 closed at 12:54:18.901 and the MSIV 311V3 at 12:54:18:926. All three MSIV valves closed due to the high steam flow. The magnet of the MSIV can hold it open against the limited steam flow. When the steam flow goes over the maximum limit the valve closes very fast. In this case the calculation time of MSIV closure is 0.1 seconds. (Heikkilä, 2010, s. 1-2)

The closure of all inner main steam isolation valves caused a fast increasing of the reactor pressure. The high pressure in the reactor actuated the condition SS6. The condition SS6 opened the relief valves V6-V13 in the system 314 and caused a scram. After the scram the cooling chains 322-721-712 started to cool the condensation pool. The relief system 314 activation caused actuation of the condition A21 at 12:54:24.280. The condition A21 caused the closure of all outer main steam isolation valves and started the diesel engines. In the reactor pressure

vessel the highest pressure was 77.7 bar and the lowest pressure 57.3 bar. The minimum water level in the reactor pressure vessel level was 3.1 m. The nitrogen leakage increased the pressure of the containment which reached a maximum of pressure 1.09 bar during this transient. The highest relative reactor power was 111.71 %. (Heikkilä, 2010, s. 1-2)

The APROS simulated MSIV control system does not include a feature to close the MSIV because of the high steam mass flow into the main steam line. The simulation was implemented by the manual closure of all four inner main steam isolation valves. The closure times were synchronized with the measured data. After the manual closure of the inner steam isolation valves, the APROS controlling model was used by the modeled automation system.

6.2. CASE 2: 2.6.2005 OL1 loss-of-load test

The purpose of the loss-of-load test was to check that the OL1 nuclear power plant can manage after a loss of load from the full power. The acceptance criterion in this case is that the plant unit remains the house load operation after the loss of load. The internal load fed by the generator is approximately 8 MW during the house turbine operation. In a general case the load drop activates the main circulation pumps to runback and the partial scram. The reactor power is stabilized at 30 % relative level. The level of the electricity generation should match with the internal consumption. The excess steam production is handled with dump to the condenser. The pressure and the level in the reactor pressure vessel should stay in the allowed area so that the reactor trip can be avoided. (Hanski, 2005, s. 1)

The test was realized by a manual opening the plant circuit breaker. The operator opened the breaker 2.621S101 manually from the control room 2.6.2005 at 14:00:50. The turbine operating speed increased rapidly. The controller of the turbine operating speed closed the control valves of the HP turbine and opened the turbine by-pass valves. The controller of the turbine operating speed set the turbine operating speed to 3000 rpm and opened the control valves of the turbine

to respond to the house load. The reactor power was stabilized at 30 % level. The maximum and the minimum pressure in the reactor dome were 69.5 bar and 68.0 bar. The highest and the lowest turbine operation speeds were 3205 rpm and 2946 rpm. (Hanski, 2005, s. 1)

The used APROS model does not include the electrical network. The simulation was implemented by a manual set of the generator power set point. The used generator set point value was 8 MW. After the generator set point was set manually, the APROS model controlling was used by the modeled automation system.

6.3. CASE 3: 7.3.2004 OL2 inadvertent closure of one MSIV

On the 7th of March, 2004, before the yearly overhaul, the reactor power was at 100 % 03:22 in the OL1. At 03:22:35.654 the high steam flow caused the closure of the MSIV 311V1. The maximum steam flow limit through the valve 311V1 was lower than normally because the surface of the holding magnet was unclean. The pressure started to increase and caused the reactor power increasing. The reactor power increased over the E-circuit limit (APRM 116 %) at 03.22.36.064. The E-circuit actuated the recirculation pump runback. The E-circuit was reset at 03.22.36.382 and the recirculation pump runback stopped. The Second MSIV closed at 03.22.36.762 and the steam dome pressure started increasing again. During the following second, the MSIV 311V4 closed at 03:22:37.395, the high reactor power released the condition SS10 (APRM 122 %) at 03:22:37.510 and the MSIV 311V2 closed at 03:22:37.689. (Lilja, 2004, s. 1)

The closure of all MSIV:s caused fast increasing of the reactor pressure. The reactor pressure increased over 74 bar and the condition SS6 was actuated. The reactor pressure reached maximum at 76.8 bar. The blow-out valve 314V12 did not opened because of a card fault. The condition A21 tripped the A-isolation and started the diesel engines at 03:22:42.688. Almost same time at 03.22.739 the low reactor liquid level activated the SS4 condition. The SS4 condition was activated during 8 seconds. (Ingvald, 2004, s. 2)

6.4. CASE 4: 20.4.2002 OL1 failure in the 400 kV grid

The OL1 NPP was at full power. The OL1 NPP was examined after a fault alarm, "error at communication of the protection system for 400 kV". During a settlement of a fault at 12:13, two switches were tripped at the station in Rauma. This caused a loss of load because OL1 NPP uses only those power lines to supply the power to the electrical network. (Lilja & Koski, 2002, s. 1-2)

After the loss of load the highest and the lowest turbine operation speeds were 3251 rpm and 2946 rpm. The loss-of-load signal will be activated if the turbine operating speed is above the limit 3045 rpm and rate of increase of the operating speed is over 60 rpm/s. This load drop signal was activated in this case. To limit the turbine operating speed all the high pressure turbine control valves closed. The reactor dome pressure increasing was controlled by opening the turbine bypass valves. The steam flow from the reactor dome decreased from 1300 kg/s to 1200 kg/s. The steam flow decrease caused a pressure increase. (Lilja & Koski, 2002, s. 1-2)

The maximum pressure in the reactor dome was 72.25 bar. The increasing reactor pressure caused the void fraction decreasing and the reactor power increased. The high reactor power activated the signal 516E3 at 12.13.26 when the relative reactor power was 110 %. The main circulation pumps were controlled to decrease the speed to minimum, but one main circulation pump was operated manually and stayed at the full operating speed. The reactor power decreased and pressure in the reactor dome dropped from 72 bar to 68 bar during 7 seconds. At 12:13:35.665 the A-isolation and the full scram signal SS12 activated. The A-isolation activated because the speed of pressure drop during 5 seconds was over the limit of 0.4 bar/s. The A-isolation started the diesel engines. The reactor water level minimum and maximum values were 3.0 m and 5.3 m. (Lilja & Koski, 2002, s. 1-2)

7 RESULTS AND COMPARISON

Result comparison between the APROS calculations and the plant measurements are presented in this chapter. The APROS calculations have been performed with using the original APROS model and the model with fixed reactor core. It is recommended to notice that all plant measurements have the difference accuracy. All calculations have been done with using the one dimensional core neutronics.

7.1. Accuracy of the plant measurements

The neutron flux measuring system (531) is designed to cover the whole range from start up to full power. The measuring range of the system 531 is from 10^{-10} to 1.50 of the nominal reactor power. (Laukkanen, 2008, s. 8) The flux measuring system is divided into two systems, the source range and the intermediate range monitoring (SIRM) and the power range monitoring (PRM). The SIRM system consist of eight SIRM-detectors which can monitor the neutron flux from subcritical conditions to criticality corresponding full power in the reactor. The SIRM system monitors both neutron flux and neutron flux doubling time. The change from the SIRM monitoring to the PRM monitoring happens at 8% power level. (Lemmetty, 2009, s. 17-18)

The PRM system consist 112 LPRM detectors located in 28 LPRM assemblies which are in operation under the normal power conditions. The measurements from PRM detectors can be displayed in the local power range monitoring system one by one or in the average power range monitoring system (APRM) with using average from groups of 28 detectors. The APRM signals are calibrated at regular intervals against the total reactor power as measured by the heat balance calculations. The APRM supplies the reactor protection system with the trip signals. The Reactor and turbine control systems uses the APRM signals to operate. The LPRM detectors can operate in a neutron flux range of 0.1 to 150 % of the nominal power. The PRM measuring accuracy for all measuring ranges is better than 0.2 % of the maximum output voltage or 0.5 % of the actual output

voltage. The time delay between the detectors current value and the output value is less than 2 ms. (Laukkanen, 2008, s. 6-45)

The reactor liquid level measurement is designed to measure the liquid level in the reactor pressure vessel annular gap. There are four different measuring subsystems A, B, C and D. The measurements are indirect. The measured magnitude is a pressure difference between two water columns. The liquid level measuring device is located under the measuring range. The liquid level is measured from closed pressure vessel. The upper part of the pressure vessel is filled with saturated steam. The method of the measurement has one great advantage that no measuring instruments are needed inside the reactor pressure vessel. The measuring instrument inside the reactor pressure vessel could cause problems because the operating conditions are so difficult. The one biggest disadvantage is that the result of the measurement is dependent on the density of the reactor water. The fluctuations of density can notably affect the results of measurements. The pressure difference is 30 % less in normal reactor operation conditions than in the normal room temperature and pressure with the same water column liquid level. The output signals are compensated against density. The water phase consists of water and steam bubbles. The density of water phase depends on temperature, pressure and void fraction. The steam phase consists of saturated steam. The density of steam phase depends on the temperature and pressure. In case of saturated steam the temperature depends on the pressure. On this account the density compensator uses the steam pressure and water temperature as input signals. The reactor liquid level measurements uncertainty of 95 % confidence interval is about 0.05m. (Laukkanen, 2010, s. 7-42)

The steam dome pressure is measured from the four reference vessels of the reactor liquid level measurement system. Every subsystem has the fine and coarse pressure measurements. The B sub has also the measurement of very high pressure. Signals from the coarse pressure measurements are high-pass filtered which make it possible to measure rapidly pressure drop. The Fine and coarse pressure measurements uncertainties of 95 % confidence interval are about 0.3 bar and 0.4 bar. (Laukkanen, 2010, s. 8-43)

The main circulation flow is measured computationally by comparing the measured and calculated flows through eight fuel assemblies. These eight measurements are divided between four subsystems. Every subsystem has two measurements. The measured magnitude is a pressure loss over the orifice plate in the measured channel. The main circulation flow measurements uncertainty of 95 % confidence interval is about 400 kg/s. (Laukkanen, 2010, s. 9-43)

The feedwater flow measurement is based on the measurement of static pressure drop over the orifice plate in the feedwater line. There are two different measuring points. The feedwater flow is calculated by the CONDIN-program. The feedwater flow measurements uncertainty of 95 % confidence interval is about 1.3 %. (Westerholm, 2007, s. 1-6)

The steam flow in the steam lines in the reactor building is measured by using Venturi tubes. There are four main steam lines and one Venturi tube in every line. Total steam flow is calculated by counting steam flows in all four main steam lines. The measuring range for one steam line has been 0-350 kg/s and for total steam flow 0-1400 kg/s. The measuring range for one steam line in the Olkiluoto 2 NPP has been changed during the outage 2011. The measuring range for one steam line is now 0-400 kg/s and for total steam flow 0-1400 kg/s. The measuring range for the total steam flow had not changed because the total steam flow with full power is 1260 kg/s. Total steam flow 1400 kg/s can be reached by nominal reactor power 110 % which is impossible situation with the presently safety limits. (Tuominen, 2011, s. 2-8)

7.2. CASE 1: 15.5.2010 OL2 inadvertent closure of one MSIV

The APROS simulation of the MSIV control system does not include a feature to close the MSIV because of the high steam mass flow in the main steam line. The simulation was implemented by the manual closure of all four inner main steam isolation valves with using the time control. The closing times were synchronized with the measured data. It could be also possible to create automation to close the valves when the steam flow increases over the limit but the exact self-closure limit

to each valve is unknown. The reactor power is measured by the APRM and the calculated reactor power is thermal power. The steady state conditions are presented in table 7.1.
The reactor power as a function of the recirculation flow is presented in appendix 11, figure 1. The calculated reactor power is higher than the measured APRM almost every point between the recirculation flow range 4800 − 6700 kg/s. The reactor power is shown in appendix 11, figure 2. The first reactor power increase begins after the first MSIV 311V1 closes and the steam dome pressure start to increase. The steam flow in the other steam lines starts to increase because the steam flow increase is dependent on the steam dome pressure increase. The reactor feedbacks reduce the reactor power and the steam dome pressure stabilizes.

Pressure starts increasing again when the second MSIV 311V4 closes. The high pressure in the reactor actuates condition SS6. The condition SS6 opens the relief valves V6-V13 in the relief system 314 and causes the scram. Around 1 second after the condition SS6 is actuated the MSIV 311V2 and the MSIV 311V3 closes and the steam dome pressure increasing continues. The reactor power increases and causes a third reactor power peak. Calculated reactor power is lower with the fixed reactor core during third power peak. The steam dome pressure reaches a maximum value around 2 seconds after closing the last MSIV. The steam dome pressure and the recirculation flow are presented in appendix 11, figure 3 and figure 4. The calculated maximum steam dome pressure is about 1.5 bar higher than measured. The higher reactor power causes the higher reactor pressure because more energy is released. The calculated reactor power is notably higher than measured during every reactor power peaks. The calculated steam dome pressure and the recirculation flow are not higher than measured until all reactor power peaks are past and all of the MSIV:s are closed. Therefore the differences in the reactor power between the calculated and measured values cannot be explained by the pressure or recirculation flow differences.

The steam flow is presented in appendix 11, figure 5-10. The calculated total steam flow in the system 311 is almost similar to the measured. Between the time

range 19-25 s all MSIV:s are closed and steam flow is measured after the valves. A measuring range of steam flow in one pipe is 350 kg/s and a calculated maximum is 400 kg/s. After the first MSIV closes the measuring values reach the maximum limit in the other steam lines. By using available measured data it is impossible to estimate how well the APROS model divides steam flow between the different lines. The feedwater system in the APROS model does not respond as fast as the feedwater system in the OL1/OL2 plants. After the scram is completed and the recirculation pumps are at the minimum rotating speed the calculated feedwater flow is much higher than measured. Thus the calculated reactor liquid level is higher than measured. The reactor liquid level is presented in appendix 11, figure 11. The calculated reactor liquid level is higher with the fixed reactor core because less energy is released.

Table 7.1 Steady-state condition case 2010

	Measured	**Calculated fixed core**	**Calculated original core**	
Thermal reactor power	90	90	90	%
Recirculation flow	6667	6670	6692	kg/s
Feedwater flow	1110	1108	1131	kg/s
Reactor liquid level	4.2	4.2	4.2	m
Steam dome pressure	69.0	69.0	69.0	bar
Steam flow 311	1145	1108	1131	kg/s
Steam flow 311V1	297	278	285	kg/s
Steam flow 311V2	280	273	279	kg/s
Steam flow 311V3	270	276	282	kg/s
Steam flow 311V4	298	280	286	kg/s

7.3. CASE 2: 2.6.2005 OL1 loss-of-load test

The APROS model does not include the electrical network. The simulation was implemented by a manual set of the generator power set point. 8MW was used as the generator set point. After the generator set point was set manually, the APROS model controlling was used by the modeled automation system. The steady state conditions are presented in table 7.2.

The reactor power as a function of the recirculation flow is presented in appendix 12, figure 1. The calculated recirculation flow is lower after the partial reactor scram than measured one. It can also be seen that the calculation with the original reactor core end up to the full scram. The reactor power is shown in appendix 12, figures 2 and 3. The measured reactor power minimum after partial scram is lower than the calculated one. The reason is that the measured recirculation flow decreases faster than calculated. The recirculation flow is shown in appendix 12 figures 4 and 5. The steam flow in the system 311 is presented in appendix 12 figure 6. It can be seen that the steam flow increased during a couple of seconds because the manual set of the generator set point does not work exactly like the real plant. The steam flow to the condenser increases too fast. The increased steam flow decreases the steam dome pressure. The steam dome pressure is presented in appendix 12, figure 7. The calculated feedwater flow goes over the measuring limit 1400 kg/s after the scram. The measured feedwater flow maximum is around 1240 kg/s. Thus the calculated reactor liquid level reaches a maximum point earlier than the measured one. The Feedwater flow and the reactor liquid level are presented in appendix 12, figures 8 and 9.

During the calculations the original reactor core neutronics crashed after 210 seconds. Reason to crash is probably the unrealistic values because both calculations were done with the same commands. The reactor power is also a little bit higher after the partial scram. Using some higher generator set points the model with the original reactor core does not crash always. The model with the fixed reactor core works fine during all tests so it is probably more stable than the original reactor core and all input details are realistic and can be easily traceable.

Table 7.2 Steady-state condition case 2005

	Measured	**Calculated fixed core**	**Calculated original core**	
Thermal reactor power	100	100	100	%
Recirculation flow	6667	6670	6692	kg/s
Feedwater flow	1110	1108	1135	kg/s
Reactor liquid level	4.2	4.2	4.2	m
Steam dome pressure	69.0	69.0	69.0	bar
Steam flow 311	1145	1108	1131	kg/s

7.4. CASE 3: 15.5.2004 OL2 inadvertent closure of one MSIV

The simulation was implemented by the manual closure of all four inner main steam isolation valves with the time control. The closing times were synchronized with the measured data. The transient methodology is mainly similar to that in the first case but the reactor power is higher when the first MSIV closes.

The reactor power as function of the recirculation flow is presented in appendix 13, figure 1. The calculated reactor power as a function of the recirculation flow is mainly between the same alarm limits but there are also lots of differences. The reactor power is shown in appendix 13, figure 2. The first reactor power increase happens after the first MSIV 311V1 closes and the steam dome pressure starts to increase. The steam flow in the other steam lines start to increase because the pressure controller tries to compensate for the increased reactor pressure by opening the turbine control valves. The steam flow is presented in appendix 13, figures 3-8. The reactor feedbacks compensate the reactor power increase and the reactor power is reduced and the steam dome pressure stabilizes. The steam dome pressure is presented in appendix 13, figure 9.

The pressure starts increases again when the second MSIV 311V4 closes. After one second also the MSIV 311V2 and the MSIV 311V3 are closed and the reactor power increase continues. The reactor power increases and causes a third reactor power peak. The calculated reactor power is lower with the fixed reactor core during the third power peak. The steam dome pressure reaches a maximum value around 2 second after the last MSIV is closed. The calculated maximum steam dome pressure is 1.5 bar higher than measured. The higher reactor power causes the higher reactor pressure because more energy is released. The calculated relative reactor power is notably higher during every reactor power peak. The calculated steam dome pressure and the recirculation flow are not higher than measured until all reactor power peaks are past and all MSIV:s are closed. Therefore the differences in the reactor power between calculated and measured values cannot be explained by the pressure or recirculation flow differences. The recirculation flow is presented in appendix 13, figure 10.

The calculated total steam flow in the system 311 is almost similar as measured. Between the time range 19-25 there are lots of differences in steam flows in the main steam lines. The reason is that all MSIV:s are closed and steam flow is measured after the valves. The measuring range of steam flow in one pipe is 350 kg/s and the calculated maximum is 400 kg/s. After the first MSIV closes measured values reach the maximum values in other steam lines. By using the available measured data it is impossible to estimate how well the APROS model divides the steam flow between different lines. The feedwater system in the APROS model does not respond as fast as the feedwater system in the OL1/OL2 plants. After the scram is completed and the recirculation pumps are at the minimum rotating speed the calculated feedwater flow is much higher than the measured one. Thus the measured reactor liquid level is higher than measured. The calculated reactor liquid level is higher with the fixed reactor core because the feedwater flow is similar but less energy is released. The feedwater flow and the reactor liquid level are presented in appendix 13, figures 11 and 12.

Table 7.3 Steady-state condition case 2004

	Measured	**Calculated fixed core**	**Calculated original core**	
Thermal reactor power	100	100	100	%
Recirculation flow	7758	7749	7748	kg/s
Feedwater flow	1250	1256	1254	kg/s
Reactor liquid level	4.2	4.2	4.2	m
Steam dome pressure	68.9	69.0	69.0	bar
Steam flow 311	1298	1256	1250	kg/s
Steam flow 311V1	336	316	315	kg/s
Steam flow 311V2	315	310	310	kg/s
Steam flow 311V3	317	312	312	kg/s
Steam flow 311V4	326	316	316	kg/s

7.5. CASE 4: 20.4.2002 OL1 failure in the 400 kV grid

The APROS model does not include the electrical network. The generator power was estimated by changing a position of valve 413V501 during the test. The circuit E3 and the isolation A21 was activated manually. After the isolation A21 activation, the APROS model controlling was used with the modeled automation system. The steady state conditions are presented in table 7.4.

The reactor power as a function of the recirculation flow is presented in appendix 14, figure 1. The calculated reactor power is not as high as measured when the E3-circuit actuates the recirculation pump runback. After the recirculation pump runback and before the A-isolation the measured reactor power is higher and more energy is released. The measured reactor power is higher because the measured recirculation flow decreased lower than calculated. The measured steam flow is

50 kg/s higher than the feedwater flow in steady state because the steam flow measurement is not exact.

The relative reactor power is shown in appendix 14, figure 2. The measured reactor power minimum after the pump runback is lower than calculated. The reason is that measured recirculation flow decreases faster than calculated. The recirculation flow is shown in appendix 14, figure 3. The calculated steam flow decreases faster than measured because the calculated reactor power is lower after the pump runback. Steam flow in the system 311 is presented in appendix 14, figures 4 and 5. The pressure increasing is also lower because less energy is released. The steam dome pressure is presented in appendix 14, figure 6. The calculated feedwater flow goes over measuring limit 1400 kg/s after the scram. The measured feedwater flow maximum is around 1240 kg/s. Thus the calculated reactor liquid level reach a maximum point earlier than measured. The feedwater flow and the reactor liquid level are presented in appendix 14, figures 7 and 8. Before the A-isolation is activated the calculated steam flow reduced much faster than the measured because the calculated reactor power is lower. After the A-isolation, the calculated feedwater flow is much higher than the measured one. The higher calculated feedwater flow causes a fast increase of the reactor liquid level and a decrease of the reactor dome pressure.

Table 7.4 Steady-state condition case 2002

	Measured	**Calculated fixed core**	**Calculated original core**	
Thermal reactor power	100	100	100	%
Recirculation flow	8000	8020	8019	kg/s
Feedwater flow	1250	1254	1255	kg/s
Reactor liquid level	4.2	4.2	4.2	m
Steam dome pressure	69.0	69.0	69.0	bar
Steam flow 311	1298	1254	1256	kg/s

8 SUMMARY AND CONCLUSIONS

The main purpose of this thesis was to settle out if it is possible to calculate the fast transients using the current Olkiluoto 1 and 2 APROS model. The main objects of the calculations were the reactor pressure vessel and the steam lines. The structure of the model is not sufficiently comprehensive to calculate transients with a minimum number of assumptions.

The most important model parts that are missing are the generator, the electrical network and the three-dimensional reactor core. The generator and the electrical network can make it possible to simulate more transients with a smaller number of assumptions. The three dimensional core neutronics will enhance the capability of the model for the transient analysis and probably reduce uncertainties. According to the results the reactor core and the feedwater systems cause most of the differences between the calculated and measured values. It is recommended to fix the feedwater system before other model updating is done.

Some unrealistic input details in the one-dimensional reactor core were updated by the author. During calculations there were still many differences in the core neutronics data because the cross sections were not updated to respond with the real situation that actually happened. It was not possible to update the cross sections with available resources.

During this thesis no problems resulting from the deficiencies in the APROS code fault were found. All of the most notable differences between the calculated and measured values can be explained by the problems in the model. The APROS model can be a good tool to make the reliable safety analysis but it requires the model to be more comprehensive and all input details to be up-to-date and easily traceable.

REFERENCES

Andersson, J. 2008. *OL 1/2 new steam isolation valves system 311.* Westinghouse Electric Sweden AB, 2008. Report: SEP 08-042 rev 3

APROS. 2011. *Well-validated, rigorous nuclear models* [online document]. Espoo : Technical Research Centre of Finland, [Accessed 5 June 2011]. Available at URL[http://www.apros.fi/en/industries/nuclear_power/well-validated_nuclear_models]

APROS. 2010. *APROS white papers: Comparison between thermal hydraulic models* [online document]. Espoo : Technical Research Centre of Finland, [Accessed 5 June 2011]. Available at http://www.apros.fi/en/ brochures_papers# White_paper

Dellby, C. & Poikolainen, J. 2004. *BISON simulation of TVO self closure of steam isolation valves 7 March 2004.* Westinghouse Electric Sweden AB, 2004. Report: SET 07-164

Hanski, O. 2005a. *OL2 - koe timo59, kuormanpudotuskoe.* Olkiluoto: Teollisuuden Voima, 2005. Report: 109463

Hanski, O. 2005b. *OL2 - koe timo59, kuormanpudotuskoe, tulosraportti.* Olkiluoto: Teollisuuden Voima, 2005. Report: 111210

Honkanen, J. 2010. *311-OL2-Reaktorin päähöyryputket-lopullinen turvallisuusseloste.* Olkiluoto: Teollisuuden Voima, 2010. Report: 136838

Heikkilä, A. 2010. *OL2 Reaktoripikasulku korkeasta reaktorin paineesta (SS6) 15.5.2010.* Olkiluoto: Teollisuuden Voima, 2010. Report: 134947

Hänninen, M. 2009. *Phenomenological extensions to APROS six-equation model.* Espoo : Technical Research Centre of Finland, 2009. ISBN 978-951-38-4

Hänninen, P. & Ylijoki, J. 2008. *The one-dimensional separate two-phase flow model of APROS.* Espoo: Technical Research Centre of Finland, 2008. ISBN 978-951-38-7224-3

Lilja, I. 2004. *Reaktoripikasulku korkeasta reaktoritehosta (SS10) 7.3.2004.* Olkiluoto: Teollisuuden Voima, 2004. Report: 104875

Jacob, M. 2008a. *Olkiluoto 1 and 2 Periodic Safety Review 2008 Feedwater flow increase/temperature decrease transients and Accidents Methodology.* Westinghouse Electric Sweden AB, 2008. Report: NTD 96-083

Jacob, M. 2008b. *Olkiluoto 1 and 2 Periodic Safety Review 2008 Pressure decrease transients and Accidents Methodology.* Westinghouse Electric Sweden AB, 2008. Report: NTD 96-085

Jacob, M. & Wallgren, S. 2008. *Olkiluoto 1 and 2 Periodic Safety Review 2008 loss of feedwater flow transients and Accidents Methodology.* Westinghouse Electric Sweden AB, 2008. Report: NTD 96-083

Jurvakainen, E. 2009. *313 - OL1/OL2 - Pääkiertojärjestelmä - Lopullinen turvallisuusseloste.* Olkiluoto: Teollisuuden Voima, 2009. Report: 107737

Jönssön, C. 2008 *Validation of S3K against the Olkiluoto 1 inadvertent closure of one MSIV (2004).* Studsvik: Studsvik Scandpower AB, 2008. Report: SSP-06/117

Kontio, H. 2008 *APROS input model for Olkiluoto 1 and 2 nuclear power plant.* Espoo: Fortum nuclear services, 2008. Report: FNS-245336

Kontio, H. 2005. *Validation of Olkiluoto 2 nuclear power plant simulation model.* Espoo : Fortum nuclear services, 2005. Report: NUCL-2958

Laakso, P. 2011a. *Lecture notes: APROS initial training course –APROS overview.* Espoo, June 6-8. 2011

Laakso, P. 2011b. *Lecture notes: APROS initial training course –Thermal hydraulic solution.* Espoo, June *6-8.* 2011

Laukkanen, J. 2010. *536 OL1/OL2 - Reaktoripaineastian instrumentointi - lopullinen turvallisuusselostus* Olkiluoto: Teollisuuden Voima Oyj, 2010. Report: 106258

Laukkanen, J. 2008. *OL1/OL2 - Final safety analysis report for system 531, part 2 - power range monitoring system (PRM).* Olkiluoto: Teollisuuden Voima, 2008. Report: 106252

Lilja, I & Koski, S. 2002. *Pikasulkuraportti: OL1 Reaktoripikasulku 400kV:n verkkohäiriön seurauksena 20.4.2002.* Olkiluoto: Teollisuuden Voima, 2002. Report: 1-KK-R6-1/02

Lemmetty, M. 2010. *Final Safety Analyses Report, chapter 1 - Scope and objectives OL1/OL2.* Olkiluoto: Teollisuuden Voima, 2010. Report: 129558

Lemmetty, M. 2009. *Final Safety Analyses Report, chapter 2 - Introduction and general plant description OL1/OL2.* Olkiluoto: Teollisuuden Voima, 2009. Report: 129490

Liuko, J. 2010. *APROS brochures* [online document]. Espoo : Fortum Oyj, [Accessed 5 June 2011]. Available at http://www.apros.fi/en/brochures_papers

Nevander, O. 2010. *Finaly Safety Analyses Report, chapter 5 - Plant function.* Olkiluoto: Teollisuuden Voima, 2010. Report: 129503

Nevander, O. 2008. *Finaly Safety Analyses Report, chapter 9.2 - General descriptions of safety systems.* Olkiluoto: Teollisuuden Voima, 2008. Report: 129529

Nousiainen, P. 2011a. *Pele 13, Pikaraportti OL2-höyrylinjojen ja -venttilien värähtelymittauksista korotetulla hyöryvirtauksella.* Olkiluoto: Teollisuuden Voima, 2011. Report: 138919

Nousiainen, P. 2011b. *OL2, SIVA-projekti, 311-sisempien eristysventtiilin koekäyttöraportti.* Olkiluoto: Teollisuuden Voima, 2011. Report: 139063

Nousiainen, P. 2010. *OL1, SIVA-projekti, 311-Sisempien eristysventtiilien koekäyttöraportti* Olkiluoto: Teollisuuden Voima, 2010. Report: 135276

Nuutinen, P. 2005. *APROS code bencmarking in boiling water reactor accident analyses.* Olkiluoto: Teollisuuden Voima, 2005

Paalanen, A. 2009. *OL1/OL2 APROS-laitosmalli* Olkiluoto : Teollisuuden Voima, 2009. Report: 113223

Paasikivi, O. 2009. *516-OL1/OL2- Reaktorin suojausjärjestelmä - Lopullinen turvallisuusseloste.* Olkiluoto: Teollisuuden Voima, 2009. Report: 106241

Puska, E. 2009a. *One-dimensional nuclear reactor physical models APROS version 5.08/5.09.* Espoo: Technical Research Centre of Finland, 2009

Puska, E. 2009b. *Three-dimensional nuclear reactor physical models APROS version 5.08/5.09.* Espoo: Technical Research Centre of Finland, 2009

Puska, E. 2006. *APROS nuclear reactor one-dimensional neutronics model user´s guide version 5.06.* Espoo: Technical Research Centre of Finland, 2006

Puska, E. 1999. *Nuclear reactor core modelling in multifunctional simulators.* Espoo: Technical Research Centre of Finland, 1999. ISBN 951-38-5361-6

Rezendes, J. 2008. Olkiluoto 1 and 2 Periodic Safety Review 2008 Recirculation flow decrease Transients and Accidents Methodology. Westinghouse Electric Sweden AB, 2008. Report: NTD 96-084 rev 2

Rezendes, J. & Jacob M. & Wallgren, S. 2008. Olkiluoto 1 and 2 Periodic Safety Review 2008 Pressure Increase Transients and Accidents Methodology. Westinghouse Electric Sweden AB, 2008. Report: NTD 96-026

TVO. 2011. *Nuclear power plants Olkiluoto 1 and Olkiluoto 2.* Olkiluoto: Teollisuuden Voima, 2011

Tuominen, L. 201. *Mittausalueen laajennus.* Olkiluoto : Teollisuuden Voima, 2011. Report: 138018

Viitanen, P. 2011. *Final Safety Analyses Report, chapter 3 - Plant site and enviroment OL1/OL2.* Olkiluoto: Teollisuuden Voima, 2011. Report: 129486

Wallgren, S. 2008. *Olkiluoto 1 and 2 perioidic safety review 2008 transients and accidents analysis methodology.* Olkiluoto: Teollisuuden Voima, 2011. Report: NTD 96-025, rev 2

Westerholm, H. 2007. *Syöttöveden virtausmittaus.* Olkiluoto : Teollisuuden Voima, 2007. Report: 118302

Westinghouse Electric Company. 2007. *Ydinvoimalaitosyksiköt Olkiluoto 1 ja Olkiluoto 2.* Pittsburgh: Westinghouse Electric Company, [Accessed 17 June 2011]. Available at http://www.westinghousenuclear.com/products_&_services/docs/flysheets/NF-FE-0034.pdf

Ylijoki, J. 2003. *Simulation model of Olkiluoto nuclear power plant for APROS.* Espoo: VTT Processes, Pulp and Paper Industry, 2003. VTT research report: PRO5/7823/03

A Cross-section of the OL1 and OL2

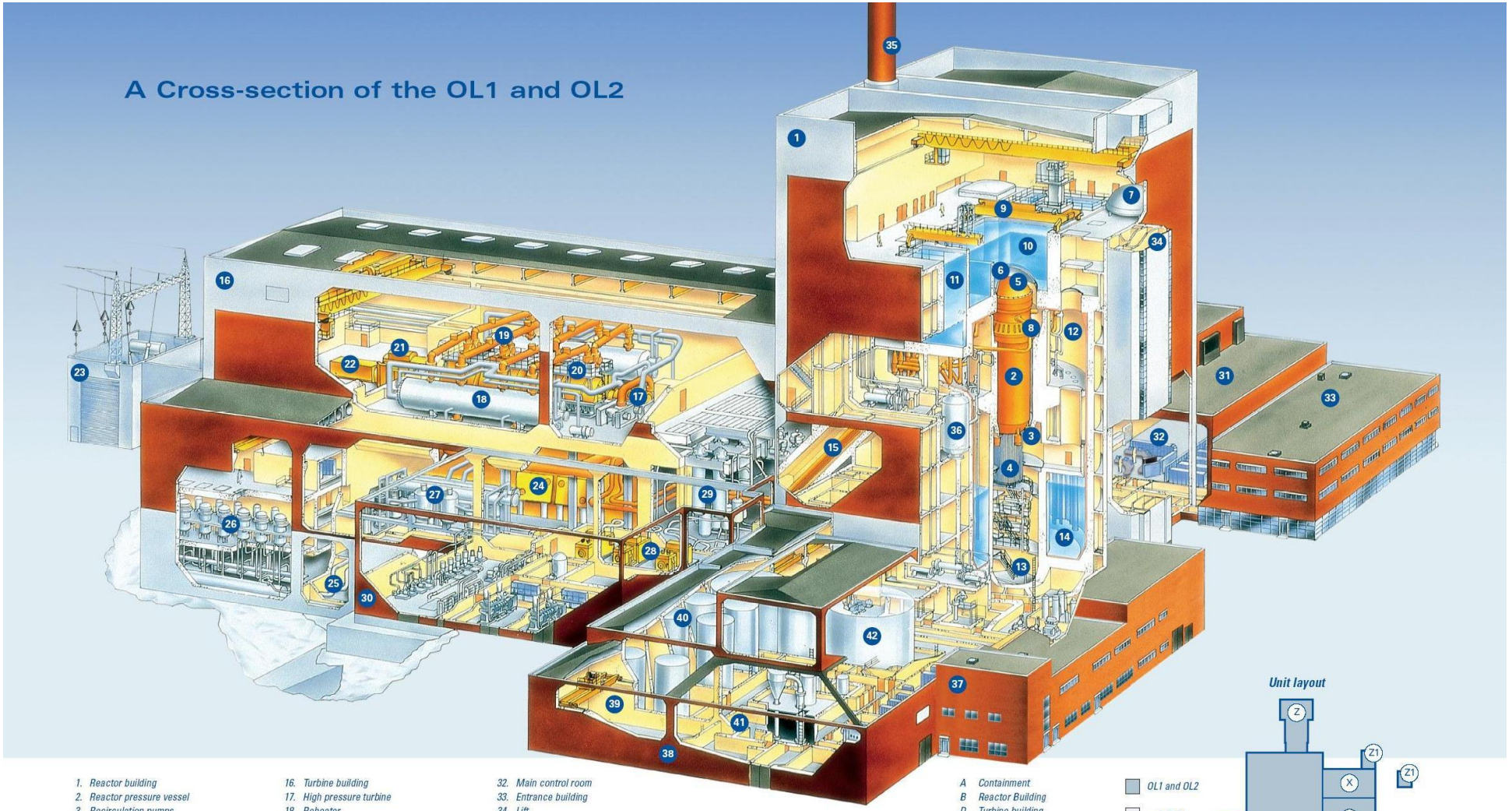

1. Reactor building
2. Reactor pressure vessel
3. Recirculation pumps
4. Control rod drives
5. Reactor pressure vessel cover
6. Containment cover
7. Containment cover lifted off (during annual outages)
8. Main steam lines
9. Reactor service bridge
10. Reactor pool
11. Fuel pool
12. Upper dry-well of containment
13. Lower dry-well of containment
14. Condensation pool of containment
15. Main steam lines
16. Turbine building
17. High pressure turbine
18. Reheater
19. Cross-over pipes
20. Low pressure turbines
21. Generator
22. Exciter
23. Main transformer
24. Condenser
25. Condensate line
26. Condensate purification system
27. Low pressure preheaters
28. Feedwater pumps
29. High pressure preheaters
30. Auxiliary systems building
31. Control building
32. Main control room
33. Entrance building
34. Lift
35. Ventilation stack
36. SAM scrubber (filtered venting system of the containment)
37. Active workshop/laboratory building (only OL1)
38. Radioactive waste building
39. Low and medium-level radioactive waste storage
40. Liquid waste storage tanks
41. Solid waste system
42. Make-up water tank

A Containment
B Reactor Building
D Turbine building
E Main control room
F Radioactive waste building
H Auxiliary buildings
N Active workshop/laboratory building (only OL1)
P Entrance building
T Cooling water supply
X Switchgear
Z Main transformer
Z1 Startup transformers

OL1 and OL2
only OL1

Unit layout

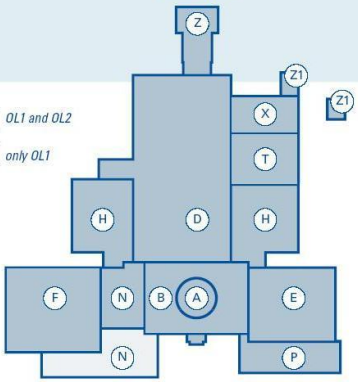

Operating principle of the boiling water reactor

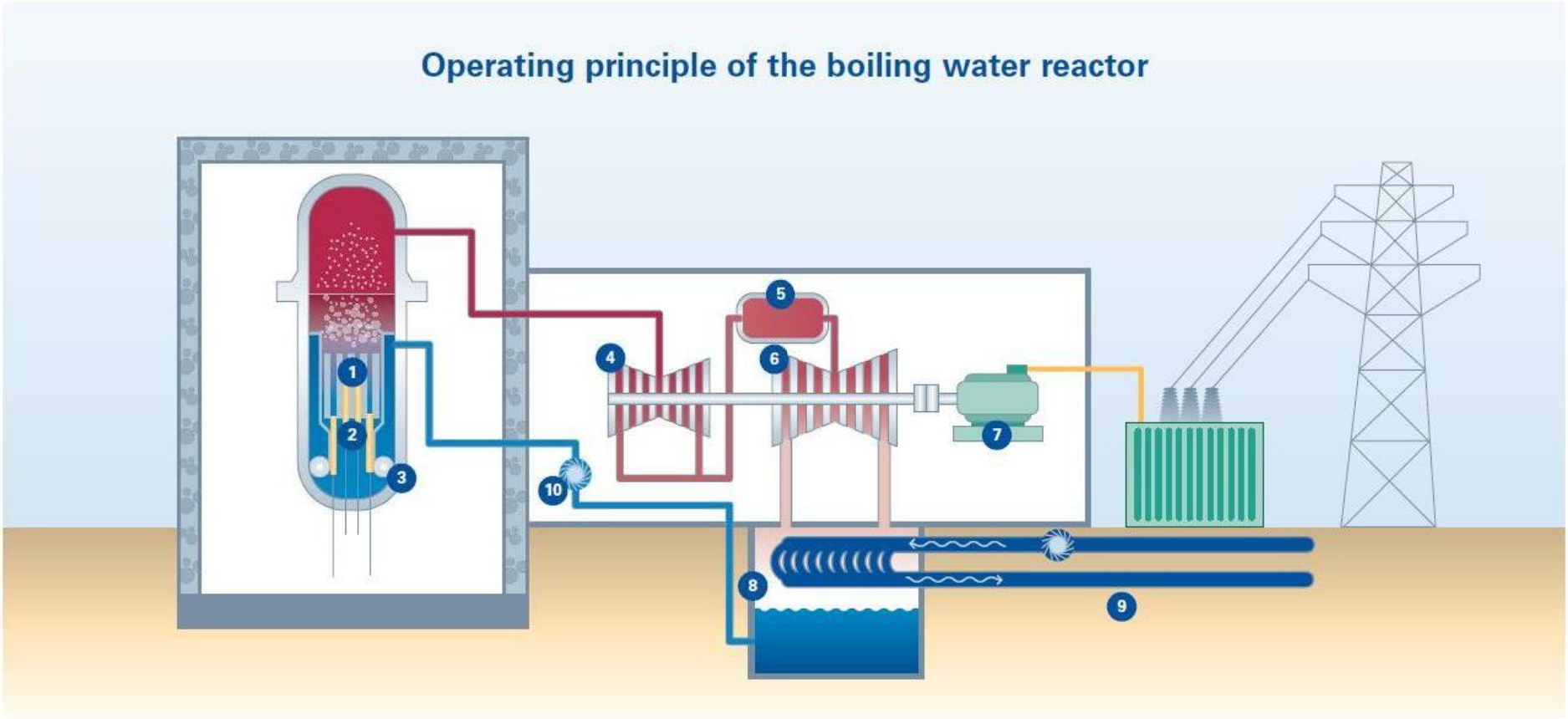

*In a boiling water reactor, the water boils as it passes between the **fuel rods (1)** in the reactor. The reactor output is regulated with **control rods (2)** and the **recirculation pumps (3)**. The steam generated in the reactor is transferred to the **high-pressure (HP) turbine (4)** through the main steam lines. Having expended part of its energy in the HP turbine, the steam is then transferred to the **re-heaters (5)**, where it is dried and superheated and then transferred to the **low-pressure (LP) turbines (6)**. All the turbines are coaxially connected to the **generator (7)**, which generates electricity that is then fed into the national grid. The steam exiting the LP turbines is condensed into water in the **condenser (8)**, using **sea water (9)** as coolant. The condensed water is conveyed through preheaters and a clean-up system to the **feedwater pumps (10)**, which feed the water back into the reactor. The heated cooling water is pumped back into the sea.*

Table 1. The reactor shutdown and isolation circuits

Reactor shutdown circuit	**Signal**
The scram circuit	SS
The electromechanical shutdown circuit	V
The start interlock system	S
The power interlock system	E
Refuelling monitoring circuit	B
BOR-circuit	BOR
Isolation circuit	**Signal**
Main steam lines break monitoring circuit	A
Reactor containment monitoring circuit	I
Feedwater system break monitoring circuit	M
Reactor auxiliary system´s outer room monitoring circuit	Y
Decay heat removal and emergency cooling systems A-room monitoring circuit	HA
Decay heat removal and emergency cooling systems B-room monitoring circuit	HB
Decay heat removal and emergency cooling systems C-room monitoring circuit	HC
Decay heat removal and emergency cooling systems D-room monitoring circuit	HD

Table 1. The monitored systems by the system 516

System		**Monitored magnitude (condition)**
211	Reactor pressure vessel	Level (SS4, SS5, I2, TB1, TBT3, TBT4, BOR4, X1, XT6) Pressure (SS6, A21, A22, MT9, BOR3, X5) Main circulation flow (SS9, SS10, SS15, E3, E4)
316	Condensation system	Temperature (V5, X3)
336	Sampling system	Turbine condensation conductivity (M2)
412	Steam reheat system	Moisture separator and steam reheat pressure (A23)
416	Control and trip oil system	Pressure (SS11)
441	Condensate system	Feedwater pump inlet pressure (SS13)
531	Neutron flux measuring system	Neutron flux (SS7, SS8, SS9, SS11, SS14, SS15, S2, S3, S5, E2, E3, E4, B3, MT9, TBT3, BOR3, BOR4) Ratio between neutron flux and recirculation flow (SS9, SS10, SS15, E3, E4)
533	Control rod operating system	"Driving screw in" -condition (SS2, V2, S4)
536	Reactor instrumentation system	Check system 211 (Appendix 7, table 1)
546	Isolation monitoring system	Leakage indicating in different rooms with pressure, pressure increasing, temperature and level: - Containment (I4, I5, I6, TB2) - Reactor building (Y2-Y16) - Steam lines (A2-A20) - Feedwater system (M3- M8) - H-rooms (HA1, HB1, HC1, HD1)
551	Steam line radiation monitors	Radiation level (I3)
555	Room radiation monitors	Dose rate in reactor hall (X2)
723	Diesel-backed normal operation secondary cooling system	Pressure (X4)

Table 1. The controlled systems by the system 516

System number	System name
311	Steam lines in reactor building
312	Feedwater system
313	Recirculation system
314	Relief system
321	Shut-down cooling system
322	Containment vessel spray system
323	Core spray system
326	Flange cooling system
327	Auxiliary feedwater system
331	Reactor water clean-up system
336	Sampling system
345	Controlled area floor drain system
351	Boron system
352	Controlled leakage drain system
354	Scram system
441	Steam turbine
445	Turbine plant feedwater system
531	Neutron flux measuring system
532	Control rod operating system
535	Control rod position indicating system
537	Feedwater control system
542	Process control
543	Valve opening system
547	Other monitoring systems
649	Frequency converters
654	Diesel engines
684	Motor sequence starting system
712	Shut-down service water system
721	Shut-down secondary cooling system
723	Diesel-backed normal operating secondary cooling system
734	High pressure purge water system
741	Containment gas treatment system
742	Reactor building ventilation system
749	Off-gas filter system
754	Compressed nitrogen system
755	Containment inerting system

Table 1. The modeled systems in the OLI/OL2 APROS model

System number	System name
112	Cooling water channels
150	Containment
211	Reactor pressure vessel and core
311	Main steam pipelines
312	Feedwater system
314	Steam blow-out system
321	Shutdown reactor cooling system
322	Containment spray system
323	Reactor core spray system
327	Auxiliary feedwater system
351	Boron system
354	Reactor scram system
411	Steam turbine
412	Steam superheating systems
413	Main steam lines to turbine
431	Condensers
436	Make-up water systems
441	Condensate systems
445	Feedwater systems
447	Steam extraction system
461	Reactor pressure control
465	Turbine protection system
516	Reactor protection system
535	Reactor power control system
537	Feedwater control system
546	Containment supervision system
712	Shut down reactor sea water system
721	Shut down reactor intermediate cooling system

Table 1. The APROS model measurements in the system 211

System 211	**Description**
211 Bypass	- Heat transfer from inside the fuel assembly to the bypass coolant beside the fuel assemblies
211 Control rods	- 31 control rod groups - All groups consist four control rods except group one consist only one control rod - All the control groups are moving with the scram or screwing speed
211 Hot channel	- Has been modeled to calculate heat and flow condition of one hot fuel rod - Pressure, liquid enthalpy, steam enthalpy and void fraction values are transferred from 211 reactor vessel nodes to the hot channel
211 Measurements	- Coarse and fine collapsed water level - Pressure differences
211 Reactor core calculation level	- Level nodes - Branches -Heat structures - Heat transfer modules - Average reactor cladding rod module
211 Neutron flux measurement	- Axial fast and thermal neutron flux - Axial power defined by the neutron flux measurement

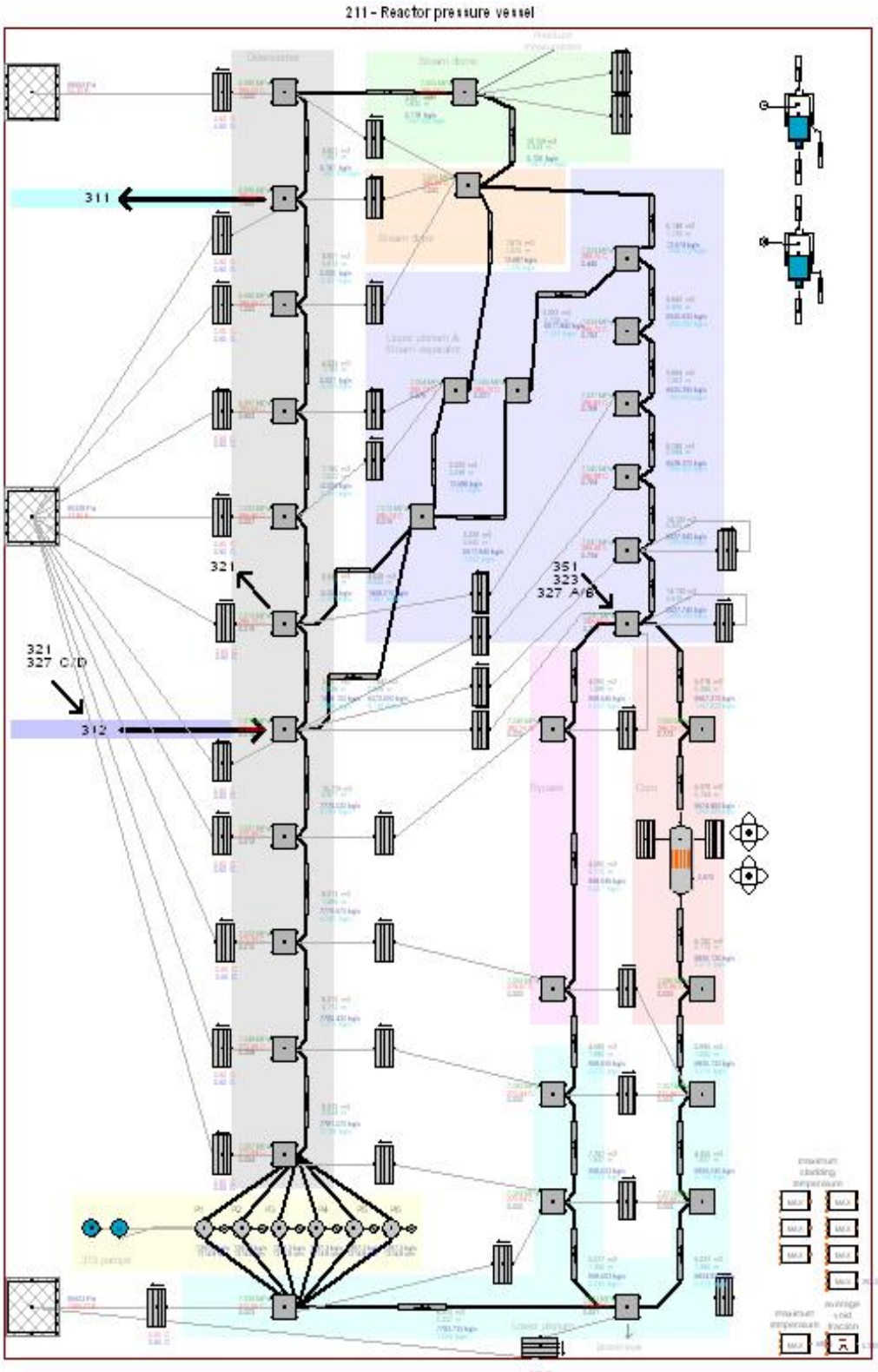

Figure 1. 211 Reactor pressure vessel

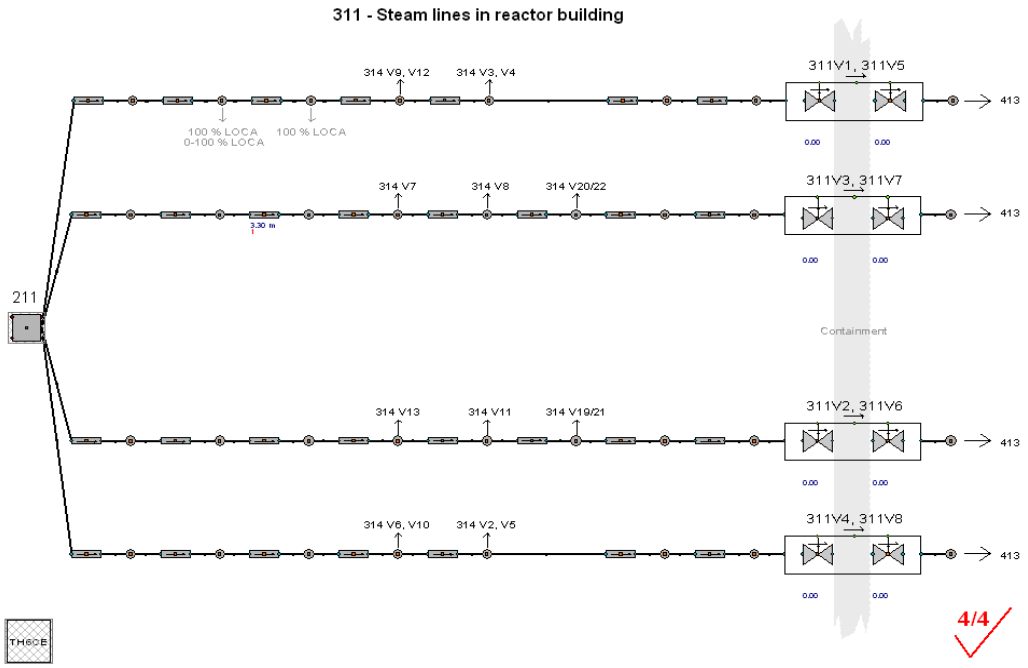

Figure 2. 311 Steam lines in reactor building

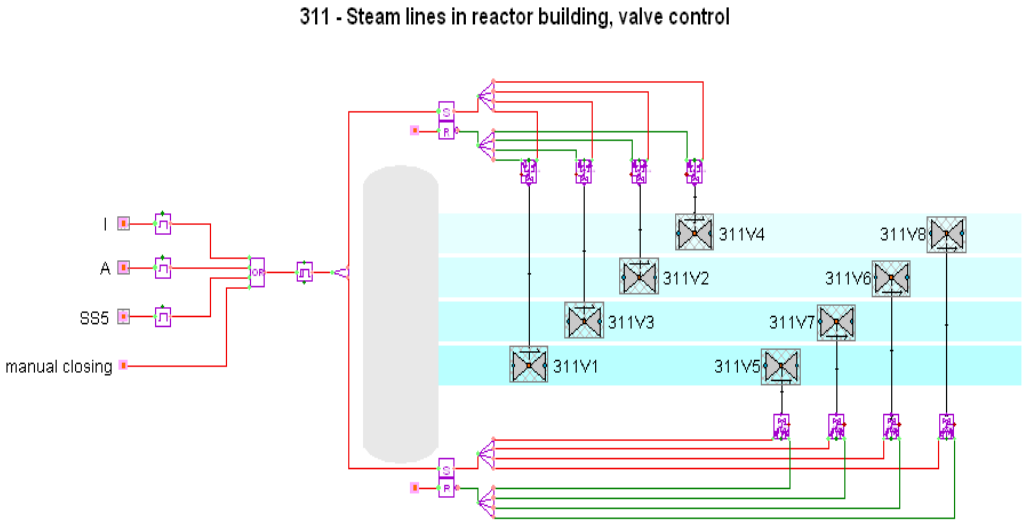

Figure 3. 311 Steam lines in reactor building, valve control

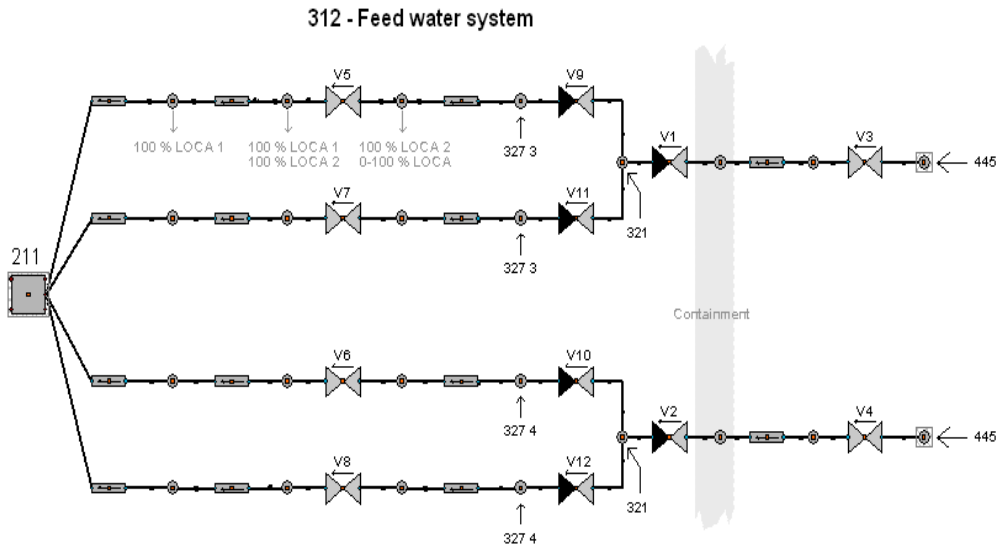

Figure 4. 312 Feedwater system

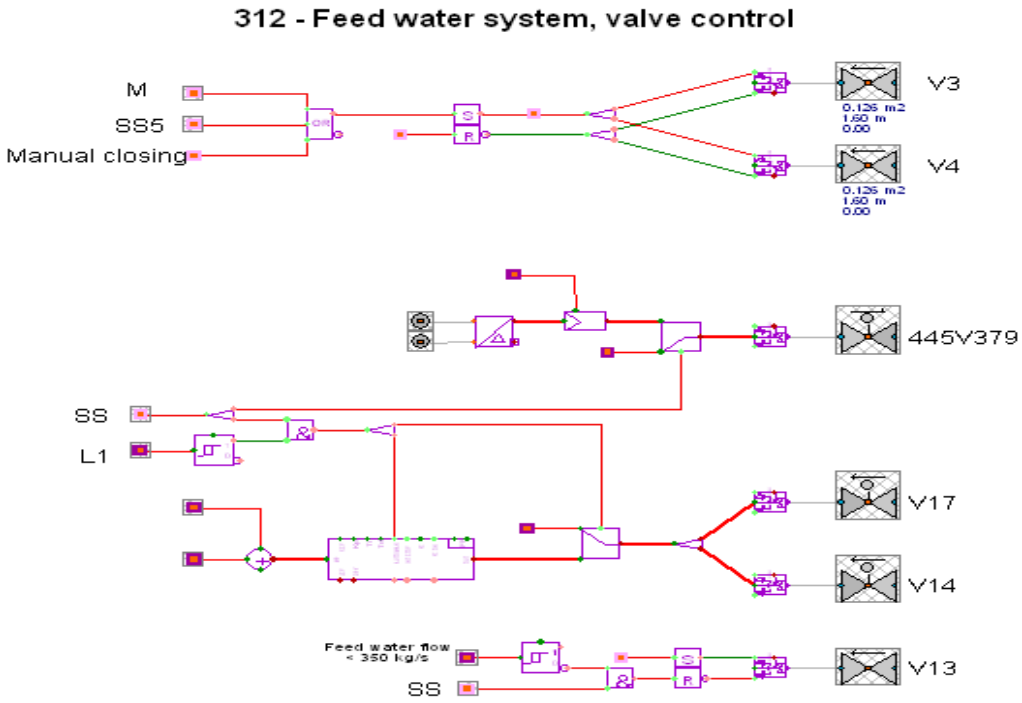

Figure 5. 312 Feedwater system, valve control

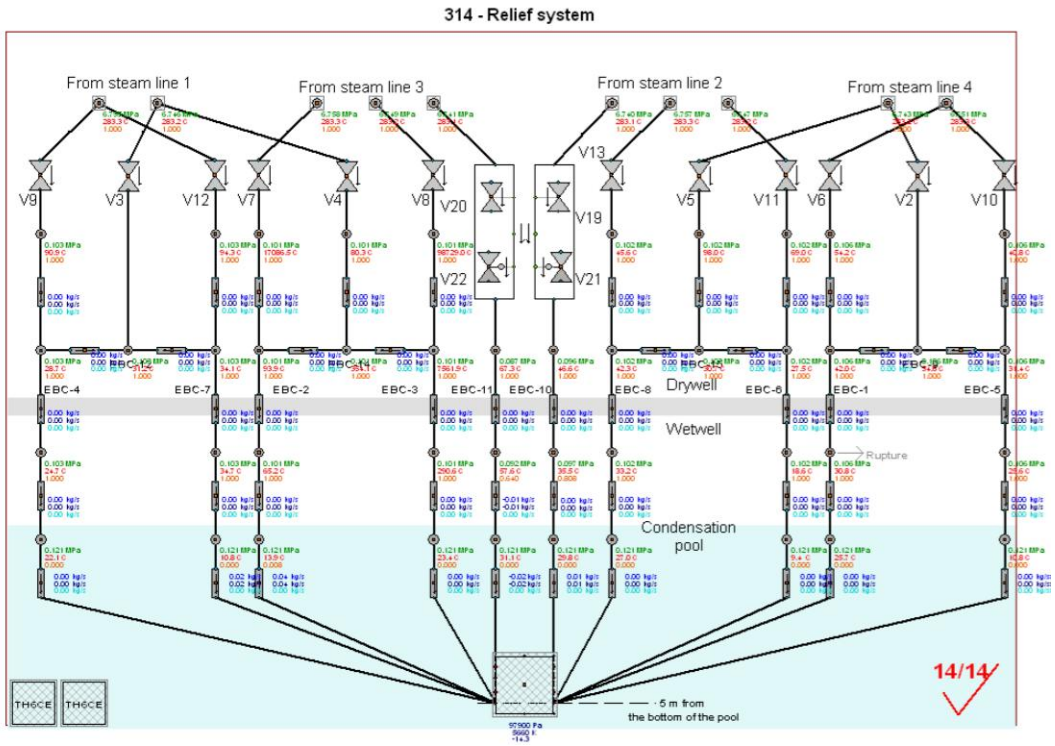

Figure 6. 314 Relief system

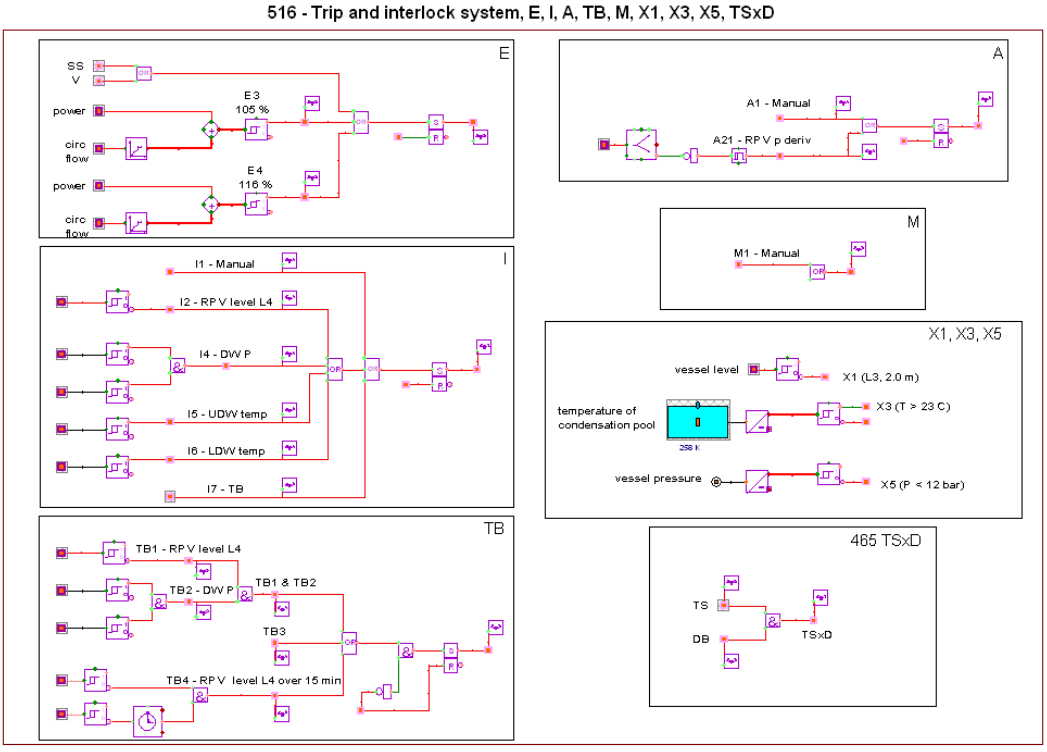

Figure 7. 516 - Trip and interlock system

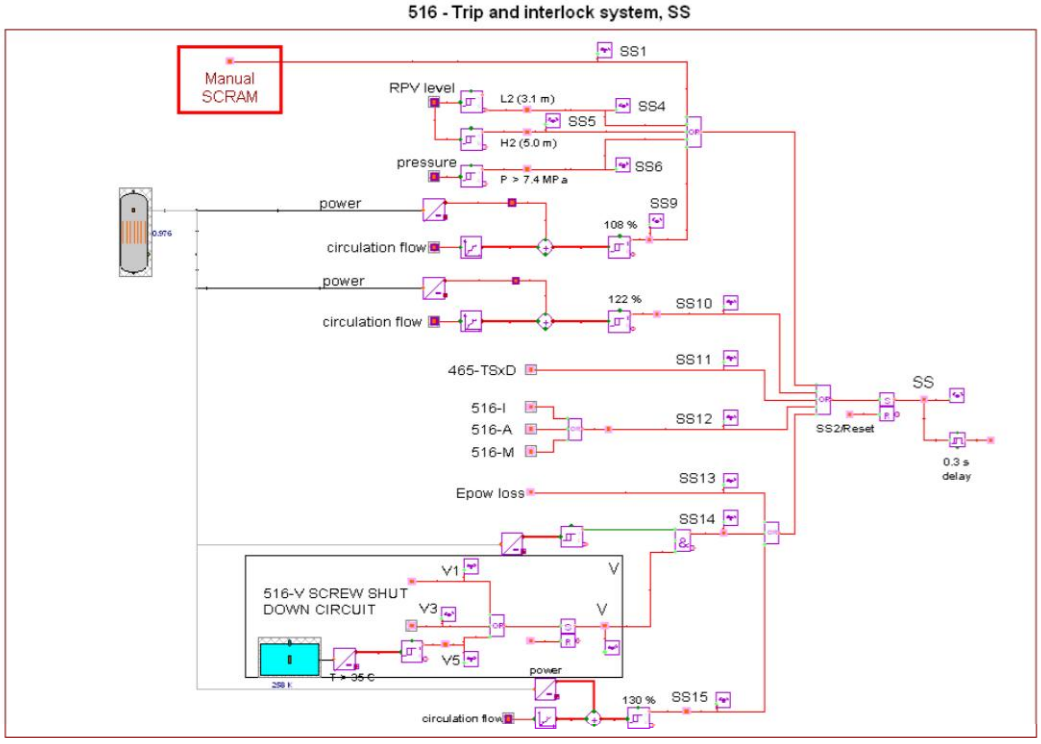

Figure 8. 516 - Trip and interlock systems, SS

Table 1. The isolation chains

Part name	**Activation limit**
E1	SS- or V-chain activated
E3	High neutron flux versus coolant flow filtered 105 %
E4	High neutron flux versus coolant flow unfiltered 116 %
I1	Manual trip
I2	Reactor pressure vessel low level L4 0.7 m
I4	Drywell high pressure P > 0.995 bar
I5	Upper drywell high temperature T > 80 °C
I6	Lower drywell high temperature T > 60 °C
I7	Activated TB-chain
TB1	Reactor pressure vessel low level L4 0.7 m
TB2	High drywell pressure P > 0.995 bar
TB4	Reactor pressure vessel low level L4 0.7 m delay 15 min
A1	Manual trip
A21	Pressure derivate -0.4 bar/s
M1	Manual trip
X1	Reactor pressure vessel low level L3 2.0 m
X3	High condensation pool temperature 23 °C
X5	Low reactor pressure 12 bar
TS	Turbine trip
DB	Forbiddance turbine by-pass, manual

Table 1. The scram chains

Part name	**Activation limit**
SS1	Manual trip
SS2	Release
SS4	Reactor pressure vessel low level L2 3.1 m
SS5	Reactor pressure vessel high level H2 5.0 m
SS6	Reactor high pressure 74 bar
SS9	High neutron flux versus coolant flow filtered 108 %
SS10	High neutron flux versus coolant flow' Unfiltered 122 %
SS11	Turbine trip and forbiddance turbine by-pass TSxD
SS12	Activated isolation chain
SS13	Low feedwater pump suction pressure 6.95 bar during 20 seconds
SS14	Activated V-chain and reactor power over 25 %
SS15	High neutron flux versus coolant flow 25 % during natural circulation
V1	Manual trip
V3	Activated SS-chain
V5	High condensation pool temperature 35 °C

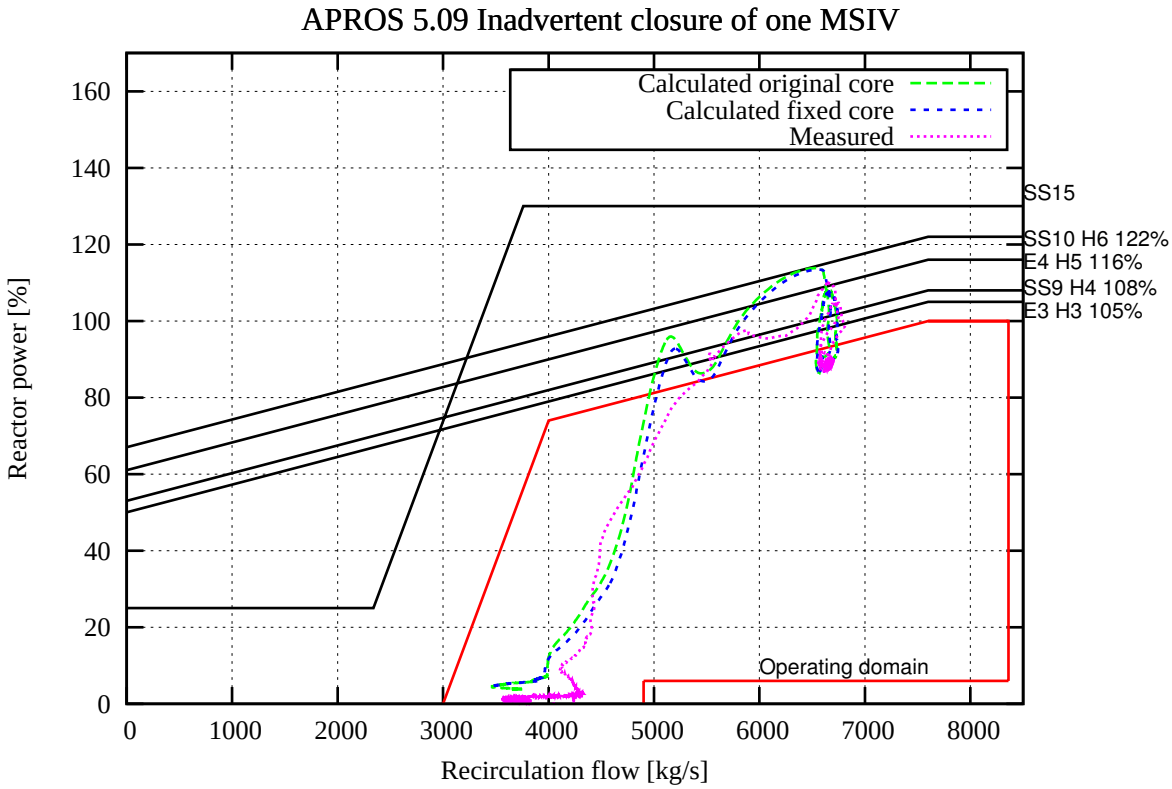

Figure 1. Reactor power as a function of recirculation flow

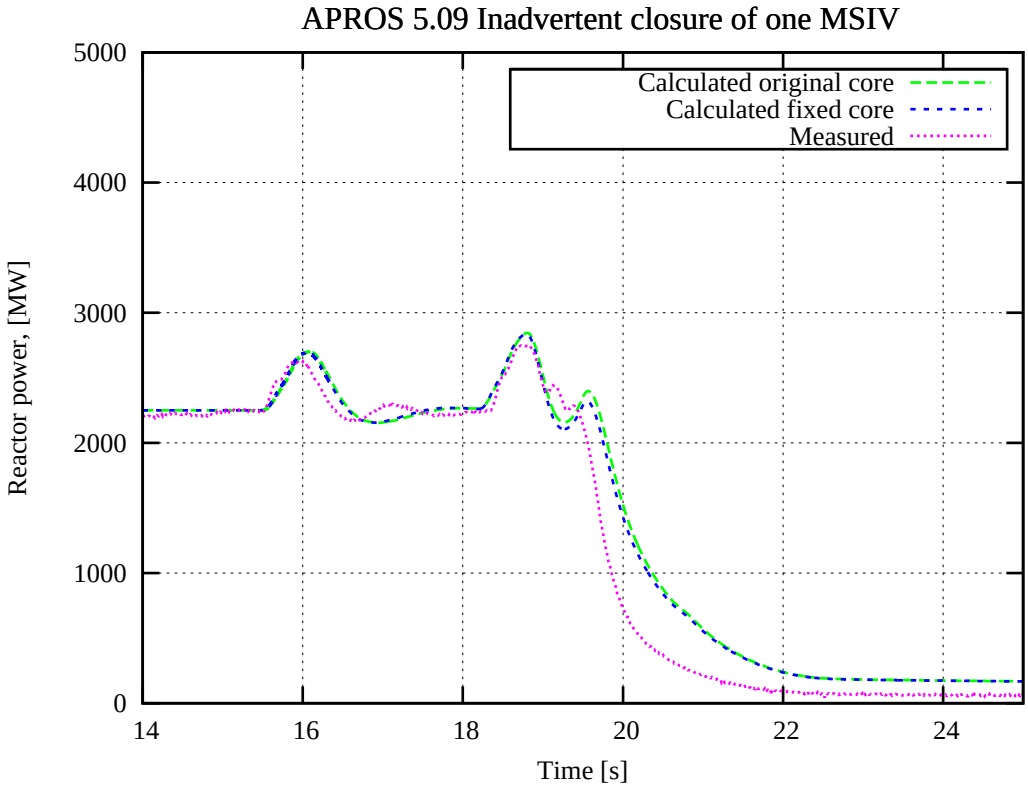

Figure 2. Reactor power

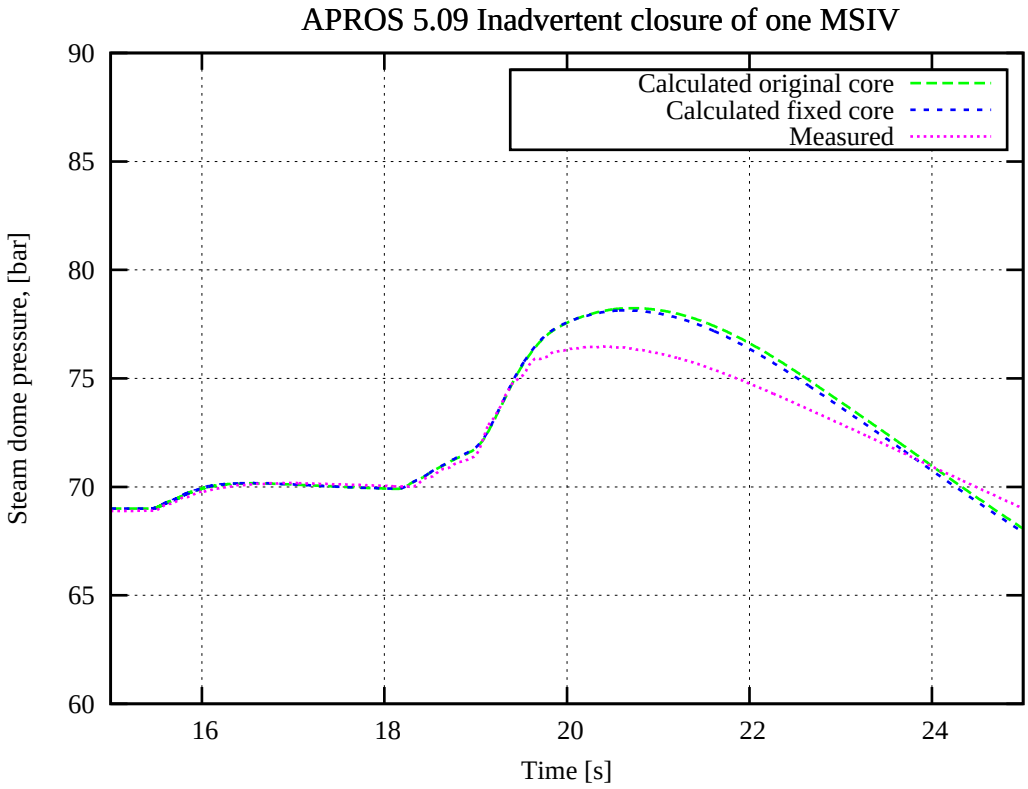

Figure 3. Steam dome pressure

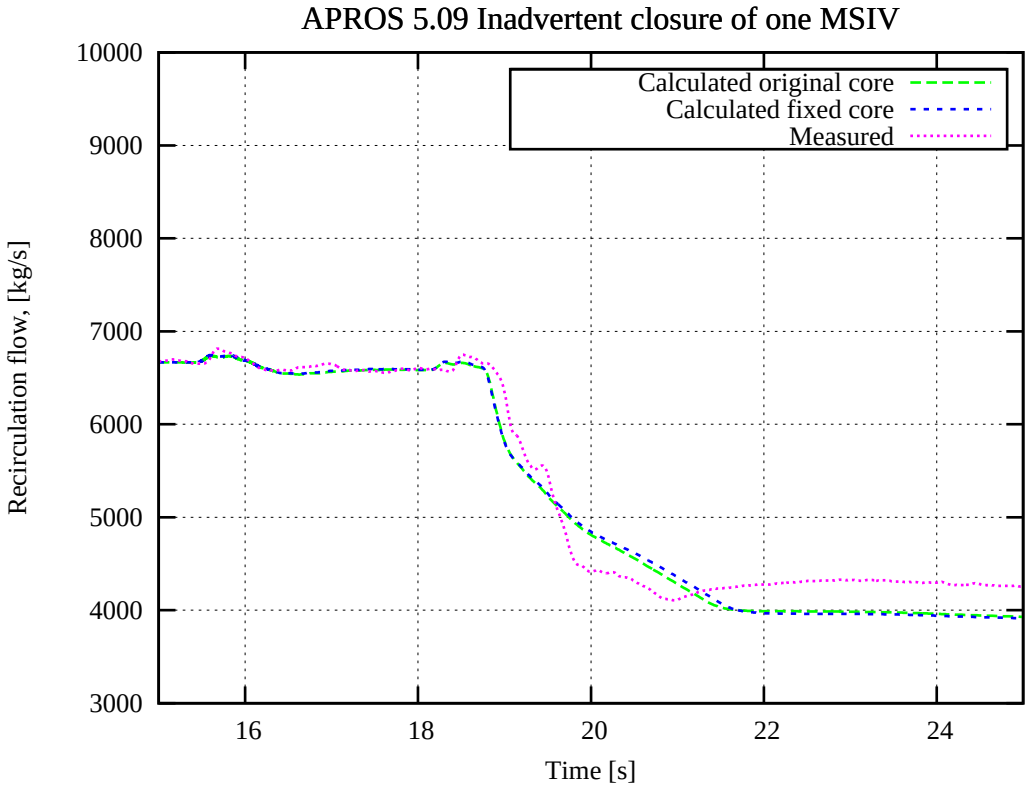

Figure 4. Recirculation flow

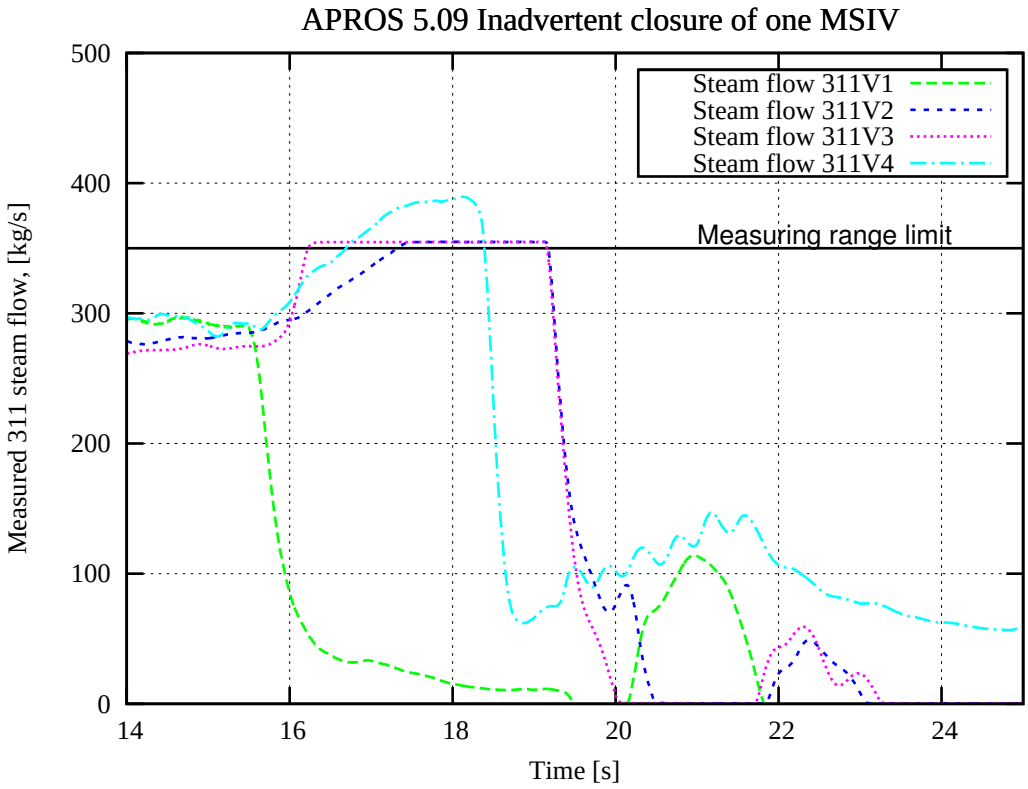

Figure 5. Measured 311 steam flow

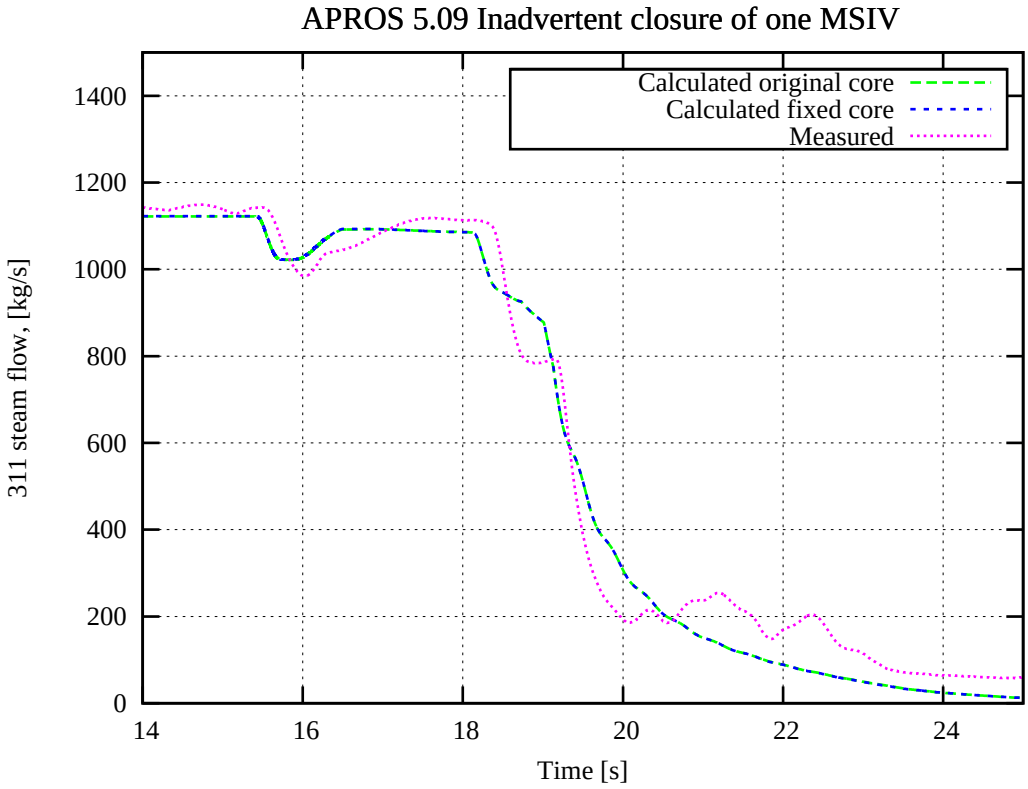

Figure 6. 311 steam flow

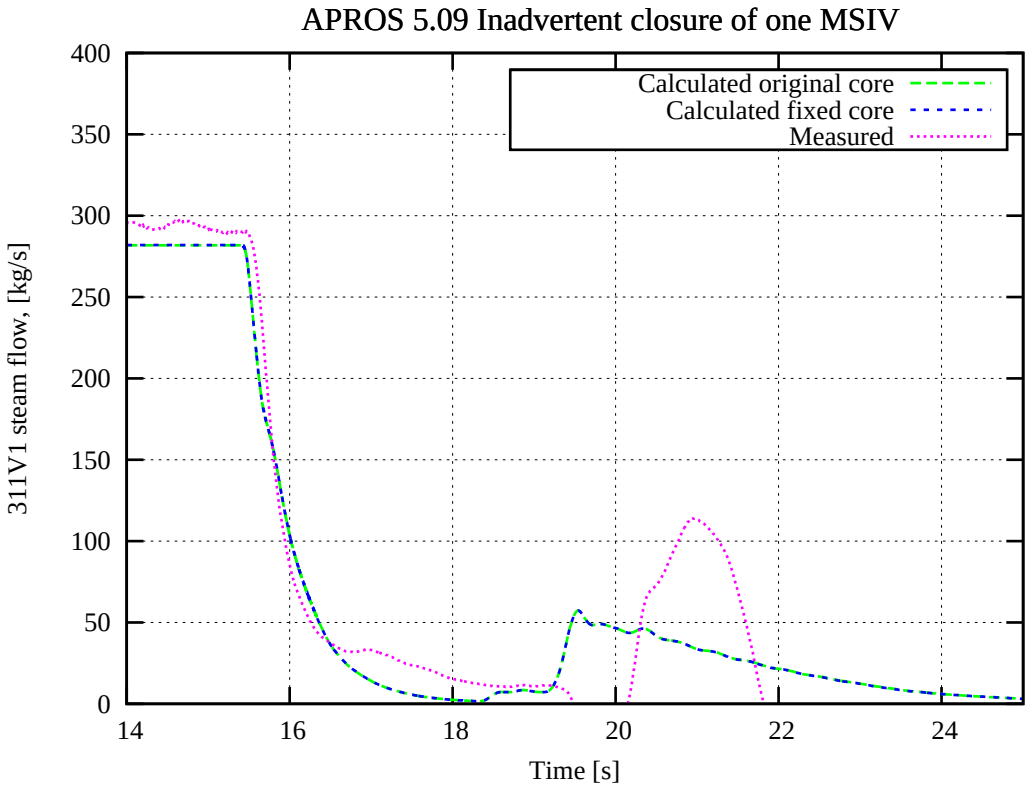

Figure 7. 311V1 steam flow

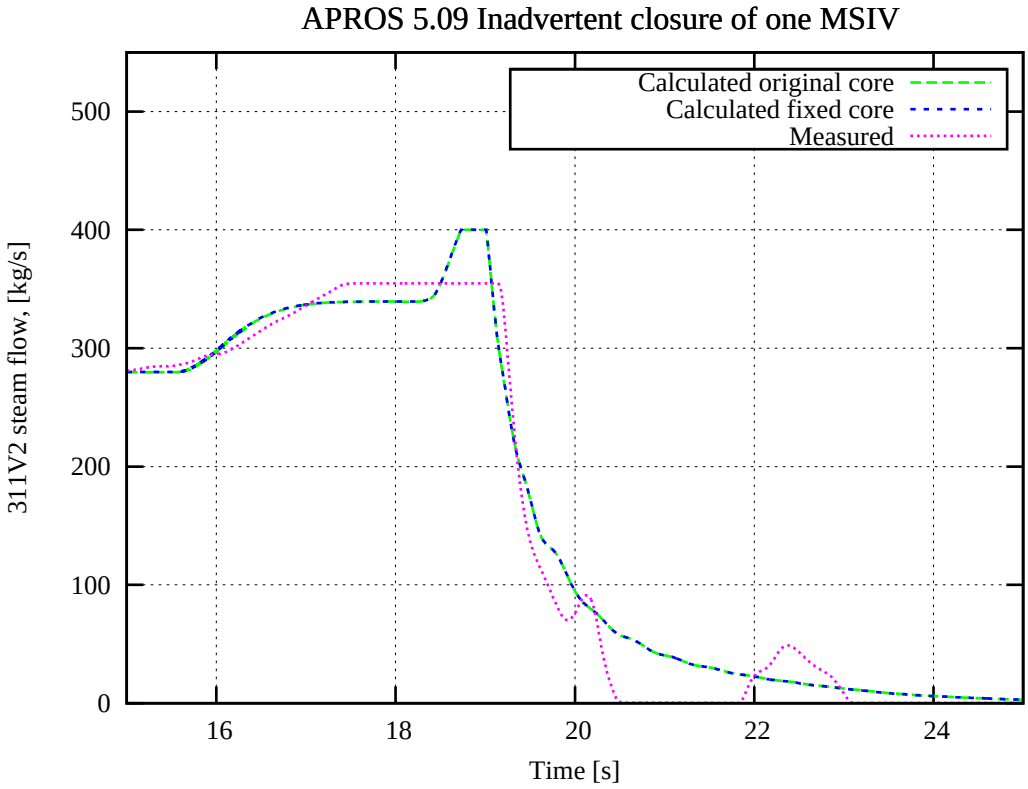

Figure 8. 311V2 steam flow

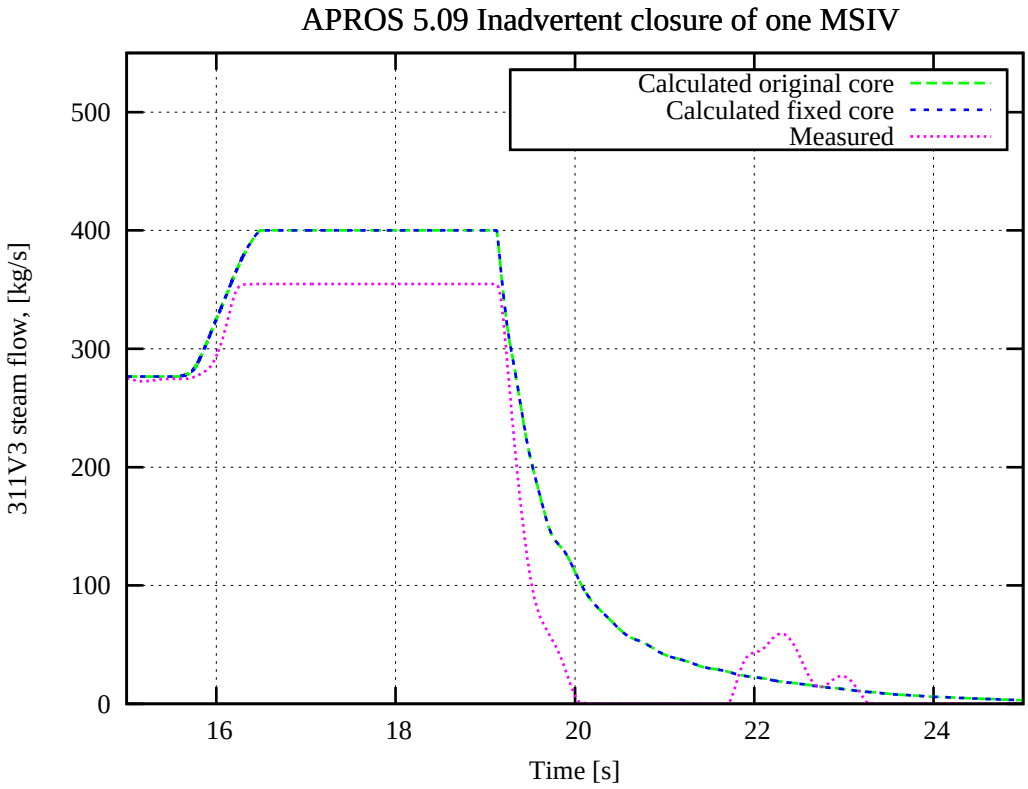

Figure 9. 311V3 steam flow

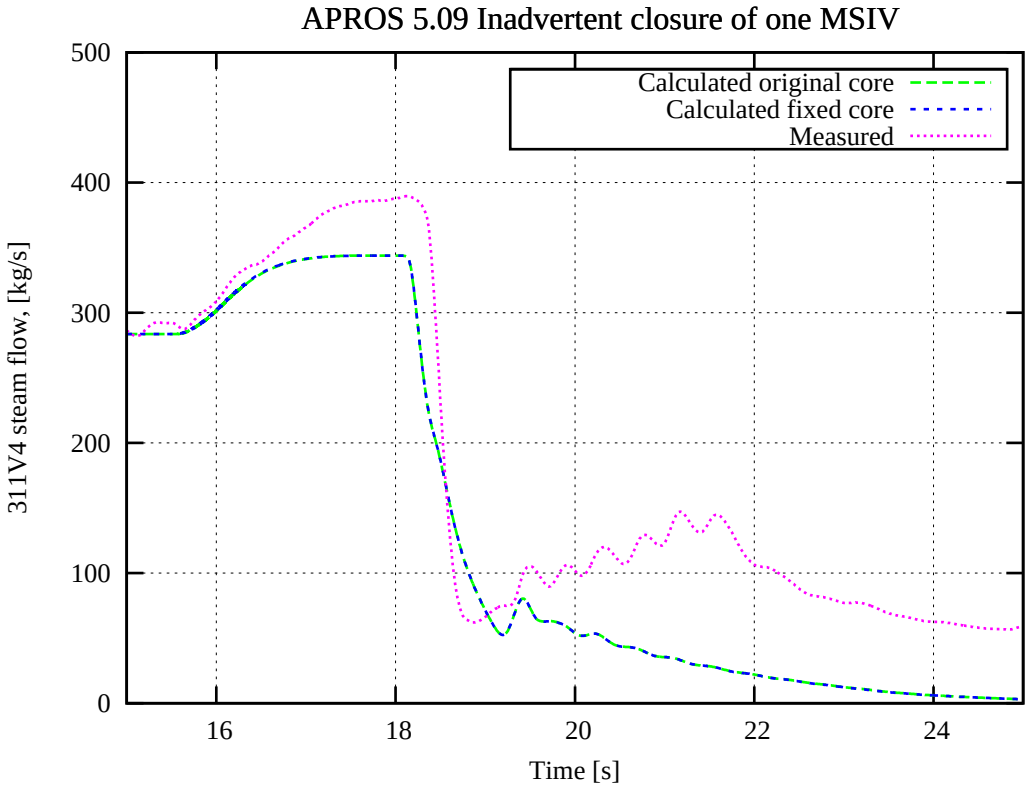

Figure 10. 311V4 steam flow

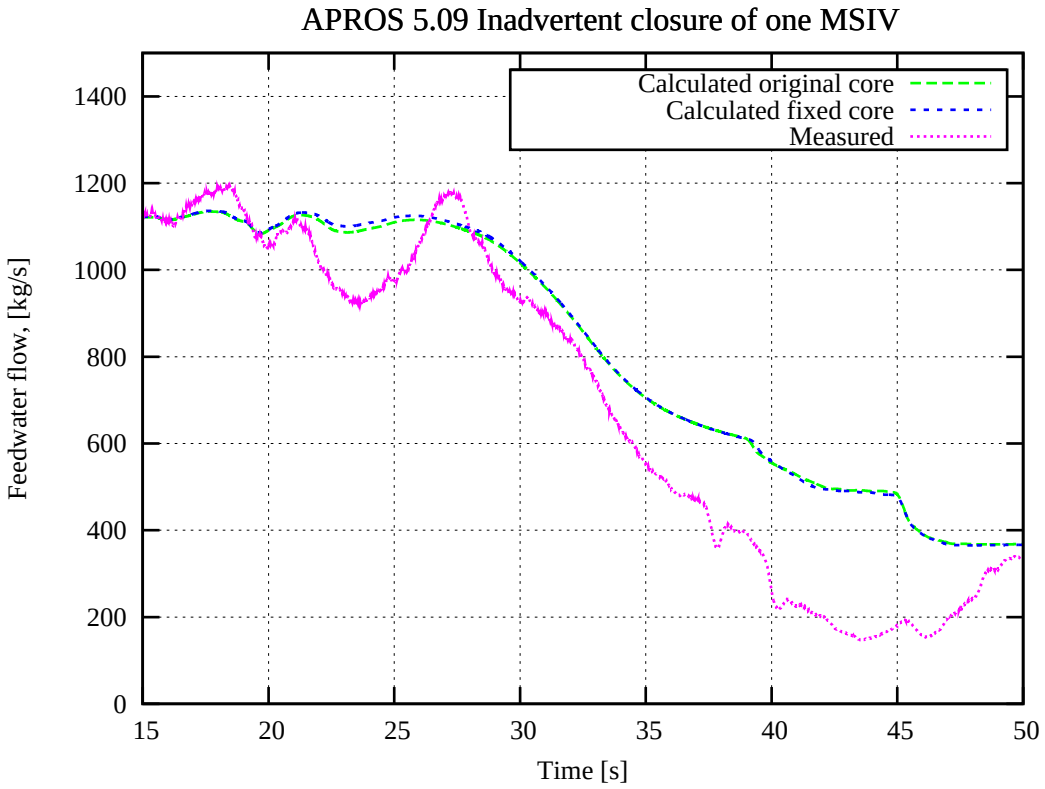

Figure 11. Feedwater flow

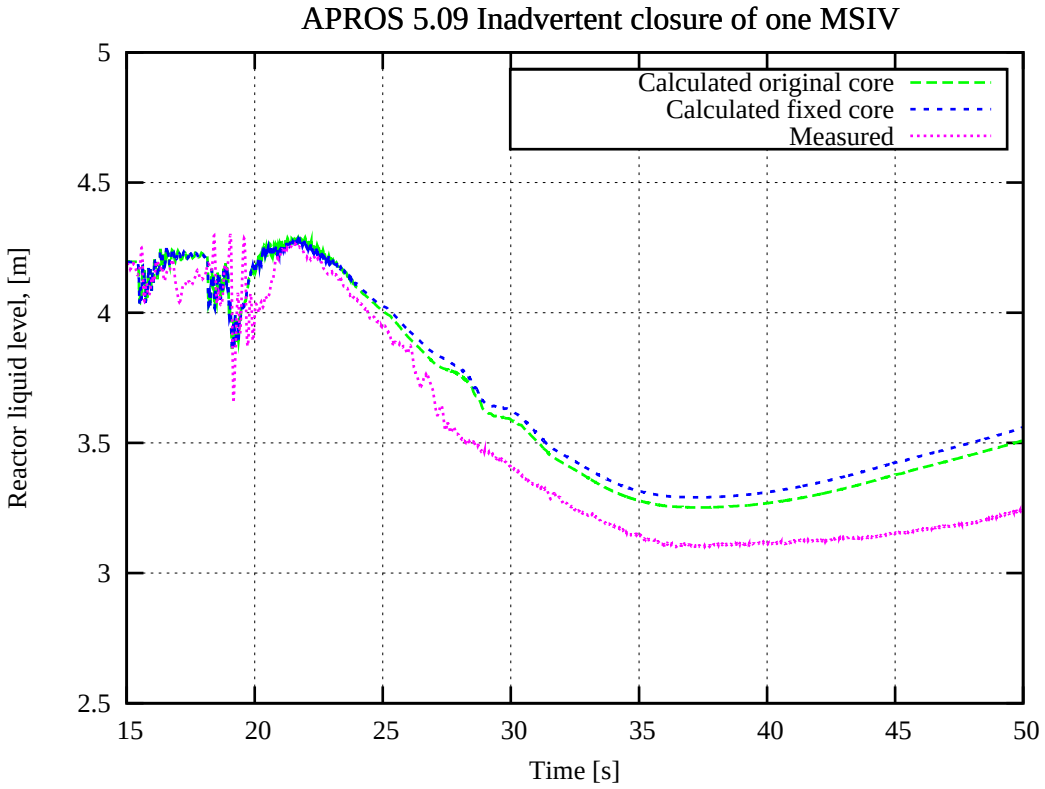

Figure 12. Reactor liquid level

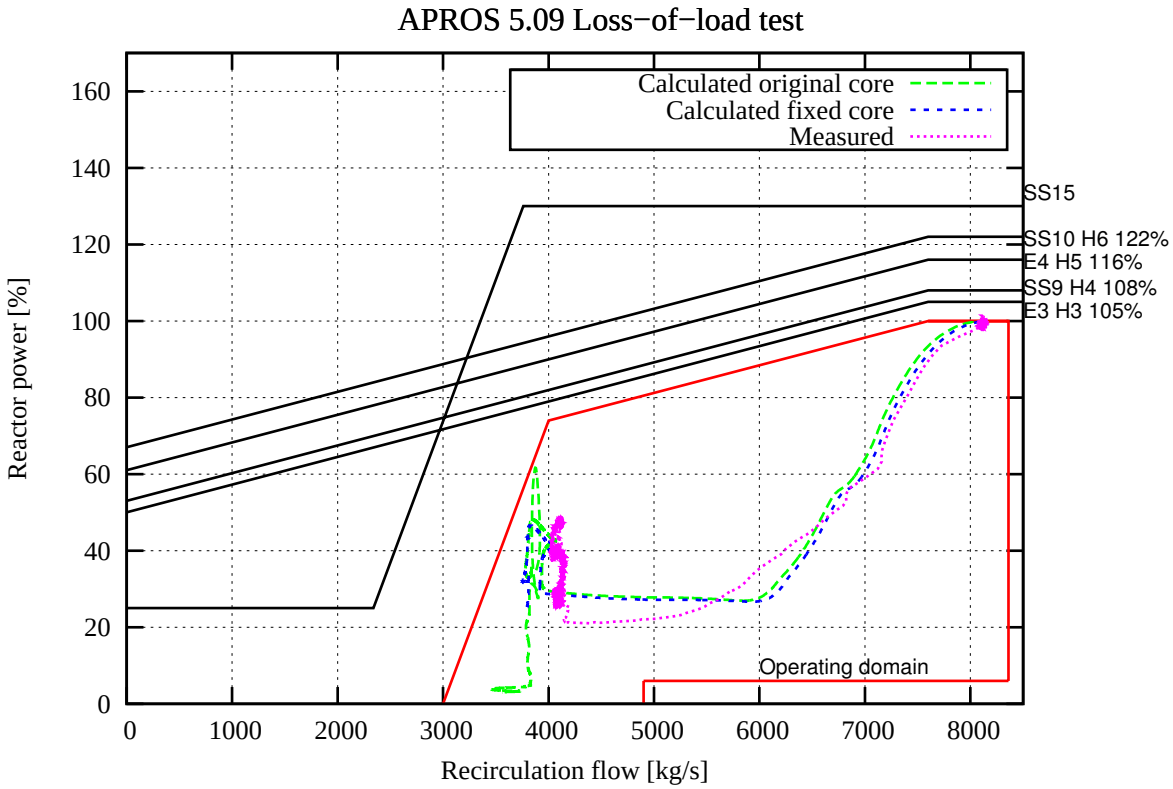

Figure 1. Reactor power as a function of recirculation flow

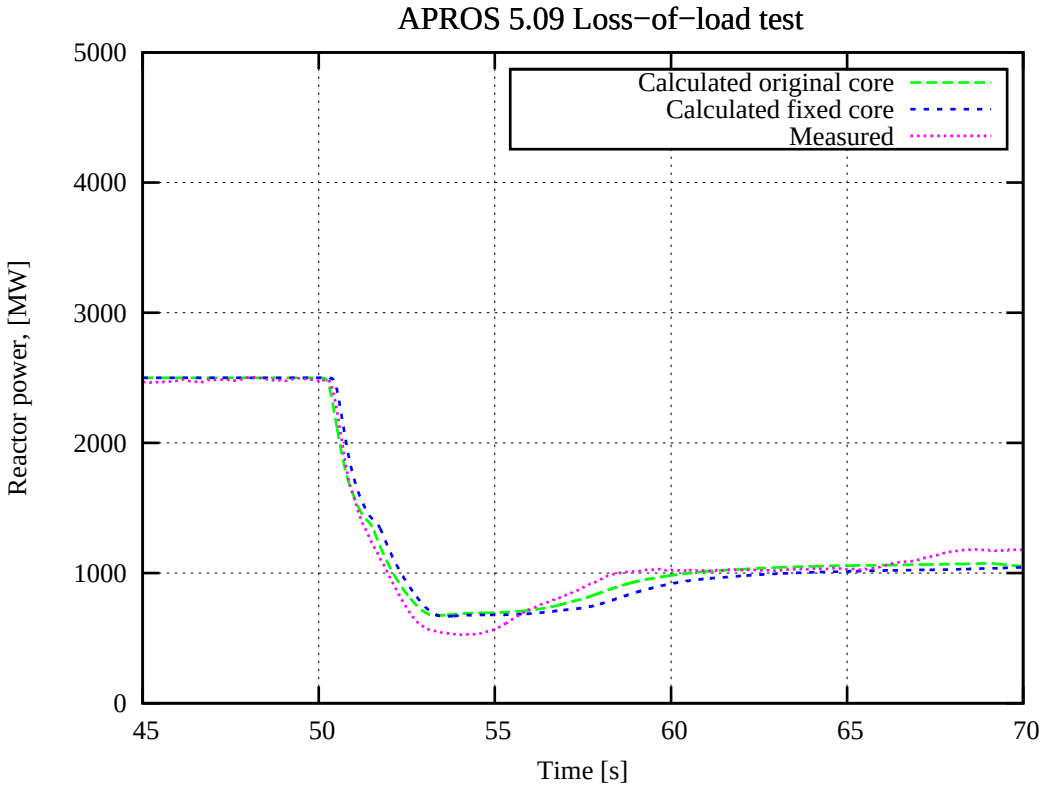

Figure 2. Reactor power short time

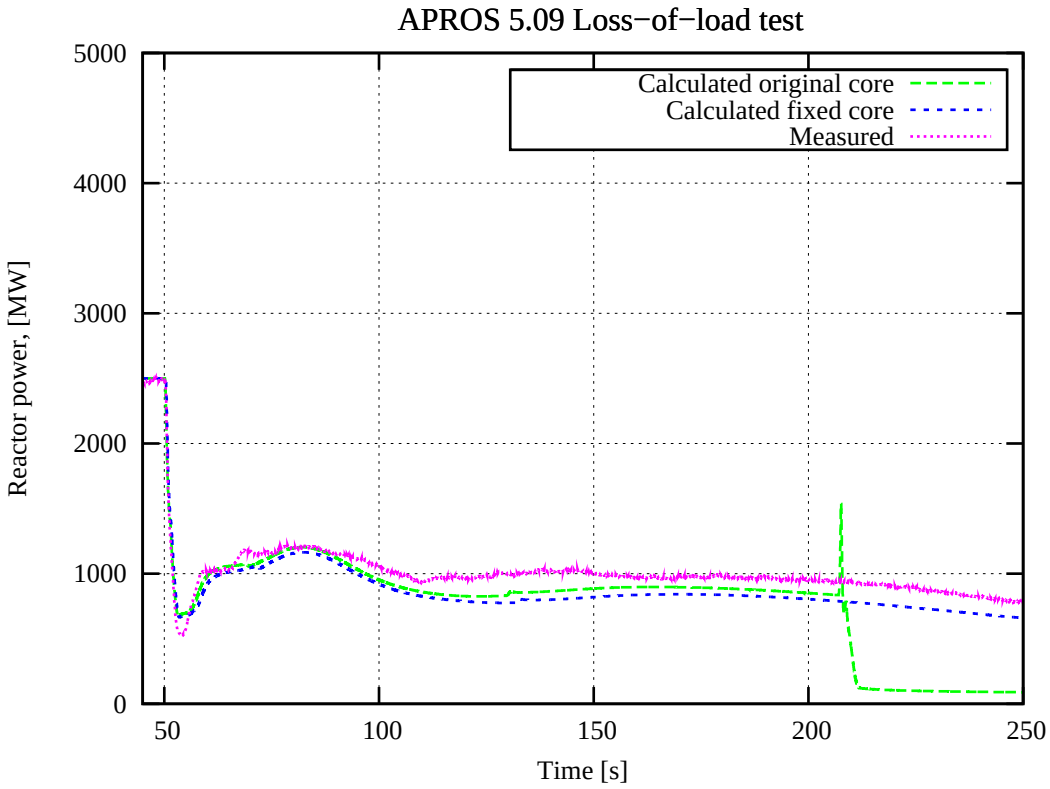

Figure 3. Reactor power long time

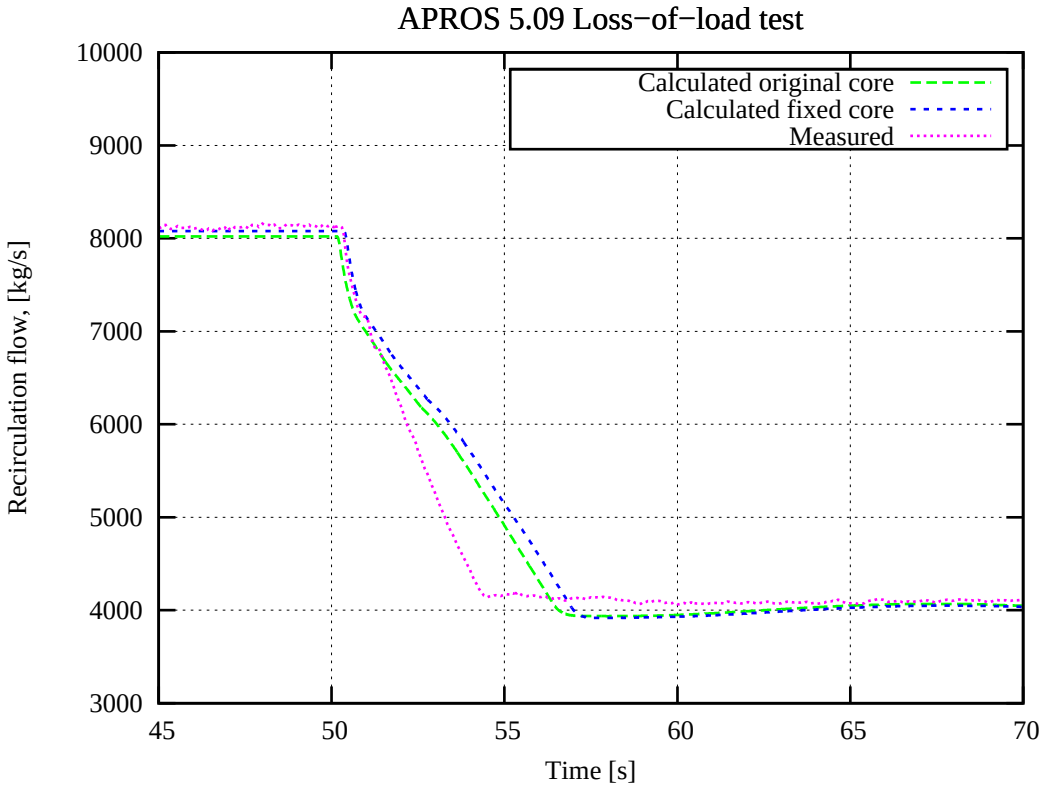

Figure 4. Recirculation flow short time

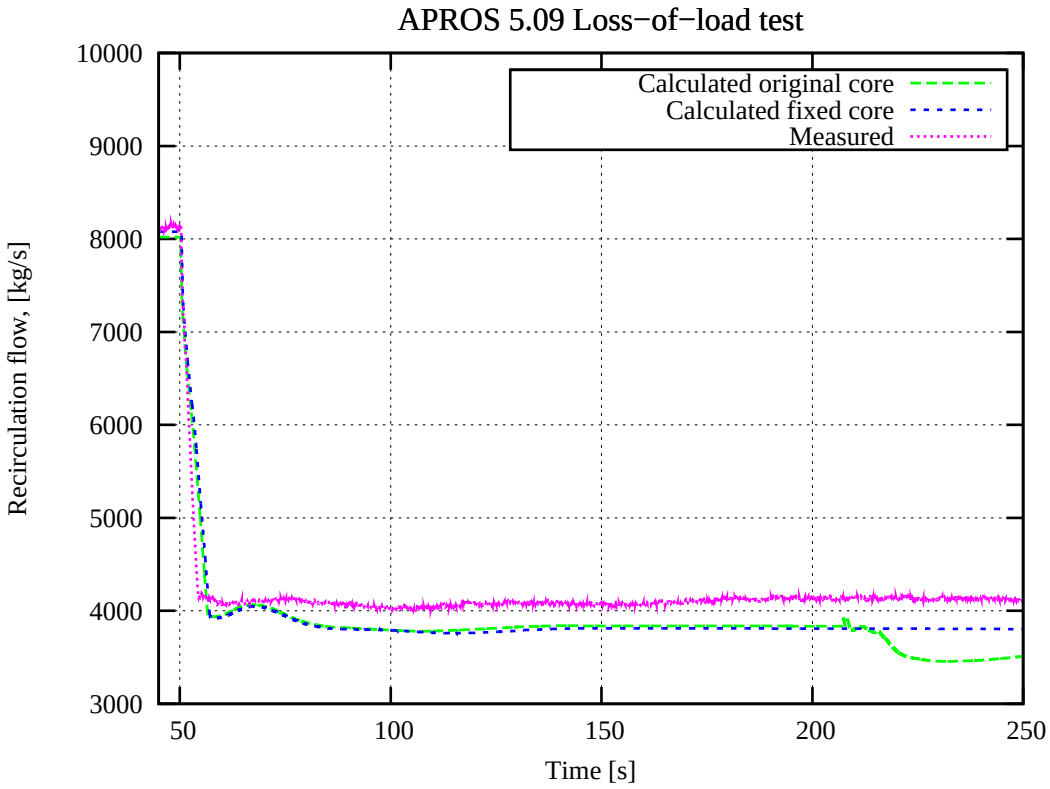

Figure 5. Recirculation flow long time

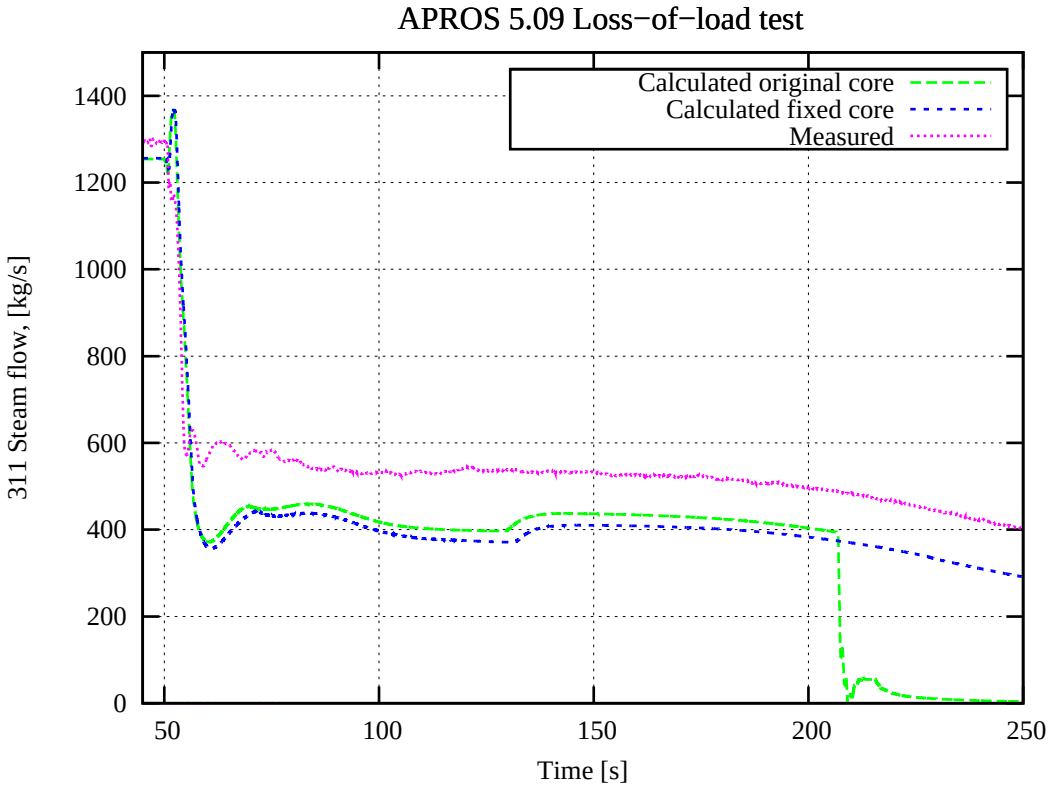

Figure 6. 311 Steam flow

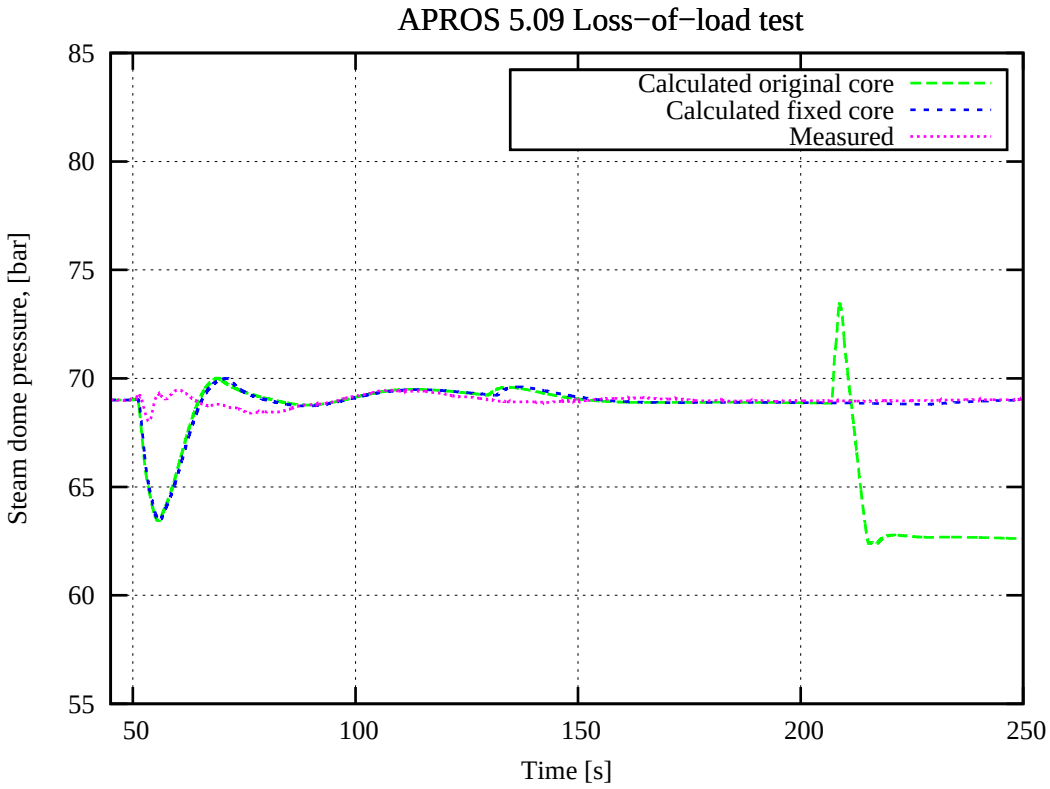

Figure 7. Steam dome pressure

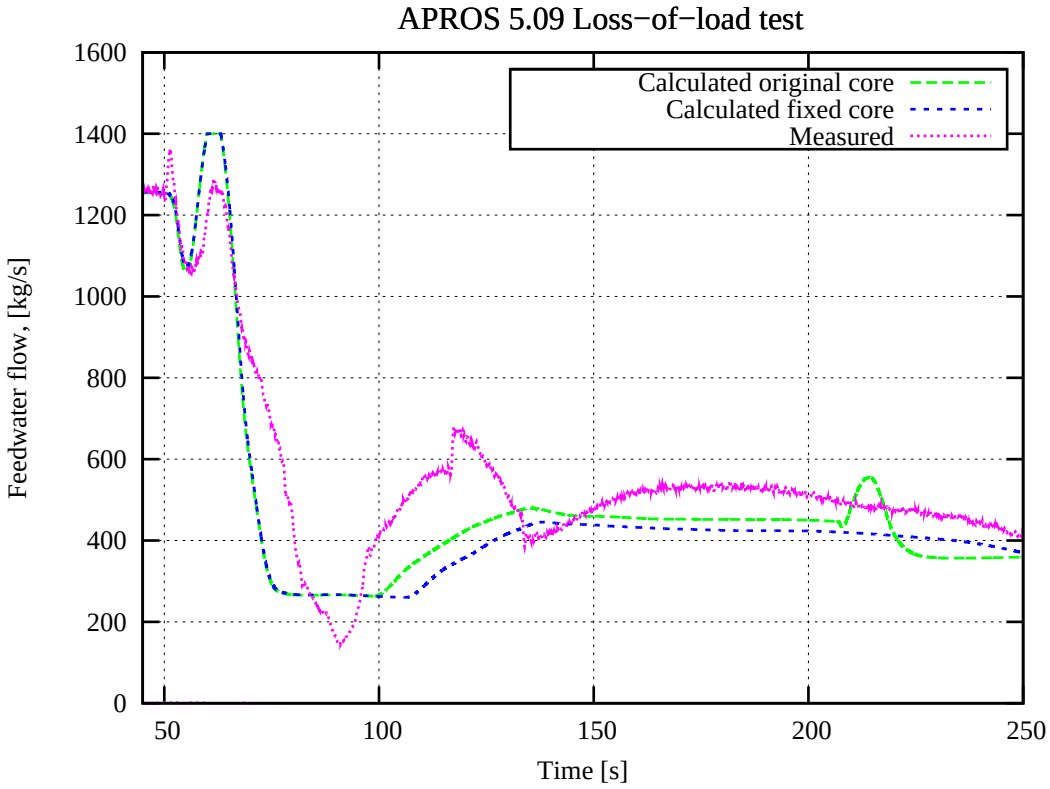

Figure 8. Feedwater flow

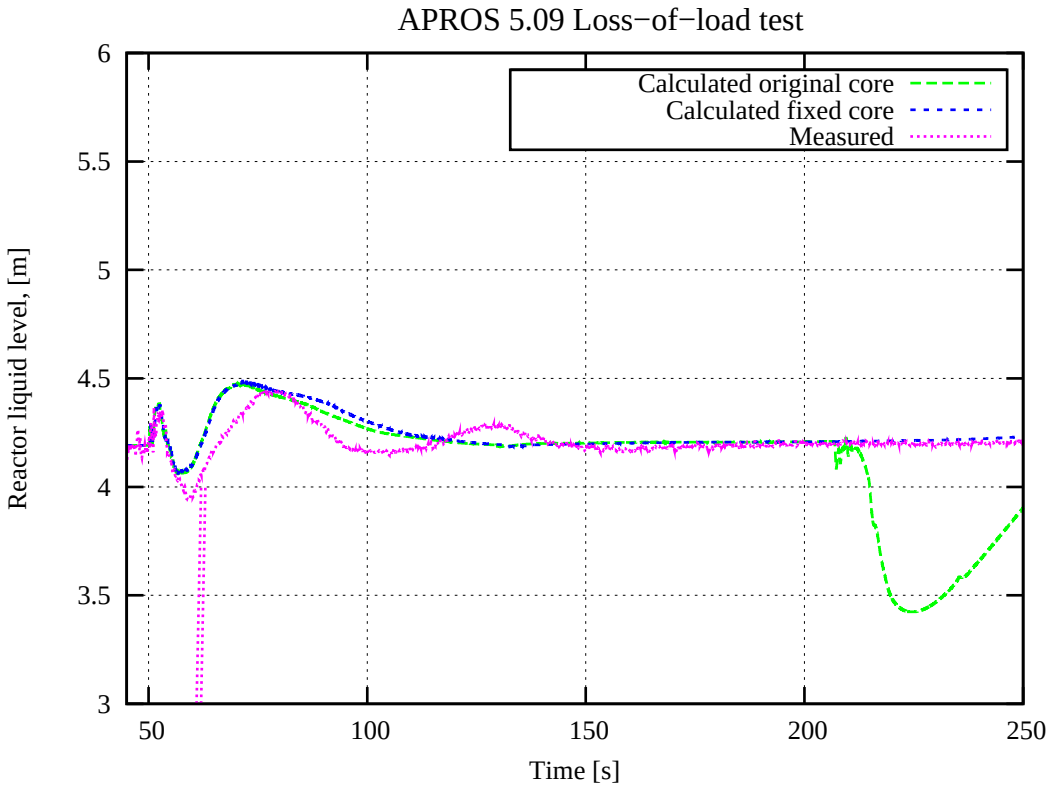

Figure 9. Reactor liquid level

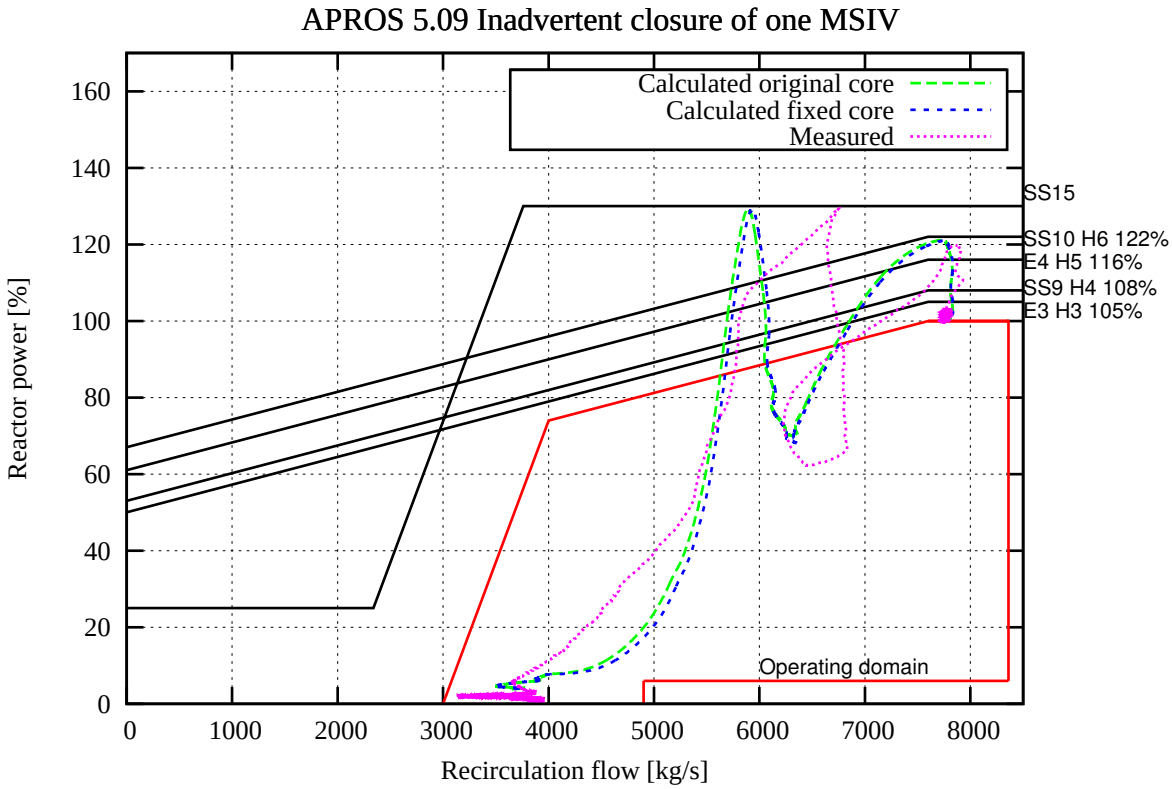

Figure 1. Reactor power as a function of recirculation flow

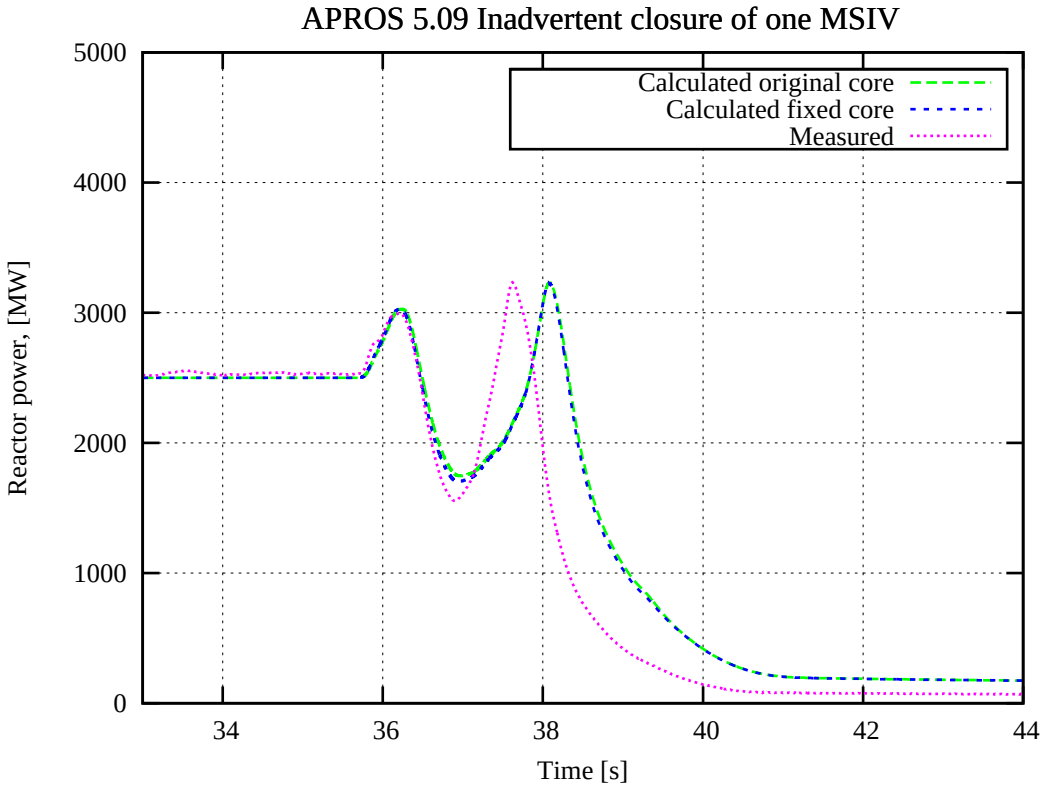

Figure 2. Reactor power

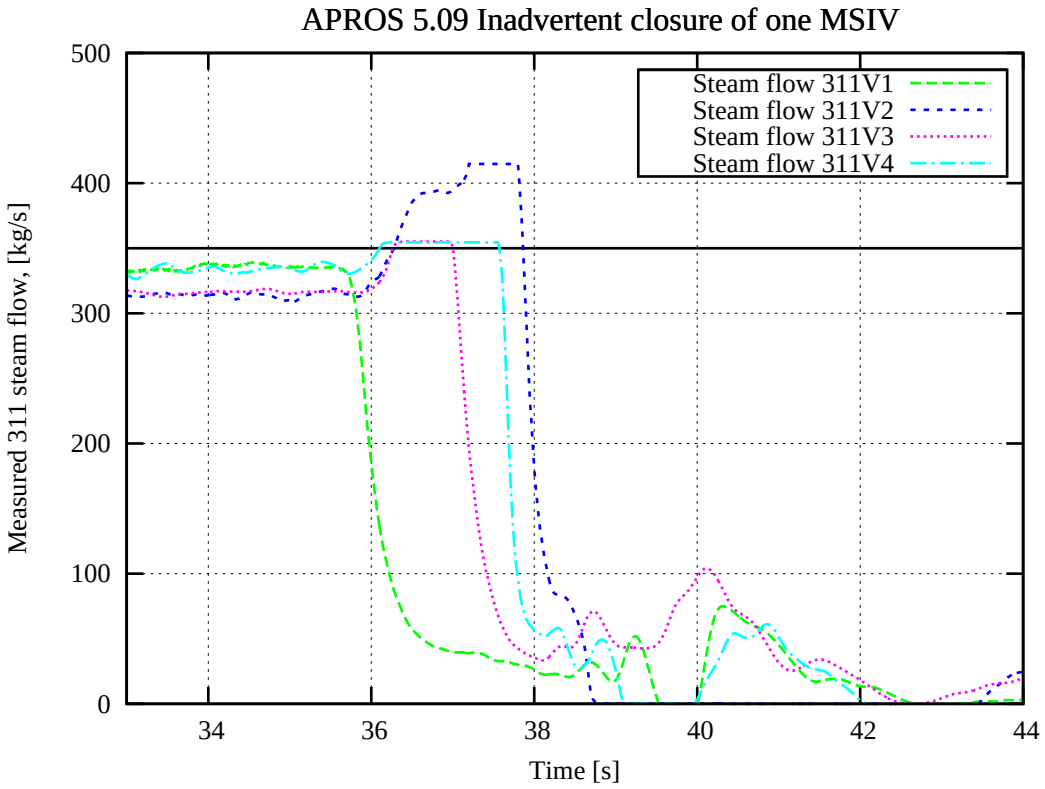

Figure 3. Measured 311 steam flow

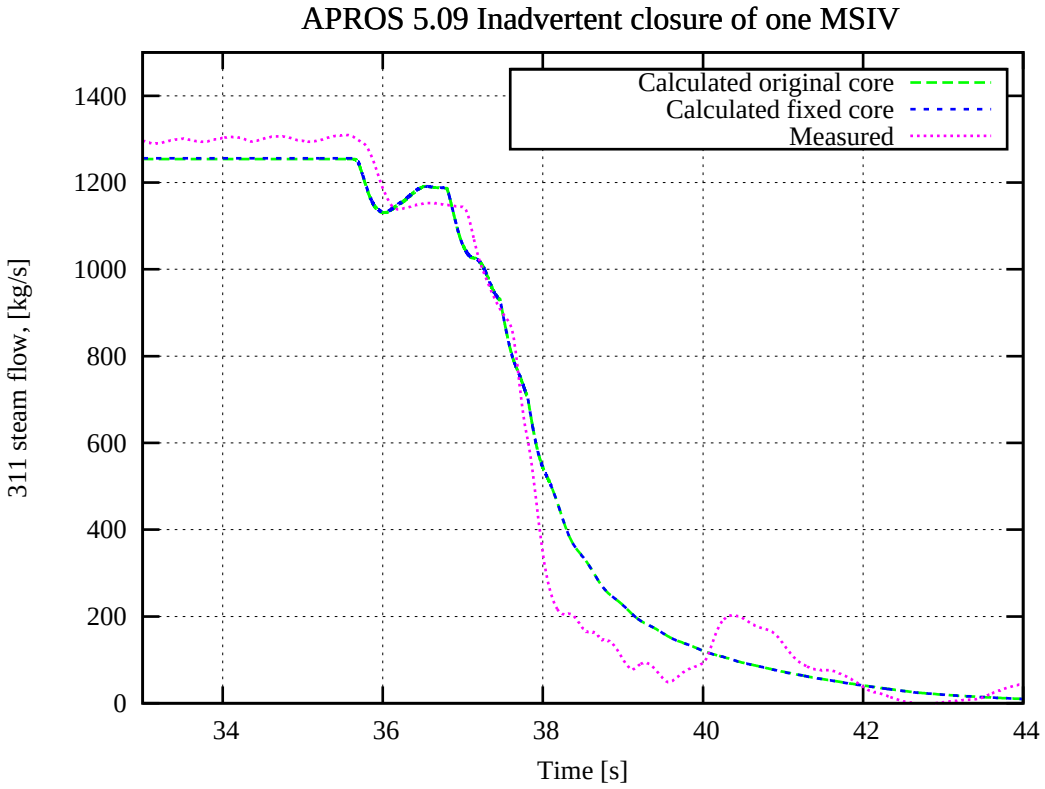

Figure 4. 311 steam flow

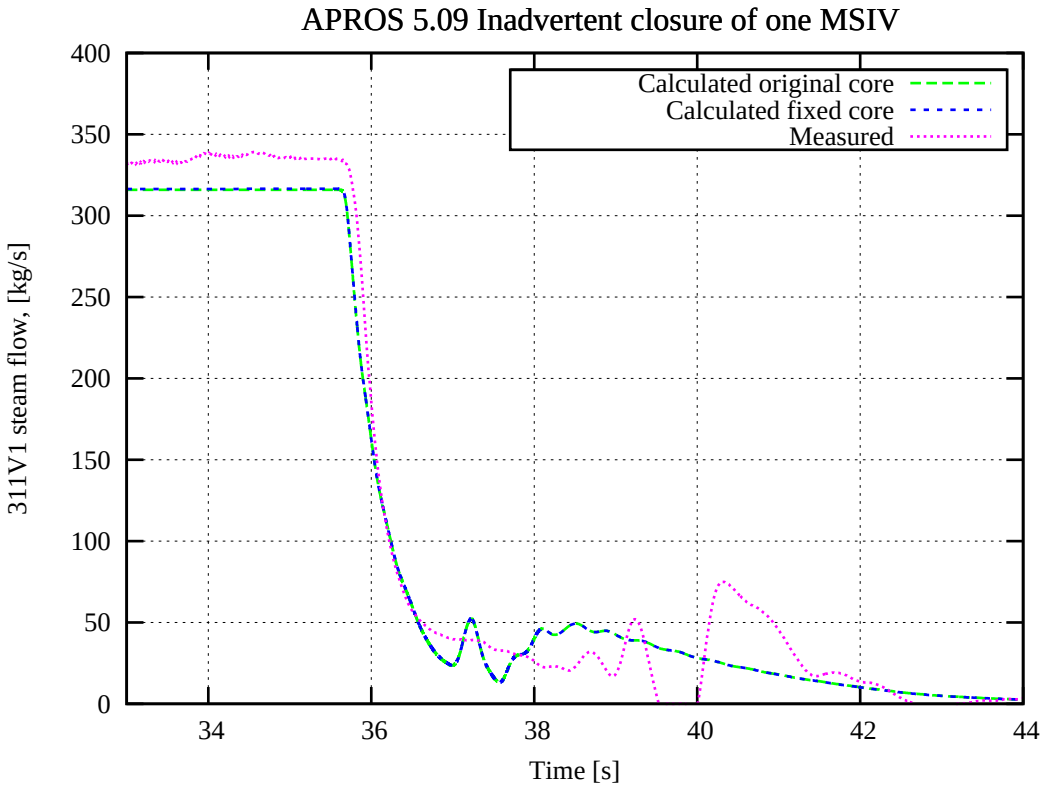

Figure 5. 311V1 steam flow

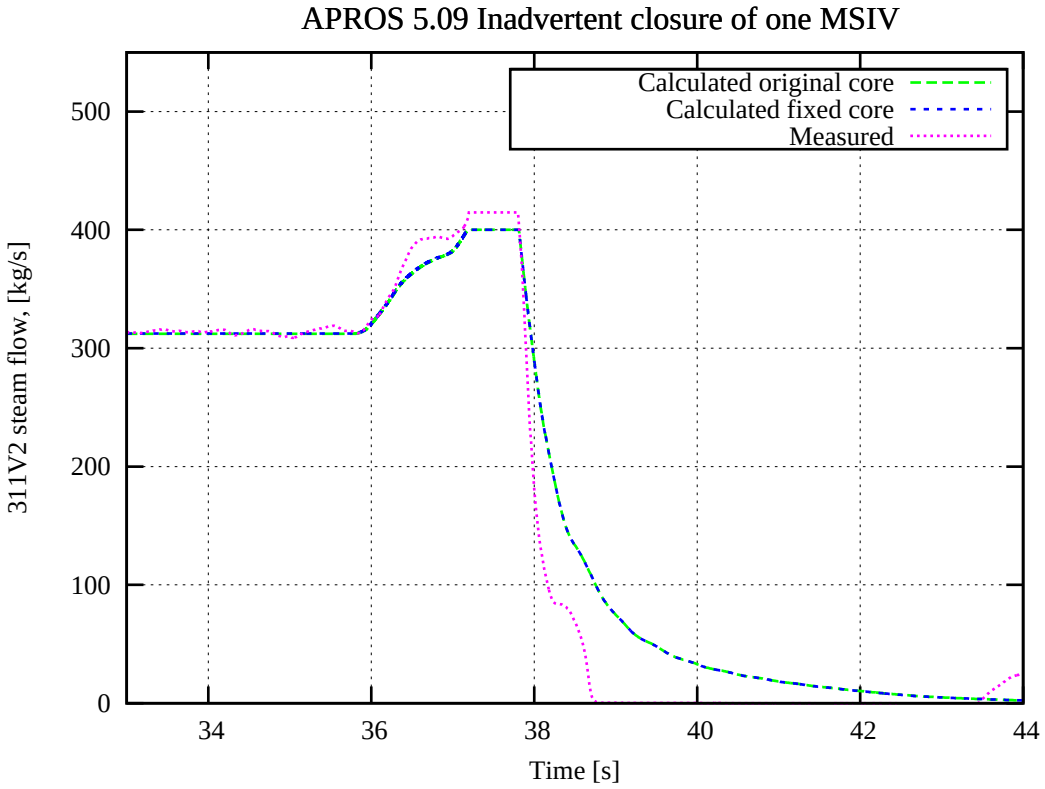

Figure 6. 311V2 steam flow

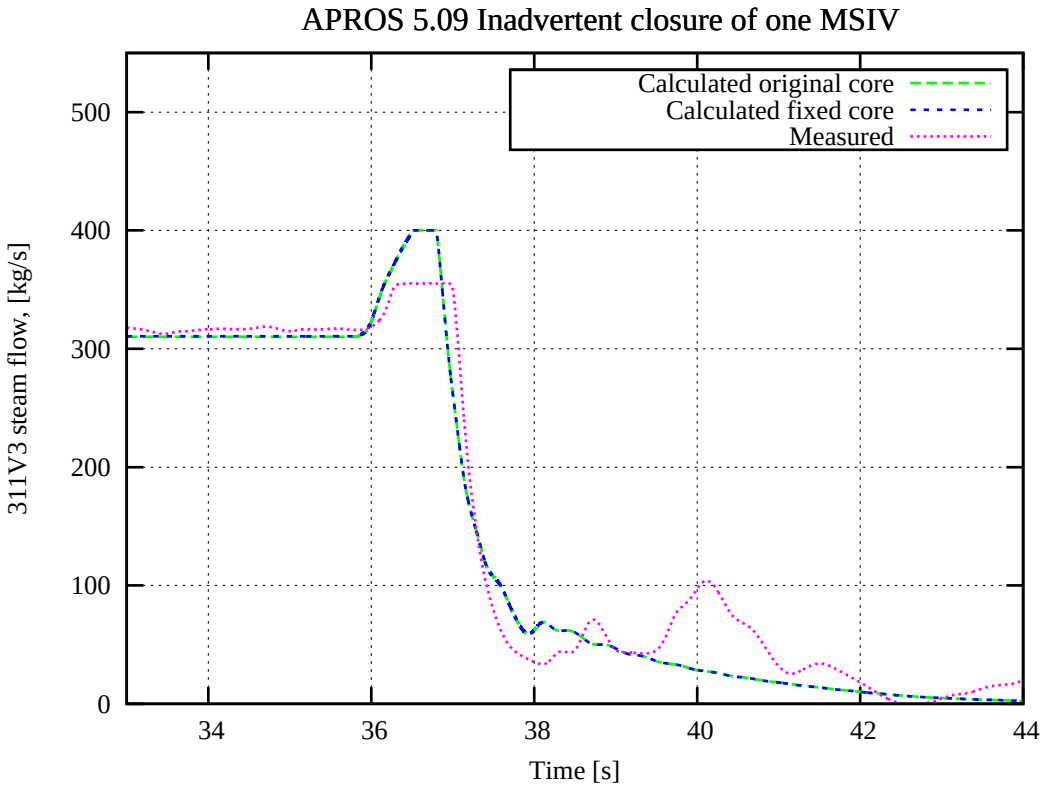

Figure 7. 311V3 steam flow

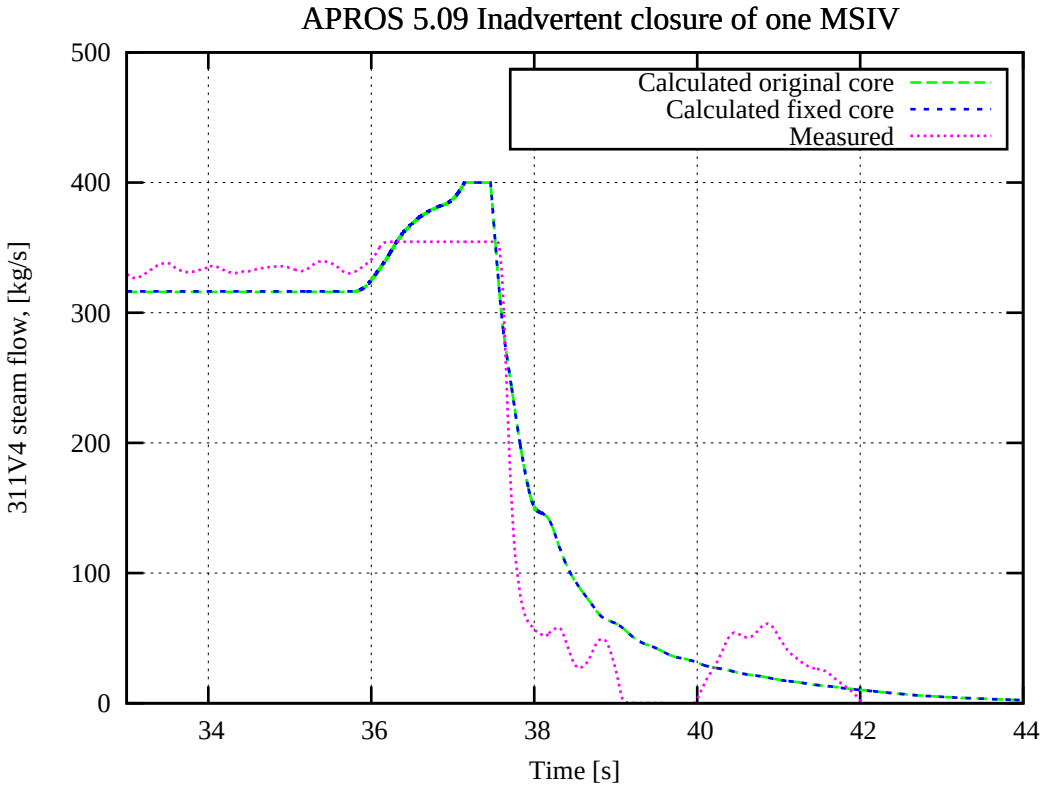

Figure 8. 311V4 steam flow

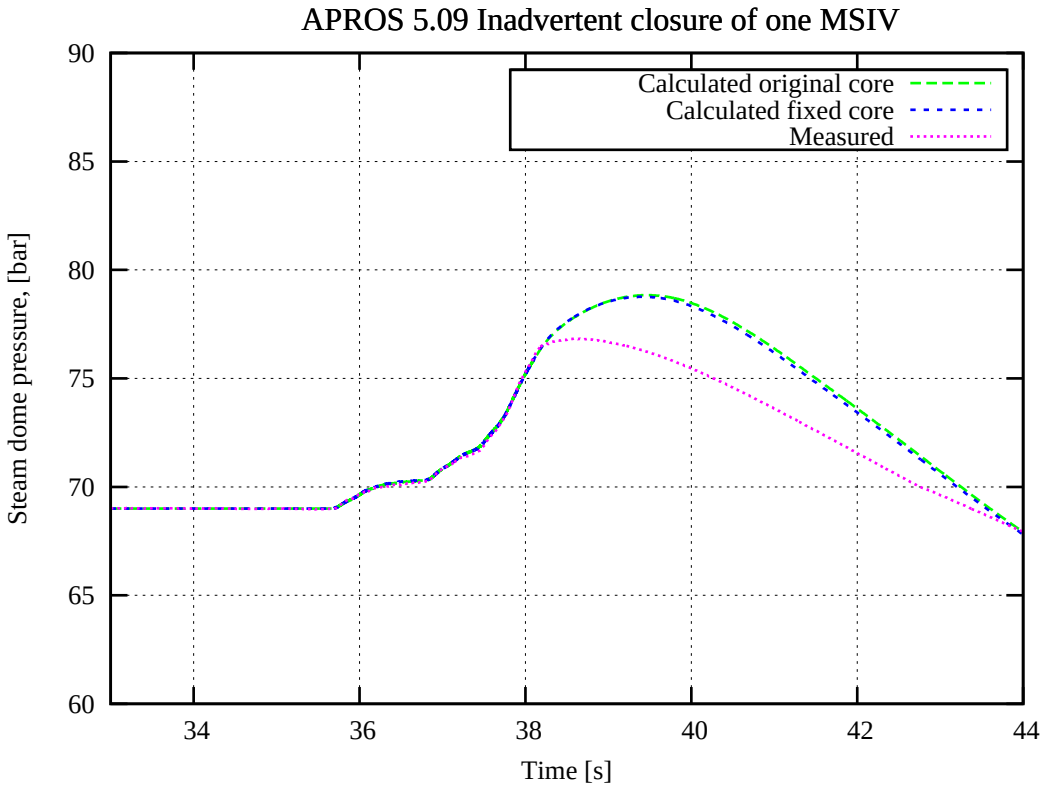

Figure 9. Steam dome pressure

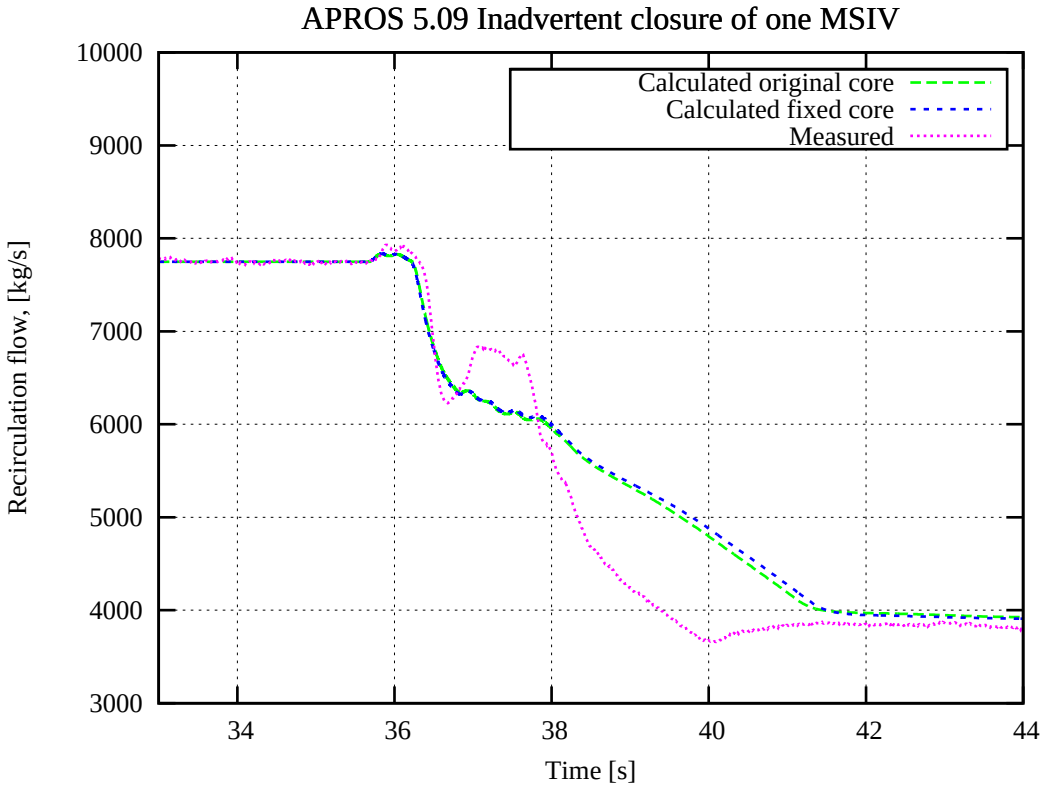

Figure 10. Recirculation flow

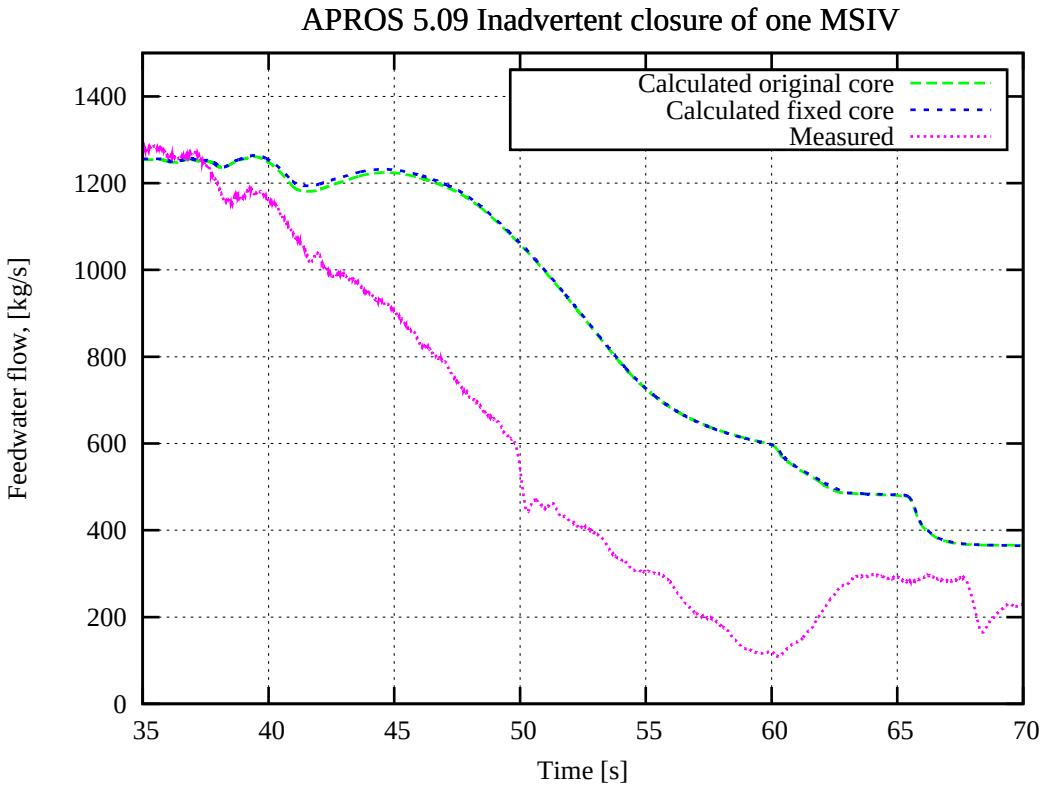

Figure 11. Feedwater flow

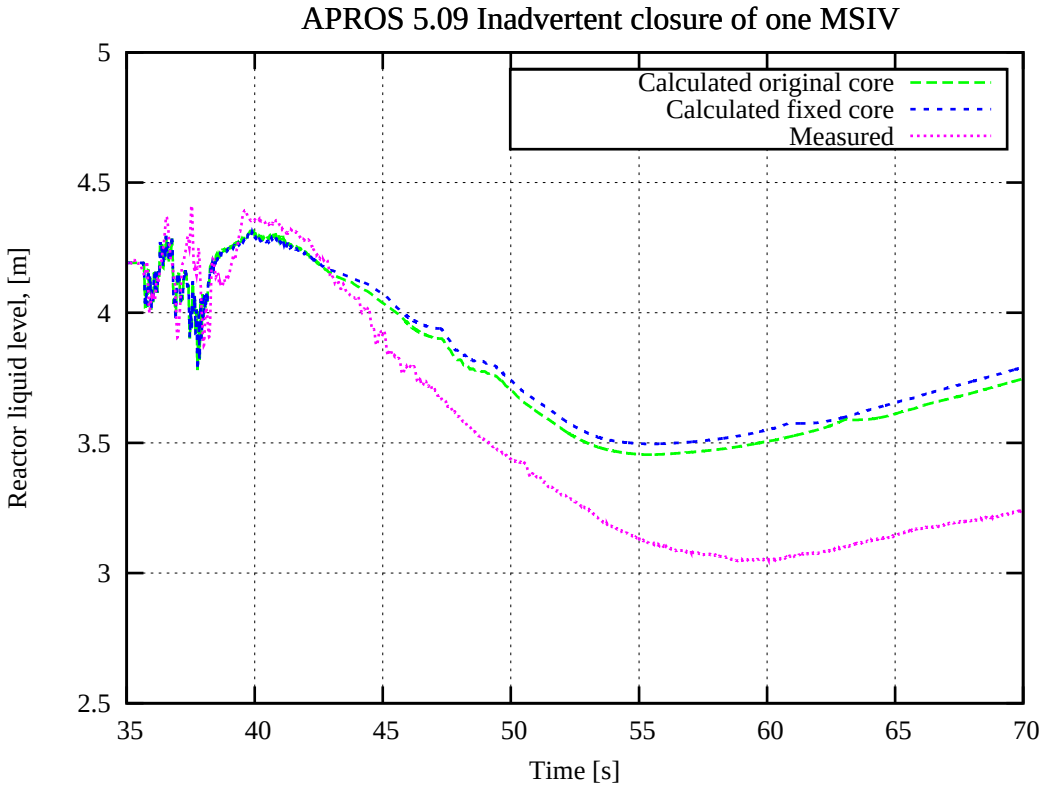

Figure 12. Reactor liquid level

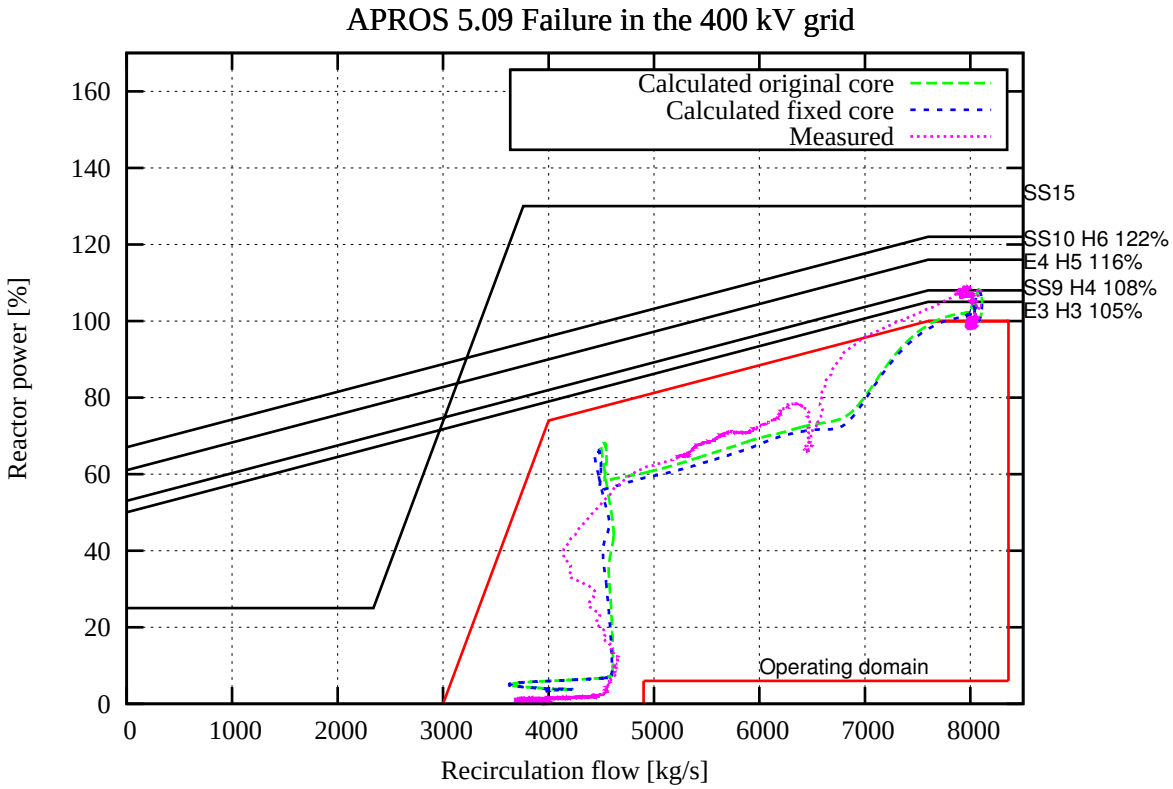

Figure 1. Reactor power as a function of recirculation flow

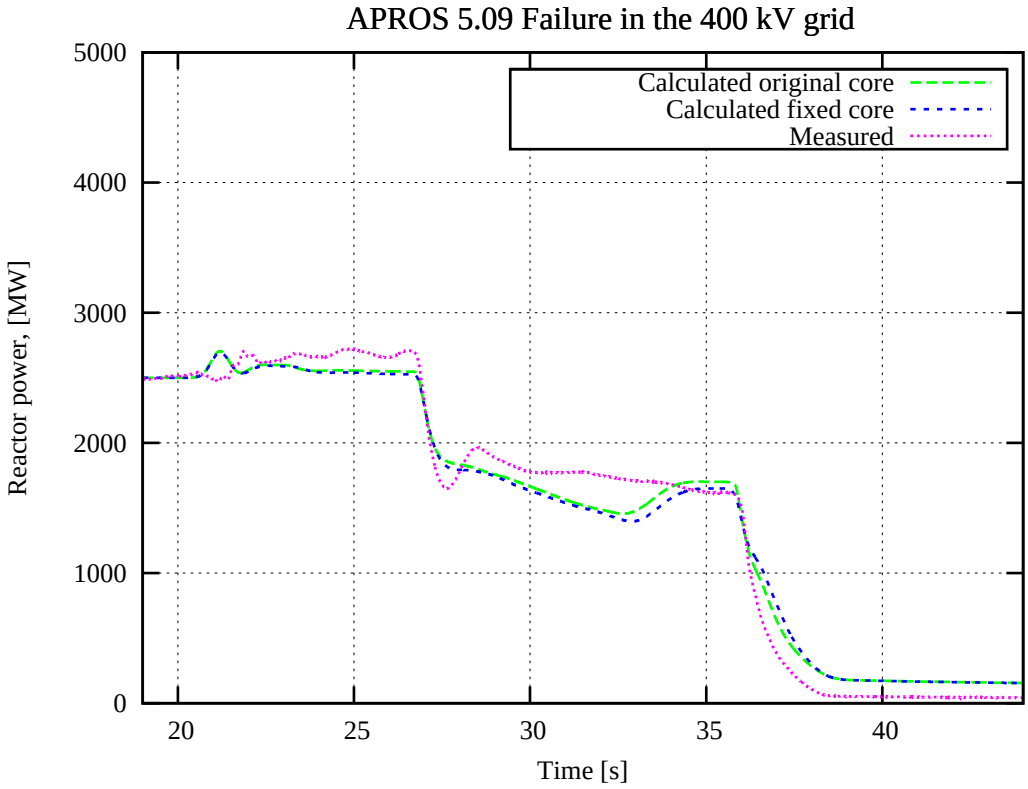

Figure 2. Reactor power

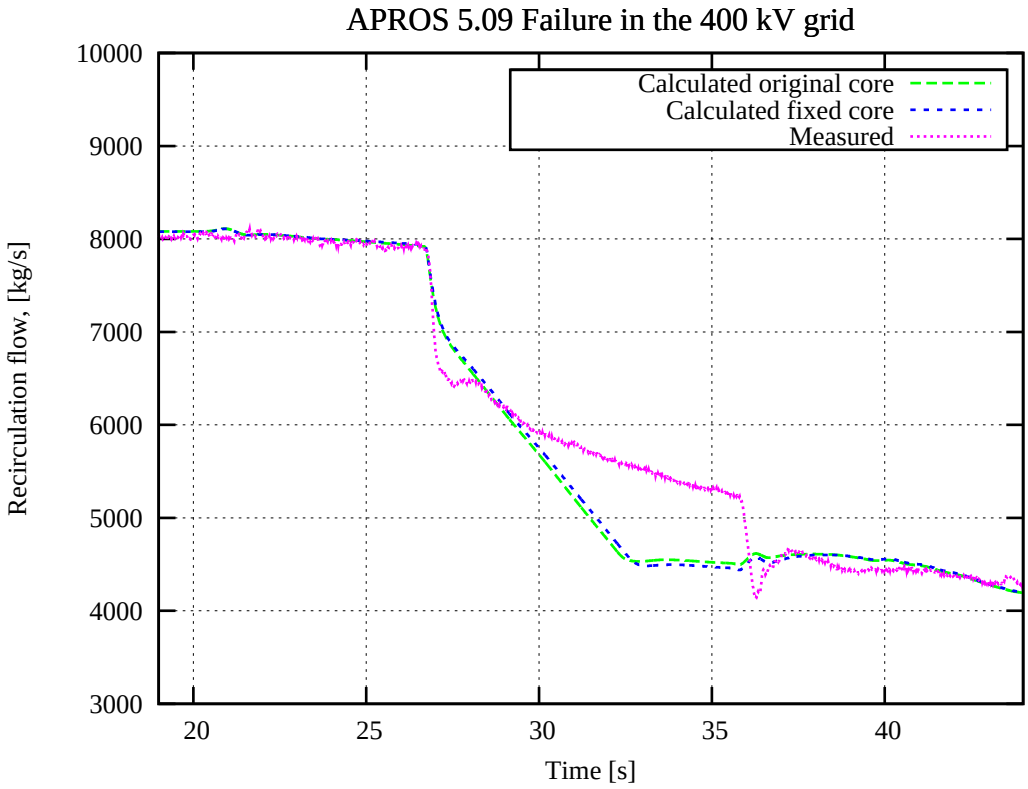

Figure 3. Recirculation flow

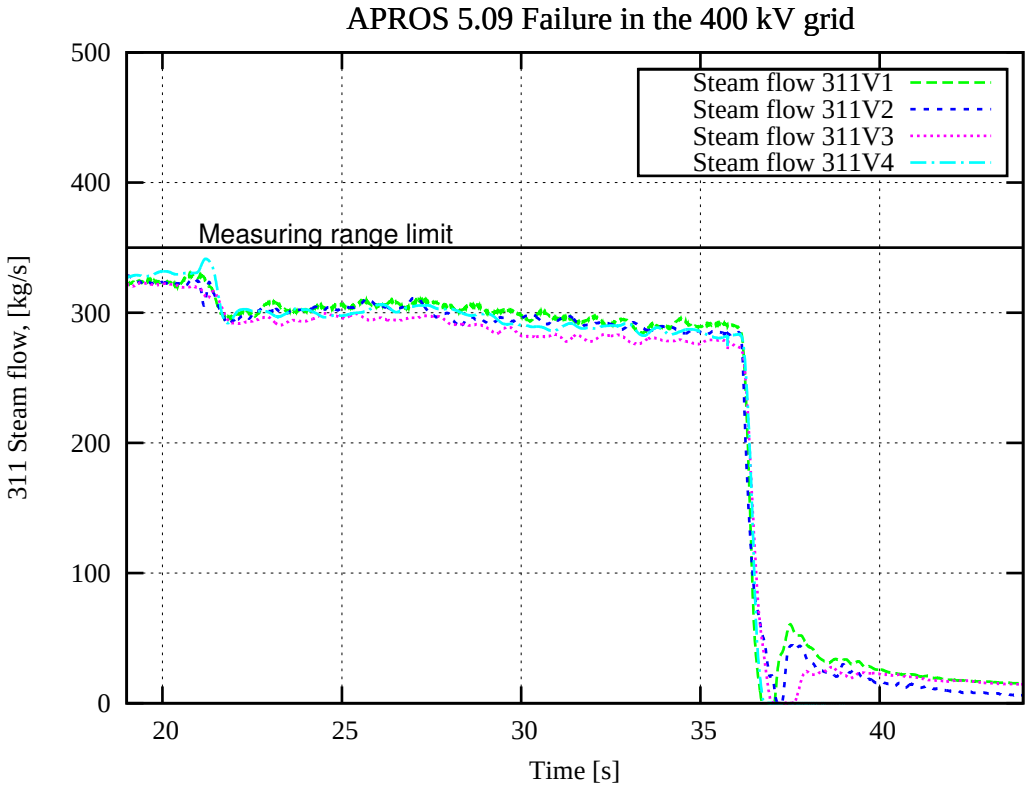

Figure 4. Measured 311V1−V4 steam flow

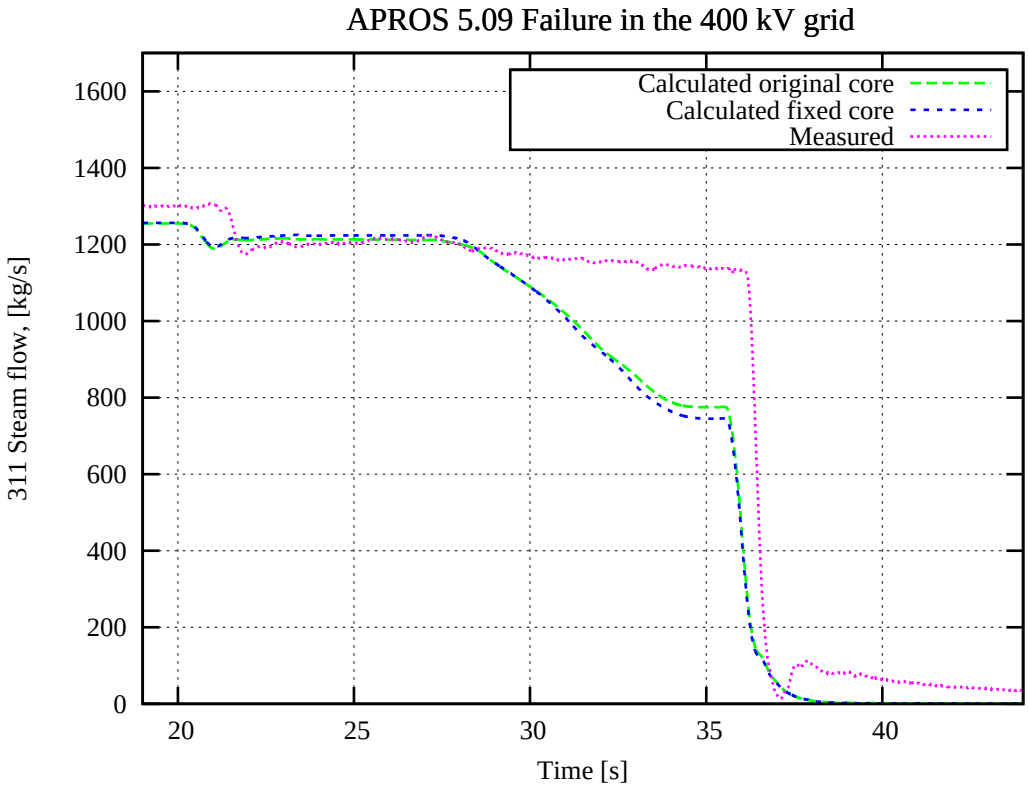

Figure 5. 311 steam flow

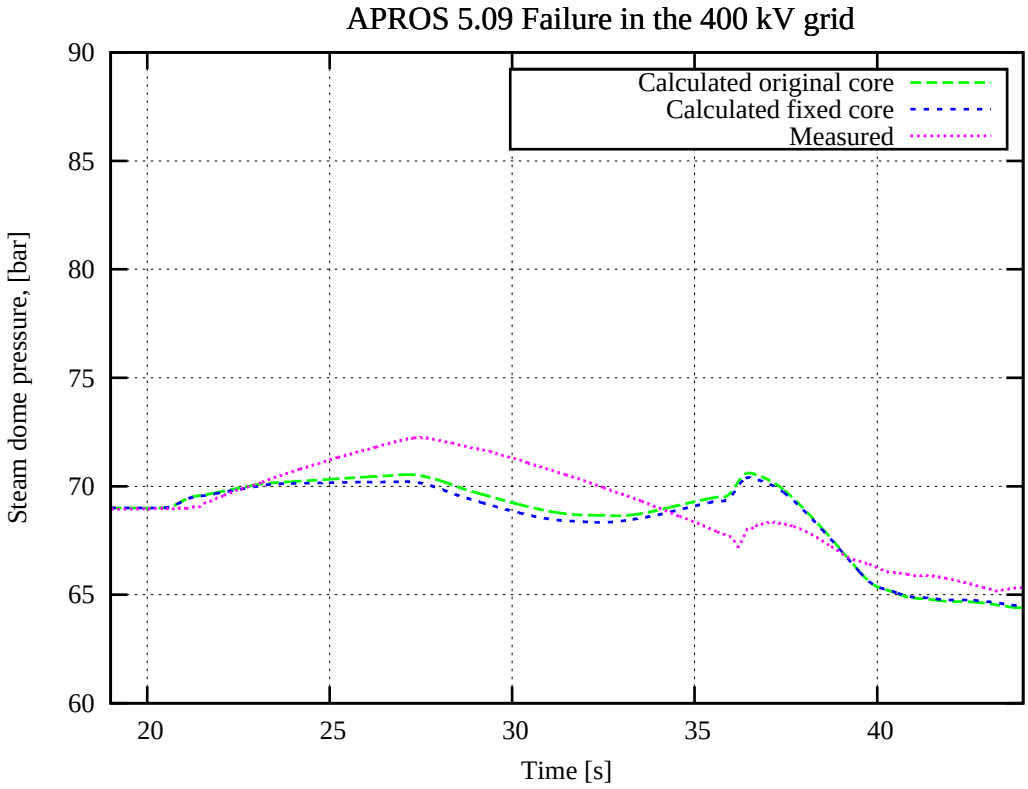

Figure 6. Steam dome pressure

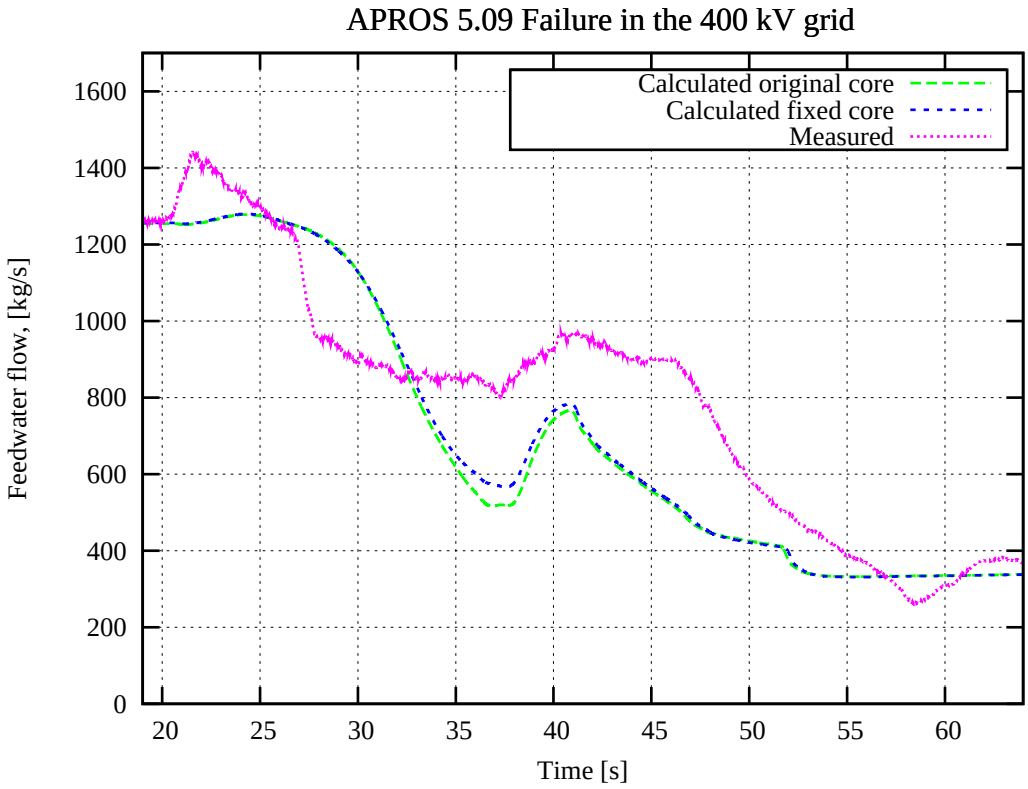

Figure 7. Feedwater flow

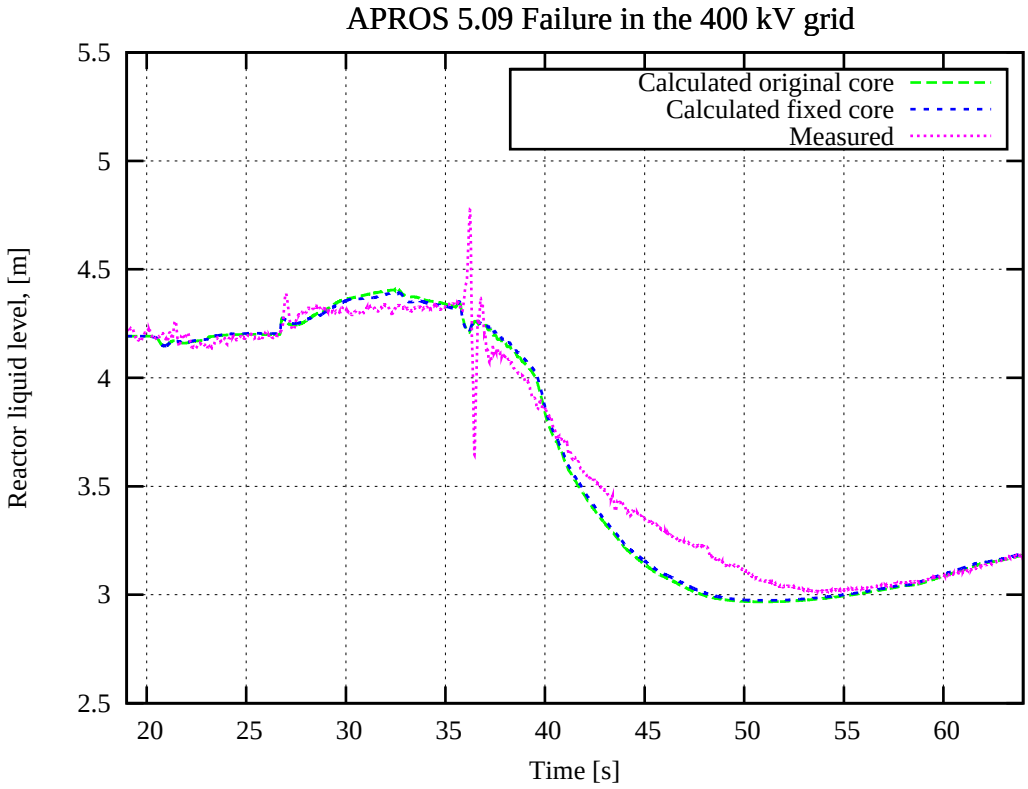

Figure 8. Reactor liquid level